ORKUSTOFNUN

National Energy Authority

Estimating Nonlinear Hydrological Rating Curves and Discharge using the Bayesian Approach

Snorri Árnason

Hydrological Service
National Energy Authority

ORKUSTOFNUN

National Energy Authority

Estimating Nonlinear Hydrological Rating Curves and Discharge using the Bayesian Approach

Master's Thesis

Snorri Árnason

Originally prepared and published for the Faculty of Engineering, University of Iceland

ORKUSTOFNUN
National Energy Authority

Key page
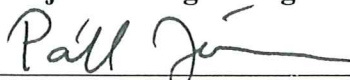
Report no.:	Date:	Distribution:	Open ☒ Closed ☐
2005/030	2006-10-04	**Conditions:**	

Report name / Main and subheadings:	Number of copies:
Estimating Nonlinear Hydrological Rating Curves and Discharge using the Bayesian Approach	20
	Number of pages:
	135

Author:	Project manager:
Snorri Árnason	Páll Jónsson

Classification of report:	Project number:
Master's Thesis	7-821201

Prepared for:

The Hydrological Service, National Energy Authority and
The Faculty of Engineering, University of Iceland

Abstract:

Here an objective methodology for establishing hydrological rating curves based on Bayesian statistics is presented. The Bayesian approach naturally combines the statistical model for the data which incorporates the hydrological model, the data themselves and a priori information which is based on previously collected data and scientific knowledge. Data collected by the Hydrological Service in Iceland at the National Energy Authority are analyzed, using scientific and heuristic methods, establishing a priori knowledge about the required parameters. The combination of data and a priori knowledge results in a posterior distribution which is used to estimate parameters of the rating curve and to predict discharge for a given water level. The Bayesian approach provides a more accurate prediction error for discharge than the current approach based on least squares.

Project manager's signature

Páll Jó...

Reviewed by:

3

Acknowledgements

Snorri Árnason

Faculty of Engineering, University of Iceland
Reykjavík, June 2005.

Abstract

Hydrological rating curves are used to convert water level time series to discharge time series. The least squares method has, until recently, been the standard method used to estimate these hydrological rating curves from data, even though new methods have been experimented with, e.g., neural networks and numerical models. However, the lack of in depth uncertainty estimates causes problems in data processing. Also, it is virtually impossible to incorporate auxiliary information objectively into this method. Furthermore, recent findings suggest that heteroscedasticity is not accounted for [1]. Finally, it has recently been reported by the Chiefs of the Hydrological Institutes of the Nordic countries (CHIN) that the subjectivity of the methodologies used in the member countries, causes uncertainties in the establishment of rating curves, resulting in different rating curve estimates between countries. Therefore, long term discharge averages and maximum values, based on the same data, are surprisingly different [2, pp. 44].

The main focus of this project is to create an objective methodology for establishing hydrological rating curves based on the Bayesian approach. Data collected by the Hydrological Service in Iceland (HS) at the National Energy Authority (NEA) is analyzed, using scientific and heuristic methods, establishing a priori knowledge about the required parameters. These data include all Icelandic rating curve parameters that have as a part of the project been gathered and organized into an Oracle database, functioning as the basis for Bayesian a priori information, as well as a plethora of other data, such as water level and discharge time series and the hydrometric network attributes. When producing discharge predictions, the Bayesian approach is utilized by using all these data from the HS.

The Bayesian approach naturally combines the statistical model for the data which incorporates the hydrological model, that data itself and the a priori information which is based on previously collected data and scientific knowledge. The result of this combination of information and knowledge results in a posterior distribution which is used to estimate parameters and to establish a rating curve as well as all derived data. The Markov chain Monte Carlo (MCMC) approach is used to sample from the posterior distribution.

Further, rating curve results from 8 case studies are compared to a recent report from a Nordic working group, established by CHIN on rating curves [2, pp. 35–44].

Application and standardization of the model is discussed as well as the general effectiveness of the methodology. Finally some issues regarding further research and development are addressed.

This project has a strong support from interested parties, both in Iceland and abroad, as the goal is a common methodology that will benefit all of the participating nations as well as other interested parties in an increased quality of data.

The ISO standardization of the methodology is very important. This means that this new methodology should follow the same principles as previous methods and adhere to ISO standards wherever possible.

Finally, it must be emphasized that the discharge data, the main product of the hydrometric network, benefits from the new and improved methodology. These data series are the foundation of many important and expensive projects including hydroelectric powerplants, bridges and other transportation structures as well as scientific research such as advanced weather models. All improvement of data integrity and quality directly influences decision making and planning in these fields.

Ágrip

Rennslislykill er samband vatnshæðar og rennslis. Hann er notaður til þess að varpa vatnshæðartímaröð yfir í rennslistímaröð. Minnstu kvaðrata aðferðir hafa hingað til verið hin staðlaða aðferð við mat á slíkum rennslislyklum. Þó hafa verið gerðar tilraunir með að nota m.a. tauganet og ýmsar tölulegar aðferðir. Skortur á nákvæmu óvissumati hamlar ítarlegri notkun rennslisgagnanna og vinnslu með þau. Auk þess er nánast ómögulegt að nota jaðargögn sem gögn við notkun allra þessara aðferða. Nýjar rannsóknir [1], gefa til kynna að ekki sé gert ráð fyrir flökti (e. heteroscedasticity) í staðlaða líkaninu. Loks hefur CHIN (Chiefs of the Hydrological Institutes of the Nordic countries) gefið út að huglægar skekkjur í hinum mismunandi aðferðum meðlimalandanna valdi óvissu í mati á rennslislyklum. Þessi óvissa veldur því að rennslislyklar geti verið mismunandi milli landa og því sé talsverður mismunur í mati landanna á langtíma meðalrennsli og hámarks- og lágmarksrennsli, byggðu á sömu gögnum, [2].

Aðalmarkmið verkefnisins er að skapa hlutlæga aðferðafræði til mats á rennslislyklum með notkun Bayesískrar aðferðafræði. Gögn frá Vatnamælingum Orkustofnunar (VM) um stika líkansins eru greind með ýmsum aðferðum og notuð til þess að meta fyrirfram upplýsingar um stikana. Þessi gögn eru meðal annars stikar allra gildandi rennslislykla hjá VM auk alls kyns annarra gagna, s.s. vatnshæðar- og rennslisgagna sem og upplýsingar um vatnshæðarmælikerfi VM. Öll gögnin eru síðan notuð til skilgreiningar fyrirframdreifinga sem notaðar eru í Bayesísku aðferðafræðinni.

Bayesíska aðferðin sameinar tölfræðilega líkanið fyrir gögnin, gögnin sjálf og fyrirfram upplýsingar sem byggðar eru m.a. á reynslu, vísindalegri þekkingu og jaðargögnum. Niðurstöður aðferðarinnar eru eftirádreifingar sem notaðar eru til þess að meta stikana í rennslislyklinum og afleiddar stærðir. Markov-keðju Monte Carlo-hermun (MCMC) er notuð til þess að safna úr eftirádreifingunni.

Niðurstöður átta tilfella eru borin saman við niðurstöður áðurnefndrar CHIN rannsóknar um rennslislykla.

Notkun og stöðlun ferlisins er einnig rædd sem og heildarkostir og gallar þess. Auk þess eru næstu skref aðferðafræðinnar og framtíðarsýn varðandi hana rædd.

Þetta verkefni nýtur mikils stuðnings hagsmunaaðila, bæði innanlands sem erlendis, þar eð markmiðið er sameiginleg aðferðafræði sem nýtist meðlimum CHIN, viðskiptavinum VM sem og öðrum áhugasömum aðilum um bætt gæði gagna.

ISO stöðlun ferlisins er mjög mikilvæg. Því var leitast við að halda sömu skilyrðum og fyrri aðferðir notast við og nota ISO staðla þar sem því var við komið.

Að lokum verður að leggja áherslu á að rennslisgögnin, afurð vatnshæðarmælikerfisins, njóta bættrar aðferðafræði. Þessi gögn eru grunnur margra mikilvægra og kostnaðarsamra fjárfestinga, s.s. vatnsaflsvirkjana og brúa og annarra samgöngumannvirkja. Einnig má minnast á vísindarannsóknir s.s. langtímaveðurathuganir. Öll aðferðafræði sem eykur gæði og heilindi rennlisgagnanna hefur áhrif á ákvarðanatöku og skipulagningu í þessum geirum.

Contents

List of Figures

List of Tables

Chapter 1

Hydrometric Networks

A short introduction is required to gain insight into this field of study. Most of the information is based on the Icelandic hydrometric network yet it is in principle comparable to the Nordic countries.

1.1   The Water Level Measurement

1.1.1   Background

The water level gauges in the Icelandic hydrometric network can be largely divided into two groups depending on the location. The first group covers 34 stations located in the highlands (400 m or more above sea level). It can be difficult to reach these stations during the wintertime and they are free from ice for only 3-6 months a year. The other group includes the remaining 131 stations which are located under 400 m above sea level. These stations are normally easy to reach all year around. In an attempt to correct for ice jams in the highlands during wintertime, major winter trips are planned to measure the low water discharge, sometimes through ice [4].

At the Hydrological Service in Iceland (HS) several methods have been used for continuous water level (or stage) measurements. Most of them are based on the previous research and experience in the field, i.e., standards, though some have been adapted to the, sometimes, unusual circumstances regarding Icelandic rivers. The oldest and most widespread methods are the stilling well and the gas pressure gauge, neither of which is constructed anymore. In fact the last one of each was built in the mid and late 1980's.

Digital technology and measurement equipment are felt to be the future of hydrological surveying and many such stations have been erected in the last 15 years, often replacing older equipment. In order to maintain the older time series, much has been dedicated to these replacements, the correct placement, calibration and scale. This revolution, however, has taken a toll. Much of the early experimental work failed in the process due to the inferior first generation of digital collectors. Many radical improvements were then made to the design and the construction of the electronic gauging stations, e.g., improved rechargeable batteries with solar cells, new digital collectors and digital pressure sensors and methods of preventing frost from damaging the equipment. Not until these corrective measures were taken and the system redesigned, did the second generation succeed.

1.1.2 Gauging Stations

These are the three most common types of Icelandic gauging stations:

Stilling Well (Analog)

A stilling well is constructed near the stream, with an intake well below the water level, preferably so that it will permit a measurement of stage to be made at all levels, from below the lowest to above the highest anticipated levels [5]. The water level of a well is measured and monitored, as well as the outside water level. The float height mechanically moves a pen upon a roll of paper that is driven by a clock. Very often, the stilling well gauging station was also equipped with a staff gauge.

Purge-Gas Pressure Gauge (Analog/Digital)

A gas pipe continuously lets out gas bubbles beneath the surface of the water and sensitive measuring equipment converts the pressure, needed to drive the gas out, to a mechanical force. This force, in turn, moves a pen upon a roll of paper driven by a clock. It is becoming more common to digitally monitor this pressure and log into computer memory.

Pressure Gauge (Digital)

A digital pressure transducer sensor, placed under water, measures pressure from the above water. This pressure reading is converted into a stage measurement and digitally logged into the memory of the collector.

1.1.3 Construction and Setup

Standard practice has been to place the measuring point, be it a well intake, a pressure gauge or a digital pressure sensor, at a relative height of 100 cm. This is to encompass all levels below it in case the intake is above the water level during draughts. Then, the intake needs to be moved deeper. This is a safety measure and a relocation of the device is rarely needed. At least one fixed reference point (or benchmark) is drilled into a solid mass, preferably lava outcroppings or structures nearby, e.g., bridges. These are then given an arbitrary height and then used for the calibration and monitoring of any changes in the height of the measuring equipment. For all these height measurements, accurate land surveying equipment is used by trained personnel.

1.1.4 Monitoring

Standard practice is to visit the station at least three times a year and perform the following checks and maintenance:

1 Check all peripheral devices and requirements such as; winding the clock, gauge gas pressure, replace ink, pen or paper if required, etc.

2 Calculate (read) and document point measurement of stage, both from paper/collector memory and if applicable, an automatic counter.

3 Measure actual water level, using a fixed reference point and/or land surveying equipment, based on relative heights. These measurements usually incorporate some kind of a stilling equipment, usually a stilling tube designed by the HS staff.

1.1.5 Data Collection and Processing

There are two ways of collecting stage data at the HS. One is to use a mechanical analog measurement equipment to continuously write the water level on paper and the other one is to log the stage electronically into digital memory.

Analog records

The digitizing of analog water level records was originally done with the aid of a digitizing table, but is now done with a scanner and processed by a LabView program. This is based on a Swedish video camera system (SKUR) used before [4]. The digital records are then stored in the HS database and the original data on paper rolls kept in a fireproof storage facility.

Digital records

Digital records are downloaded from the collector memory with a laptop computer or through an automated dial-up system, and stored in the HS database.

The results are a digital water level time series for each gauging station that define the continuous water level curve with acceptable accuracy. These time series are, however, not equally sampled over time and are called primary data. The primary data are converted into discharge using the rating curve (see Section 1.3). These discharge time series are then converted to secondary data, equally spaced in time, usually with daily values. These secondary data, time series with ice jams and other discrepancies corrected, are then published in annual reports. Finally, the equally sampled discharge time series are converted back into water level time series with daily values, again using the rating curve.

1.2 The Discharge Measurement

1.2.1 General

It must be clear that a data set of discharge measurements at different water levels is neither a uniform nor a homogeneous set. Each measurement is subject to many variable factors, environmental and other. Those of the most concern to the rating curve establishment process are discussed, e.g., the measurement method, the type of river runoff being measured and the steadiness of flow during the discharge measurement.

It is also important to observe that Iceland and especially its highlands are a very harsh and inaccessible environment. Measuring discharge is confined by weather conditions and logistics during winter and spring, to short windows of opportunity, leaving summer and fall discharge to be measured more frequently. This may in part, explain the relative lack of high and low discharge measurements in the HS data sets.

Defining the water level for a discharge measurement is an integral part of the measurement process. Usually, the mean of the water level during the measurement, weighted over time, is a

sufficient estimate. The discharge measurement is also given the label *steady*, *rising* or *falling* (see Section 1.2.6), according to the state of flow.

1.2.2 Discharge Measurement Methods

There exist, however, many methods of measuring discharge. The method used in each case depends heavily on local conditions and the current situation. A vast majority of the HS discharge measurements have been collected using a standard propeller measurement equipment. Usually, if the stream is wadable, it is measured on foot and these measurements are often considered to be of the best quality. If the river is too deep or the flow is too strong, a boat is used. Boat measurements are considered to be of a somewhat less quality. The third most popular method and the one considered to be of the lowest quality is the cableway suspended propeller.

The discharge measurement method mainly used is the complete profile method, 4-7 points per profile and a minimum of 18 profiles across the river. All the small rivers are waded with a guideline. Where it is not possible to wade, a boat or a cableway installation is used. There are as many as 34 cableway installations in use, crossing the largest rivers in Iceland. These installations are of Icelandic design, with some input of ideas from Russian hydrometric textbooks [4].

The measurement equipment is in almost all cases a propeller type current meter. In some cases, for example at freezing temperatures or at high levels of bottom vegetation, a magnetic current meter is used. In the Icelandic West- and Eastfjords where rivers are both fast and shallow or during flash floods where it impossible to measure in the usual way, dilution methods have been used to some extent, both dye and chemical (salt).

1.2.3 Types of Runoff in Iceland

The nature of the Icelandic rivers is varied. Based on their origin, they are classified as spring (ground water) fed rivers, direct runoff rivers and as glacially (glacier) fed rivers. Many rivers are mixtures of all these runoff types, for example, both spring fed and glacially fed. A mixed river is categorized by the governing runoff type.

Seasonal snow cover, glaciers and groundwater play a large role in the hydrology of Iceland. The largest contribution to the runoff is by rivers fed directly by rain and snow melt. However, glacial contribution to annual runoff is estimated to be approximately 20% of the total runoff and another 20% of the runoff is estimated to be ground water, some of which is originated from glacial melt. The distribution of precipitation between seasons, and temperature evolution throughout the year, determines how much of the precipitation falls as snow. It, therefore, determines whether a large fraction of the runoff will be snow melt floods in the spring or whether autumn or winter floods will be larger. The summer and fall temperature affects how much glacial melt water will be in the glacial rivers during the summer; the higher the temperature, the more melt water. The different geophysical characteristics of watersheds in Iceland give an extra basis for variability, especially due to large areas of post glacial, highly permeable lava fields. Groundwater storage masks some of the climate variability and glaciers create their own variability of runoff through changes in mass balance, forced by climatic variations [3].

Icelandic rivers are divided into 3 basic categories, spring fed, glacier fed and direct runoff rivers.
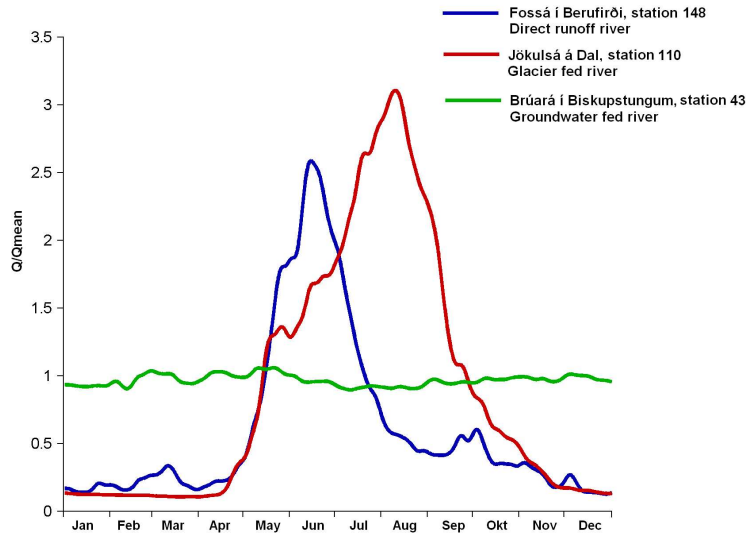
Figure 1.1: These rivers are representative for each of the three types of runoff. This figure shows the daily runoff of each river in m^3/s as a proportion of the mean discharge over one year [3].

1 Spring Fed Rivers A spring fed river has a predictable water level pattern. It consists of a steady unvaried flow throughout the year, affected only by considerable amounts of precipitation, in particular, during the winter when the ground is frozen. Notable annual events are floods at the beginning of snow melt in early spring. The relative change in the flow over the course of one day can be expected to be very low. Spring fed rivers can be found in regions with relatively recent lava fields, as the young rock has the highest permeability.

2 Direct Runoff Rivers A direct runoff river consists of a network of rivers. Its flow is mainly weather dependent, it oscillates over the year depending on precipitation and snow/glacial melt. Notable annual events are spring floods and floods in the late summer/early fall, coinciding with the maximum glacial melt and warm rainy weather. It can be expected to change rapidly and unpredictably over the course of day, representing weather events on the catchment area. For example, during snow melt, a substantial diurnal variation is observed. The direct runoff rivers can be found on the oldest rock on Iceland, i.e., the East- and Westfjords. Direct runoff rivers have also been divided into two categories, direct runoff rivers with lag, where snow and vegetation delay the runoff, and direct runoff types that respond directly to rain.

3 Glacially Fed Rivers Glacial rivers, like the spring fed ones, have a relatively predictable flow pattern. Over the winter, snow and glacial melt is negligible and river flow contains only the spring fed part of the river, as such it follows a similar flow pattern. This flow is often around 1% of the maximum summer discharge. As soon as snow melt begins with the spring the discharge increases steadily until snow melt is over and glacial melt begins.

5

At that time the discharge is dependent on weather events on the glacier catchment area, i.e., temperature, wind and sun. Given steady weather conditions, the diurnal pattern of flow becomes very predictable with a low glacial melt during the night and a high melt during the day.

One very important feature encountered in Icelandic glacial rivers is their extreme sediment transport. Often the riverbed at the control section contains only sand and fine sediment. This means that the control section may be unstable and subject to change.

Shifts have been observed in rating curves for gauging stations in all river types, seemingly because of an unstable control section (see Section 1.3). Sometimes, in glacial rivers, extreme sediment transport is to blame [6]. In spring fed rivers, sand drift is often to blame and following floods in direct runoff rivers, drastic changes in the control section are often observed.

In recent years it has been attempted at the HS to establish if and when the rating curve shifts. These attempts have been relatively successful yet some problems have followed. Some have pointed out the lack of predictive power in these shifted rating curves, as the estimate of the shift is usually based on historical data instead of predictable patterns, such as a rating curve dependant on seasonal events such as the summer growth of river bottom vegetation. Rather, the shift is thought to depend on unpredictable events, natural occurrences, such as floods, earthquakes or such. Shifts can be thus, be loosely divided into two types, predictable and unpredictable.

It has also been put forth that the scatter or variance of the data does not support such accurate analysis. It is, however, evident from the data that it is possible to track the shifts, if the frequency of discharge measurements is high enough. The value of the improved information is not very significant with regard to the long term mean discharge, but it is very important with respect to annual flows as well as to the seasonal flows [6]. Further analysis on shifts in rating curves can be inspected in various reports published by the HS, for example: [7], [8], [9] and [10].

Thesis *It is proposed, that the analysis of rating curve shifts, high frequency or not, needs better estimates of data variance and prediction intervals, in order to judge whether the data is reliable enough for further inspection. If, for example, 19 of 20 discharge measurements fall within the 95% prediction intervals, it should be hard to justify further shift analysis unless, for example, the data set demonstrates some attributes that enable it to be divided into subsets. Then, prediction intervals may be constructed around each of the subsets and decisions made on that basis e.g. the frequency and cause of the shifts between the different rating curves, and the nature, or shift type. This demonstrates, even further, the importance of dependable prediction intervals.*

1.2.4 The Manning Equation

The Manning equation is the most widely used of all uniform-flow formulas for open channel flow computations. It describes steady state flow in an open channel as a function of friction, slope and geometry, e.g., the desired flow for most rating curves. It is relatively precise when flow is steady and the channel is uniform. The formula is an empirical relationship and n can not be deducted from any natural laws of physics.

$$S_f = \frac{n^2 Q^2}{2.21 A^2 R^{(4/3)}}$$

6

where

- S_f is the friction

- A is the

- n is the

- R is the

- Q is the

1.2.5 General Open Flow Equations

The general equations for open channel flow are based on the continuity equation and Newton's second law of conservation of linear momentum. Mathematical models for various simplified and approximate special cases have been developed and applied to engineering problems (Chow, 1959; Henderson, 1966). More rigorous derivations were done, by Strelkoff (1970) and Chen and Chow (1971). In both cases, the one dimensional incompressible open channel flow equations were derived by the integration of the point form of the continuity equation and the Navier-Stokes equation. In a series of paper, Yen (1973, 1975) derived the equations describing an unsteady, spatially varied, turbulent, free surface flow of a viscous nonhomogeneous fluid in a channel of arbitrary cross-sectional and alignment geometry with an erodible boundary. This was done rigorously by integrating the point form of continuity, momentum and energy equations over a cross-sectional area of the channel [11].

For an incompressible fluid, the integrated equation of continuity is, (Yen, 1973)

$$\frac{\partial A}{\partial t} + \frac{\partial Q}{\partial x} = \int_{\sigma} \widehat{q} d\sigma$$

in which

- A is the active cross-sectional area of flow

- Q is the discharge through A

- σ is the perimeter bounding A

- x is the lateral distance

- t is the time

- $\widehat{q}$ is the time of lateral flow per unit length of σ, having dimension of length/time, and being positive for lateral inflow and negative for outflow.

7

The one-dimensional momentum equation integrated over the area, A, for a gravity oriented coordinate system with depth, Y, measured vertically is, (Yen, 1975) [11],

$$\frac{1}{gA} + \frac{\partial Q}{\partial t} + \frac{1}{gA}\frac{\partial}{\partial x}(\frac{\beta}{A}Q^2) + \frac{\partial}{\partial x}(kY) + (k - k')\frac{Y}{A}\frac{\partial A}{\partial x} \qquad (1.1)$$

$$= S_0 - S_f + \frac{1}{\gamma A}\frac{\partial T}{\partial x} + \frac{1}{gA}\int_\sigma \widehat{q}u_x d\sigma$$

in which

- g is the gravitational acceleration

- S_0 is the channel slope $= \tan(\theta)$ for gravity oriented coordinates, where θ is the angle between the channel bottom and a horizontal plane

- S_f is the friction slope, evaluated from the Manning equation for uniform steady flow

- γ is the specific weight of the fluid

- u_x is the x-component velocity of the lateral flow joining the channel flow

- k and k' are pressure distribution correction factors

- β is the momentum flux correction factor

- T represents the force acting normal on A due to internal stresses.

- t is the time

This equation can be simplified, based on the Saint-Venant equations (Fread, 1977) [12], the continuity equation:

$$\frac{\partial(A + A_0)}{\partial t} + \frac{\partial Q}{\partial x} = q$$

and a conservation of momentum equation

$$\frac{\partial Q}{\partial t} + \frac{\partial(\frac{Q^2}{A})}{\partial x} + gA(\frac{\partial h}{\partial x} + S_f + S_e) = 0 \qquad (1.2)$$

where

- h is the water surface elevation,

- A is the active cross-sectional area of flow

- A_0 is the inactive (off-channel storage) cross-sectional area

- x is the longitudinal distance along the channel (valley)

- q is the lateral inflow or outflow per linear distance along the channel (inflow is positive and outflow is negative in sign)

- S_e is the expansion-contraction slope

8

1.2.6 Conditions of Flow

When measuring discharge for a stage-discharge relationship it is important to know which of two possible cases is being studied. The general case of developing a steady relationship between stage and discharge is one and the other is studying the hysteresis effect sometimes found in the discharge measurement data sets. This hysteresis is a phenomenon that is sometimes observable when measurements are made at unsteady water levels. It can be shown that discharge measurements done at rising water levels can be expected to give more discharge. Sometimes, though more seldom, falling water levels during a discharge measurement result in less discharge. When measuring Icelandic rivers, this behavior is important to understand, as most of them have a very varying diurnal flow.

The hysteresis is hard to identify and quantify and is one of the main reasons why it is necessary to establish prediction intervals for measurements. Without these intervals, it is very hard to distinguish the hysteresis from regular or normal noise in the data set.

The practical conditions of a steady water level are not universally accepted even though they have been derived mathematically. Usually water level peaks are considered to be steady and of course spring fed rivers have a stable water level almost all of the time. The hysteresis effect is, therefore, practically unknown in discharge measurement data sets made in these rivers. In fact, for each flood a unique hysteresis will be formed.

The steady state rating curve is usually preferred for its wider utility. The flow reaches a steady state when the differential factors in (1.1) and (1.2) are equal or close to zero. This is also the time interval when the Manning equation is in effect and valid.

The reason for more discharge during an increase in water level than during the decrease is described with complicated differential equations. During an increase in the water level one of these differential factors is dominant, as the increase in water level happens faster than the following decrease. During the decrease in water level, the magnitude of the dominant differential factor is less than in the case of the increase. This can be compared to a large wave that crashes violently onto a beach and then dissipates slowly back into the ocean.

1.3 The Rating Curve

1.3.1 General

The control of flow in an open channel is the establishment of a definitive stage-discharge relationship. When control of flow is achieved at a certain section of the channel, this section is a control section [13].

To develop a reliable stage-discharge rating curve with dependable predictability power, two things are needed. A water level time series gauged at the control section and point discharge measurements of the flow through that control section.

In Figure 1.2 an obvious pattern can be seen in the data set. A line through these points is called a rating curve and establishes the connection between water level and discharge, thus enabling the conversion of water level time series into discharge time series.

The usually accepted form of a rating curve is known as the equation $Q = a(w - c)^b$. This equation is derived from equations regarding free flow in open channels. The variables are

- Q is the calculated discharge, usually in m^3/s.
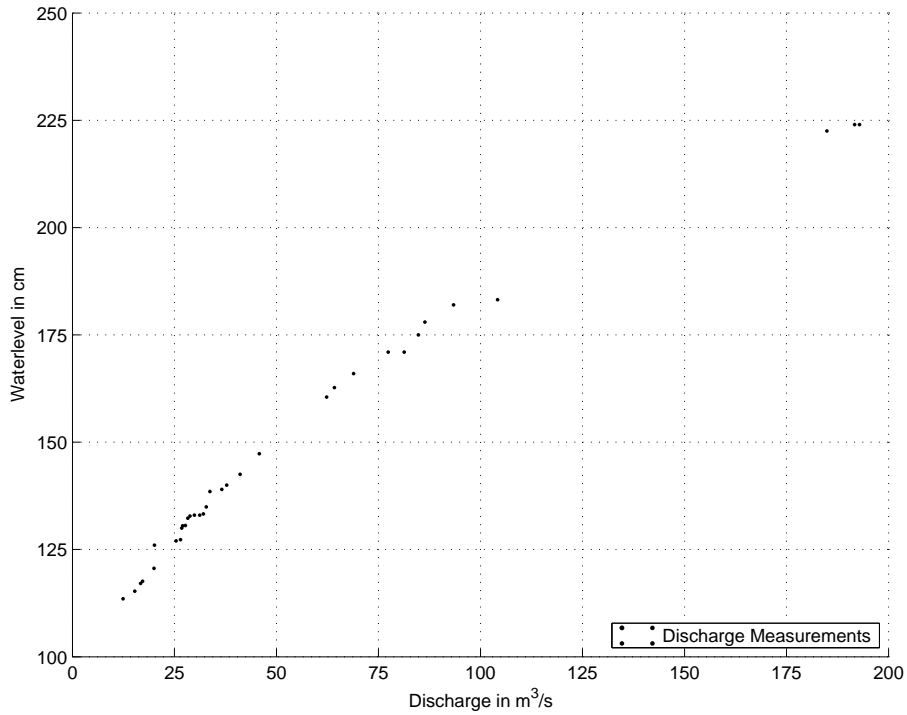
Figure 1.2: Discharge measurements from the Icelandic river Fnjóská as a function of water level.

- W is the water level, usually in cm or m.

- a is a quantifying constant, describing friction and to some extent, the form of the control section. It depends on the acceleration of gravity and the measuring units used. It has no unit.

- b is a positive constant, contributing information about the shape of the control section and the river channel. It has no unit.

- c is the relative height of the channel bottom, usually in cm or m.

1.3.2 The Rating Curve Parameters

- $W_{\min}$ is the lowest observed water level at the survey station, usually in cm or m.

- $W_{\max}$ is the highest observed water level at the survey station, usually in cm or m

- W_{Q_n} is the data set of all discharge measurements with their relative water levels at the survey station, usually in cm or m versus m^3/s

- $W_{Q_{\min}}$ is the water level of the lowest discharge measurement at the survey station, usually in cm or m.

- $W_{Q_{\max}}$ is the water level of the highest discharge measurement at the survey station, usually in cm or m.

10

- $Q_{\max}$ is the highest measured discharge at the survey station, usually in m^3/s

- $Q_{W_{\max}}$ is the estimated discharge at the highest observed water level, according to the official rating curve, usually in m^3/s.

- a is a positive constant that has a negative correlation with parameter b, if b increases, a must decrease to preserve scale.

- b is a positive constant, contributing information about the shape of the river channel and control section. Natural channel sections are in general very irregular, usually varying from an approximate parabola to an approximate trapezoid. For streams subject to frequent floods, the channel may consist of a main channel section carrying normal discharges and one or more side channel sections for accommodating overflows [13]. Using the geometric elements of the control section and Newtonian physics, it can easily be derived that a $\vee$ shaped control section in a free fall has a b value of 2.5 and a $\sqcup$ shaped control section in a free fall has a b value of 1.5. Channel cross sections are thus, estimated to have some permutation of those two values, given of course, some leniency to both values. This dictates that the expected value of b is larger than 0 and less than 5. One reason for limiting b at 5 is that it has the potential of yielding unrealistically high discharge when the rating curve has a low α value (see Section 1.4) and b is large, i.e., when extrapolating the curve way beyond $W_{Q_{\max}}$.

- c is an estimate of the channel´s bottom, relative to the water level, i.e., the bottom of the $\vee$ and $\sqcup$ shape, defined as the water level point of zero discharge. Sometimes it can be measured with land surveying equipment or estimated during draughts and these estimates usually assist in calculating the rating curve. As c is a physical constant, relative to the arbitrary constant of 100 cm (see Section 1.1.3), the value of c is expected to be greater than 100 cm and hopefully never less, as that indicates the measuring point has not been placed deep enough to cover all levels of stage. The actual value of 100 cm is a safety measure to avoid that c will take a negative value, in case, the depth sensor needs to be extended deeper under the water surface.

1.4   Rating Curve Quality

1.4.1   Estimates of Data Coverage

$W_{\max}$ and $W_{\min}$ (see Section 1.3.2) of the time series are expected to change with time, fast for perhaps the first ten years of gauging, providing statistical coverage of annual floods and draughts. Later, the changes happen in jumps that coincide with so called statistical events such as 10, 20 or 50 year events, i.e., floods or draughts that are expected to happen, on the average, once every 10, 20 or 50 years. It is seldom possible to measure the discharge during the peak event, therefore, some extrapolation of the rating curve is expected, from the lowest $W_{Q_{\min}}$ down to $W_{\min}$ and from $W_{Q_{\max}}$ up to $W_{\max}$. This means that one expects better discharge data generated through rating curves with higher values of $\alpha = W_{Q_{\max}}/W_{\max}$ and $\beta = W_{\min}/W_{Q_{\min}}$ (α and β are not the same parameters discussed in Section 1.2.5). This, however, is not always the case, if the following is considered. A well defined rating curve has α and β equal to 90%. A singular event, e.g., a spring flash flood which lasts for one day, raises $W_{\max}$ to a higher level,

thus reducing α to say 80%. While the peak discharge of that single day needs to be calculated using an extrapolated rating curve, that is only a fraction of the cumulative discharge of the day. When compared to the cumulative water level curve for the whole time series the effect is negligible.

It is, therefore, proposed that

$$\gamma = \frac{\int_0^T W(t_{\mathrm{lim}})dt}{\int_0^T W(t_{tot})dt}$$

where

$$W(t_{\mathrm{lim}}) \in [W_{Q_{\mathrm{min}}}, W_{Q_{\mathrm{max}}}]$$

and

$$W(t_{tot}) \in [W_{\mathrm{min}}, W_{\mathrm{max}}]$$

is a better predictor of rating curve quality. It is important to note that for this to become a standard procedure, the water level time series must be equally sampled, for the purpose of comparison. In that case, it is easier to work with sums than integrals.

As an example of the procedure, the water level time series for three Icelandic gauging stations are shown in red, in Figure 1.3. For each station, the whole water level time series is sorted in decreasing order. In order to standardize the series, it is divided by its respective W_{max}. The respective $W_{Q_{\mathrm{max}}}$ and $W_{Q_{\mathrm{min}}}$ of each series are shown in blue. The aforementioned α, β and γ values can be estimated roughly from the figures. The exact values are, however, shown in Table 1.1. The α value can be read off the y-axis, e.g the upper blue line. The β value is the ratio of the lower blue line to the bottom of the graph. The γ value is the area between the blue lines, i.e., the water levels of the rating curve, supported by discharge measurements, divided by the total area. All three values are needed to gain perspective of the rating curve quality. Figure 1.3 and Table 1.1 enable some deductions to be made about the gauging stations.

Table 1.1: A compilation of the rating curve quality parameters for the Icelandic gauging stations no. 268, no. 150 and no. 411.

Gauging station	α	β	γ
268	0.3810	0.2678	0.6266
150	0.5241	1	0.9664
411	0.0282	0.4241	0.1741

Station no. 268 is in a spring fed river, located in a remote place deep in Iceland's highland. The river is monitored for the energy sector, hence, gathering reliable information about the total discharge is the main objective. The lack of both high and low discharge measurements is apparent and explained by difficult logistics. It can be deduced that an effort must be made to increase the γ and lower the β value. This effort might be a winter expedition to measure low discharge.

Station no. 150 is in a direct runoff river, crossed by Iceland's main highway. This optimal location, among other things, has enabled the HS to make a variety of discharge measurements, especially low discharge, explaining the high β value. In addition, the time series is a relatively
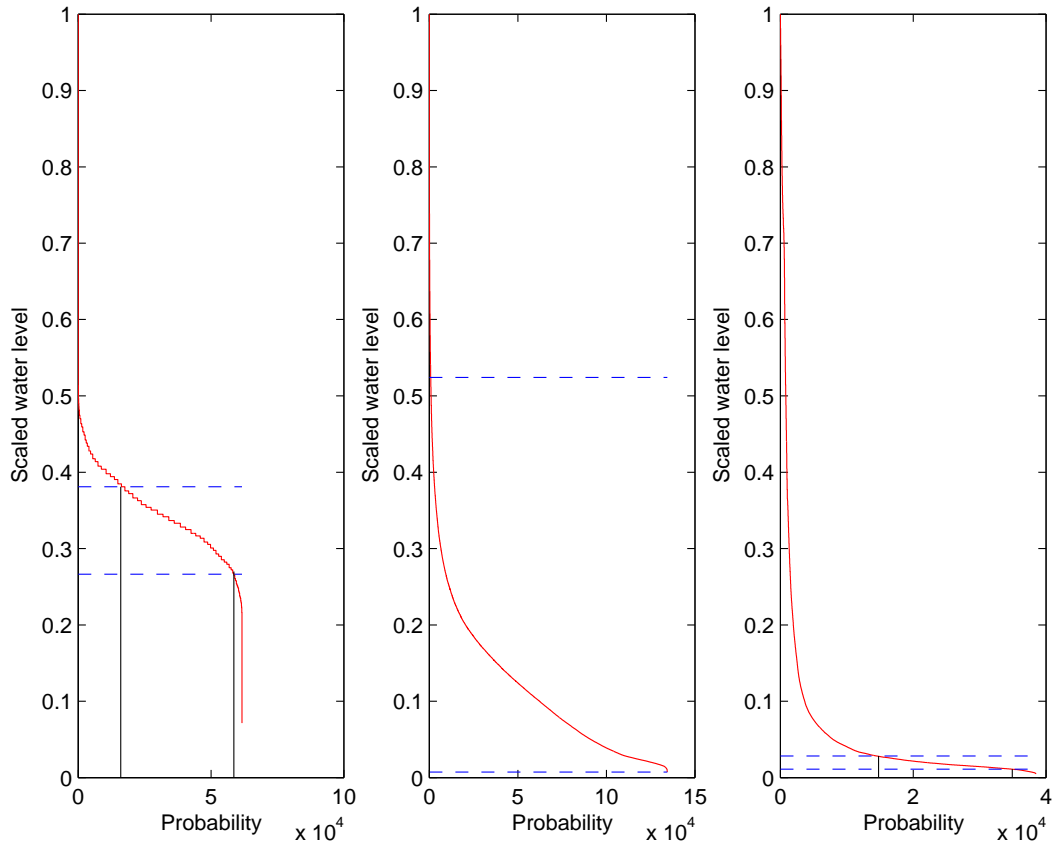
Figure 1.3: **Left to right:** Examples of rating curve quality diagrams for the Icelandic gauging stations no. 268, no. 150 and no. 411.

long one so the river's behavior is known to some certainty. As the river is crossed by Iceland's main highway, the Icelandic Public Roads Administration might be interested in the peak discharge for designs of a new bridge. This means that in this case, the high γ and β values are of no interest, and only the α value matters. Here, an effort to increase the α value must be made. This can be achieved by monitoring weather, precipitation and temperature, for the possibility of high discharge events. Sometimes, however, local conditions do not allow higher discharge measurements to be made.

Station no. 411 is similar to station no. 268. It is a spring fed river, monitored for the energy sector. The desired information is, therefore, total discharge. This river is located in a canyon that can be reached most of the year with motorized transport. Here, difficult logistics do not explain the abysmally low α, β and γ values, but rather, the natural surroundings. The river is in a deep canyon, and impossible to measure with a boat. The range of discharge measurements is, therefore, confined to waded measurements. To rectify this situation, the HS must construct a cable way or experiment with other measurement methods to increase α and γ values. Steps must also be taken to measure low discharge during the winter.

Thesis *From these stations, it is apparent, that the proposed rating curve quality parameters can be used to identify problematic rating curves, to prioritize scheduled discharge measurements and aid in the decision making process, based on individual needs or desired information. The α and β are a measure of how well the rating curve handles extreme values, floods and droughts. This is important for the design and construction of various structures. The γ value is a*

measure how well the total discharge is defined by the rating curve. This is important to get a better estimate of the water resource, e.g., for water supply or power production.

1.4.2 Estimates of Data Scatter

Another predictor of quality is the number and variance of discharge measurements at different water levels, $W_{Q_i}, i = 1, ..., n$. The scatter of W_{Q_n} is often a problem in rating curve estimation. The problem is to quantify the coverage of the data set over the measured span of W. In context to the problem above, all the parameters, α, β and γ will be very high, with only one very high measurement and one very low, in an extreme case. This is usually not the case, although, there will often be holes in the W-Q pattern and/or clustering of data points. To address this problem, two estimators of data integrity are introduced, each quantified with high/low number of measurements: unified or clustered. Most cases will fall into one of these four categories, (see Figure 1.4).
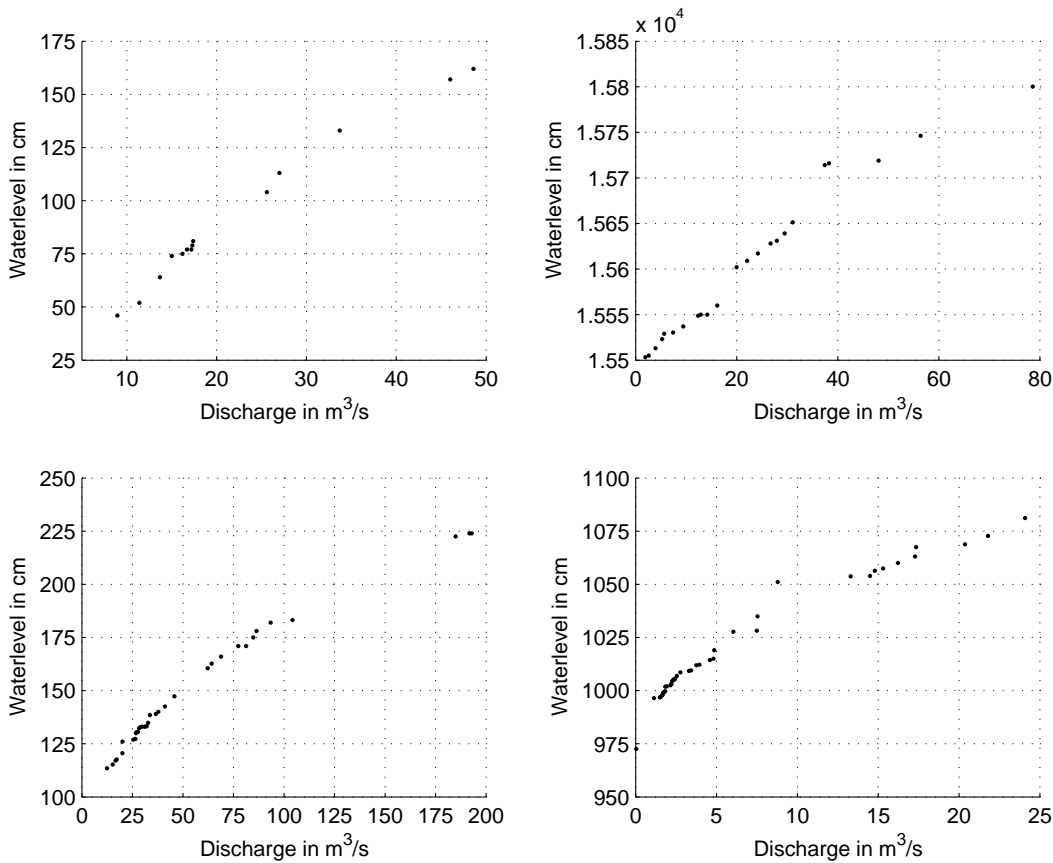
Figure 1.4: A sample of various clustering behavior in discharge measurement data.

First, to identify clusters, sophisticated cluster analysis can be used or simple heuristic methods. One such might be to identify gaps which are larger than the average gap of the data set. If $\delta W = (W_{Q_{\max}} - W_{Q_{\min}})/n$ is less than, for example, $C(W_{i+1} - W_i)$ for some $i = 1, ..., n - 1$ assuming, that the data set is sorted in increasing order and that n is at least greater than 2. A suitable constant C, may then be chosen, for example, $C = 1.5$. Those gaps larger than δW are then identified. It must be emphasized that only distances *within* the data set are used and

14

not from the distance (gap) between $W_{Q_{\max}}, (W_{Q_{\min}})$ and $W_{\max}, (W_{\min})$, as that factor is already incorporated into parameters α, β and γ. As the problem is to easily classify rating curves, it may be of use to introduce as a parameter, the identified gaps as a fraction of measurement span,

$$\frac{1}{\delta W} \sum_{j \in A} (W_{j+1} - W_j)$$

where

$$A = \{j \in \{1, 2, ..., n-1\} | C(W_{j+1} - W_j) > \delta W\} \subseteq \{1, 2, ..., n-1\}.$$

Thesis *To accurately plan discharge measurements, some measure of rating curve quality is needed. It is not possible to improve rating curve quality if there is no basis for comparison. Two methods are proposed and can either be used separately or in unison as they are not estimators of the same variability. These methods provide an opportunity to define future goals concerning rating curve quality and have the potential to become very useful for organizing and planning of field work.*

Chapter 2

The Bayesian Approach

Estimating the parameters of the hydrological rating curve using the Bayesian approach is in many ways feasible and easily justified. The Bayesian approach allows the incorporation of prior information in a natural way, that is, any available scientific knowledge can be utilized, whether it is based on theoretical knowledge, experience or auxiliary data, while the classical or frequentist approach does not.

For the purpose of obtaining prior information about the parameters in the rating curves that are established in this thesis, data from the Hydrological Service in Iceland are utilized. This is the subject of Chapter 3. In this chapter an introduction to the Bayesian approach is given along with computational techniques for numerical evaluations. Statistical models for discharge measurements and water levels are given and it is described how the Bayesian approach can be applied to the model that will be selected for data analysis in Chapter 4. By applying the Bayesian approach to rating curves, the main objective of this thesis is accomplished, that is, improving the rating curve error estimates. Due to this fact and other advantages of the Bayesian approach, it will be proposed as the common methodology for analysis of rating curve data.

2.1   Previous Publishings

The use of Bayesian methods for fitting rating curves, is described in a very recent paper (2005) by Moyeed and Clarke [14]. In that paper, the importance of rating curves in virtually all hydrological procedures concerned with flow in rivers is discussed, including rainfall runoff models, stochastic modeling of discharge time series, flood flow estimation of flows with T-year return periods and analysis of time series in regard to climate change.

By successfully constructing rating curves for 7 watersheds, the authors maintain that Bayesian methods enable credible regions to be estimated for discharges and quantities derived from them. They also claim that prior information about the nature of the rating curve can be included into the method, and that the Bayesian approach can be extended to allow for uncertainty in the stage measurements.

All of these findings are further established in this thesis. However, some of the key differences between *the paper* by Moyeed and Clarke and *this thesis* are outlined in the following.

- In this thesis the prior parameter distributions are studied carefully and estimated through in depth analysis of historical data while Moyeed and Clarke use uninformative prior distributions (except for b).

- Due to the lack of a thoroughly established estimated prior distribution in the paper, no comparisons between the prior and the posterior distributions are made as is done in this thesis.

- In this thesis, rating curve or data quality parameters are introduced and compared to the estimated posterior distributions, providing an interesting relationship to be studied.

- To reduce correlation between the estimators for the parameters a and b, the original model of $Q = a(w - c)^b$, is reparameterized in this thesis. A possible new interpretation of the parameter a results from this reparameterization.

- To account for heteroscedasticity in the data, the most current statistical model for discharge measurements is used in this thesis, i.e., the heteroscedastic model introduced by Øverleir [1].

- Residual analysis, which would likely shed light on the shortcomings of the original model, is not performed in the paper. All of the models in this thesis are subject to rigorous residual analysis, as well as comparative scrutiny.

- Moyeed and Clarke make no attempt to compare the Bayesian results to the results of the current methodology. In this thesis, maximum and minimum discharge, as well as annual mean discharge, and corresponding credible regions, are compared to the results of a working group of rating curve experts working with the same data.

2.2 An Introduction to Bayesian Statistics

2.2.1 The Elements of Bayesian Statistics

Bayesian statistics lay on the foundations of probability theory. All unknown parameters are treated as if they were random variables. The Bayesian approach requires a fully specified prior distribution for these unknown parameters, and a fully specified statistical model describing the observed data. The prior knowledge and the observed data are sources of information that the Bayesian approach naturally combines in a probabilistic framework. Its advantage is that all uncertainty can be taken into account, allowing for an accurate inference about the unknown parameters. It can be considered a disadvantage that all probability distributions need to be fully specified.

The prior distribution of the unknown parameters is formed based on historic data and on scientific and expert knowledge. The prior distribution can be difficult to obtain and extensive work may be necessary to achieve a satisfactory prior distribution.

The mathematical presentation of the Bayesian approach is a follows. Let X denote a random vector that represent the data whose distribution depends on the unknown parameter vector θ. The distribution of X given θ is denoted by $f(x|\theta)$ and is called the likelihood function. The prior information about θ is quantified probabilistically in the prior distribution of θ which is denoted by $\pi(\theta)$.

The joint distribution of X and θ is given by

$$\pi(x, \theta) = f(x|\theta)\pi(\theta).$$

Given that the observed data take the value x, the prior distribution of θ can be updated with respect to the data using Bayes Theorem [15], resulting in the conditional distribution of θ given $X = x$,

$$\pi(\theta|x) = \frac{f(x|\theta)\pi(\theta)}{\int f(x|\theta)\pi(\theta)d\theta} \propto f(x|\theta)\pi(\theta),$$

which is called the posterior distribution of θ. All inference about θ is based on its posterior distribution.

2.2.2 Markov Chain Monte Carlo based on the Gibbs Sampler and the Metropolis–Hastings Algorithm

In most cases analytical results cannot be used to do inference on θ, one reason being that the posterior distribution of θ is only known up to a constant, that is, the constant $\int f(x|\theta)\pi(\theta)d\theta$ is not known. In the Bayesian approach, the likelihood function $f(x|\theta)$ and the prior $\pi(\theta)$ are known and the fact that $\pi(\theta|x) \propto f(x|\theta)\pi(\theta)$ can be utilized to obtain samples from $\pi(\theta|x)$.

One of the algorithm for posterior sampling is called the Gibbs sampler, also called alternating conditional sampling, see [16] and [17] for a general discussion on the Gibbs sampler. Assume that the vector θ has been divided into K subvectors, $\theta = (\theta_1^T, \ldots, \theta_K^T)^T$. In each iteration t, a sample of each subvector is obtained by sampling from the distribution of the subvector θ_j, conditioned on the latest value of the other subvectors. Let

$$\pi(\theta_j|\theta_{-j}^{t-1}, x)$$

be the conditional distribution of θ_j given the data and the other subvectors at their current value, denoted by θ_{-j}^{t-1}, where

$$\theta_{-j}^{t-1} = (\theta_1^t, \ldots, \theta_{j-1}^t, \theta_{j+1}^{t-1}, \ldots, \theta_K^{t-1})^T.$$

The Gibbs sampler is then formed by selecting initial values for θ, $t = 0$, and then by sampling from the K conditional distribution for each $t = 1, \ldots, B$, where B is the total number of iterations. The Gibbs sampler is given by

$$\begin{aligned}
\theta_1^t &\sim \pi(\theta_1^t|\theta_{-1}^{t-1}, x) \\
\theta_2^t &\sim \pi(\theta_2^t|\theta_{-2}^{t-1}, x) \\
&\vdots \\
\theta_K^t &\sim \pi(\theta_K^t|\theta_{-K}^{t-1}, x).
\end{aligned}$$

Each of the distributions in the above Gibbs sampler can either be identified as a known distribution which can be simulated directly from or their functional form is known up to a constant as the posterior. In the latter case the Metropolis–Hastings algorithm can be applied to obtain samples from the given conditional distribution.

The Metropolis–Hastings algorithm proceeds as follows for the j-th subvector of parameters, θ_j, in the t-th iteration.

19

1. Sample a proposal θ_j^* from a proposal distribution $q_t(\theta_j^*|\theta_j^{t-1})$.

2. Calculate the ratio of the densities

$$r = \frac{\pi(\theta_j^*|\theta_{-j}^{t-1}, x) q_t(\theta_j^{t-1}|\theta_j^*)}{\pi(\theta_j^{t-1}|\theta_{-j}^{t-1}, x) q_t(\theta_j^*|\theta^{t-1})}.$$

3. Set $\theta_j^t = \theta_j^*$ with probability $\min(r, 1)$, otherwise set $\theta_j^t = \theta_j^{t-1}$.

In most cases it is easier to work with r on the logarithmic scale in terms of numerical computation and for analytical results. The logarithm of r is:

$$\log(r) = \log\{\pi(\theta_j^*|\theta_{-j}^{t-1}, x)\} - \log\{\pi(\theta_j^{t-1}|\theta_{-j}^{t-1}, x)\} + \log\{q_t(\theta_j^{t-1}|\theta_j^*)\} - \log\{q_t(\theta_j^*|\theta^{t-1})\}.$$

The Metropolis–Hastings step is an adaptation of a random walk that uses an acceptance/rejection rule to converge to the specified target distribution. According to [16], this acceptance ratio is recommended to be around 40% to ensure proper convergence. This acceptance ratio is *tuned* by changing the variance of the proposal distributions.

2.2.3   Parameter Estimates

The most commonly used Bayesian point estimates of a parameter vector θ are the mean of $\pi(\theta|x)$ (posterior mean) and the median of the marginal distribution of each element of θ (posterior median). However, before any estimates can be made, properties of the generated Markov chains need to be inspected.

It is suggested by [17] and [16] to run a few (3 to 5) parallel chains. The mixing of the chains is an indicator of how well the chains represent the posterior distribution. The mixing can be measured with the Gelman and Rubin statistic [18], $\widehat{R}$. If the value of $\widehat{R}$ is near 1 (below 1.1) for the chains, they are considered satisfactory, and it is said that the chains have converged and represent a sample from $\pi(\theta|x)$. If the value of $\widehat{R}$ is greater than 1.1 for some parameters then it is suggested to run the chains further. This evaluation should be based on visual inspection as well.

If the Markov chains are considered satisfactory, the autocorrelation of the series is checked. Slow convergence and strong autocorrelation implies that the parameters are still dependent and/or that the simulation is not efficient enough.

If these criteria are fulfilled, inference about the posterior distribution can be made by collecting and treating the latter part of the simulated chains as identically distributed samples from the target distribution. The first part of the chains is not used since a burn-in period is always needed, see [16] for evaluation of the burn-in period. And finally, point estimates of the parameters can be computed from the simulated posterior samples, using either the sample mean or median. In this paper the posterior mean has been chosen as the preferred point estimate.

2.3   Statistical Rating Curve Models

The most commonly used statistical model describing the relationship between discharge measurements and water level measurements is given by

$$Q_i = a(w_i - c)^b + E(Q_i)\epsilon_i, \quad \epsilon_i \sim N(0, \sigma^2), \quad i = 1, \ldots, n, \tag{2.1}$$

(e.g. [1], [14], [19] and [20]) where Q_i and w_i are the i-th discharge and water level measurements, respectively, out of a total of n measurements, a, b and c are as in Section 1.3. The parameter σ^2 is a scale parameter for the mutually independent errors, ϵ_i, $i = 1, \ldots, n$. This model assumes no measurement errors in the water level. The mean and variance of the discharge under the model in (2.1) are

$$E(Q_i) = a(w_i - c)^b, \qquad Var(Q_i) = \sigma^2 E^2(Q_i) = \sigma^2 a^2 (w_i - c)^{2b}, \quad i = 1, \ldots, n.$$

A functional relationship between Q and w different from $Q = a(w - c)^b$ has been applied by Gawne and Simonovic, [21], but they proposed the Box-Cox transformation to discharge, resulting in

$$\frac{Q^\phi - 1}{\phi} = \beta_0 + \beta_1 w$$

when the parameter $\phi \neq 0$ and $\ln(Q) = \beta_0 + \beta_1 w$ otherwise.

The model in (2.1) was extended by Øverleir [1], by introducing a more flexible model for the variance of Q, namely, a model of the form

$$Q_i = a(w_i - c)^b + E^\psi(Q_i)\epsilon_i, \quad \epsilon_i \sim N(0, \eta^2), \quad i = 1, \ldots, n. \tag{2.2}$$

The mean and variance of the discharge under the model in (2.2) are

$$E(Q_i) = a(w_i - c)^b, \qquad Var(Q_i) = \eta^2 E^{2\psi}(Q_i) = \eta^2 a^2 (w_i - c)^{2b\psi}, \quad i = 1, \ldots, n.$$

The effect of the parameter ψ is such that if $\psi = 1$ then the model in (2.2) is the same as the model in (2.1), while if ψ approaches zeros, the variance of Q approaches a constant. Values of ψ larger than one, imply larger variance for Q for large w relative to smaller values of w.

Due to dependence between estimators for the parameters a and b induced by the likelihood function (see Chapter 3), we propose a reparameterization of a of the form

$$a = \exp(\alpha_0 + \alpha_1 b + \epsilon),$$

introducing the parameter ϵ instead of a. The parameters α_0 and α_1 are constants. Their values are found in Chapter 3. Further, by reparameterizing with the parameter τ^2 instead of η^2 where

$$\tau^2 = \eta^2 a^{2\psi},$$

the model in (2.2) can be rewritten as

$$Q_i = \exp(\alpha_0 + \alpha_1 b + \epsilon)(w_i - c)^b + (w_i - c)^{b\psi}\epsilon_i, \quad \epsilon_i \sim N(0, \tau^2), \quad i = 1, \ldots, n. \tag{2.3}$$

The mean and variance of the discharge under the model in (2.3) are given by

$$E(Q_i) = \exp(\alpha_0 + \alpha_1 b + \epsilon)(w_i - c)^b, \qquad Var(Q_i) = \tau^2 (w_i - c)^{2b\psi}, \quad i = 1, \ldots, n.$$

The statistical model in (2.3) will be used to analyze the data described in Chapter 4.

21

2.3.1 Posterior Inference through Markov Chain Monte Carlo (MCMC)

Here the posterior distribution of $(\epsilon, b, c, \psi, \tau^2)$ in (2.3) is derived and the corresponding Gibbs sampler is given. Let q_i denote the i-th observed discharge. Further, let $q = (q_1, \ldots, q_n)^T$ and $w = (w_1, \ldots, w_n)^T$. Then the model in (2.3) provides a likelihood function given by

$$f(q|\epsilon, b, c, \psi, \tau^2, w) = \prod_{i=1}^{n} \frac{1}{\sqrt{2\pi\tau^2(w_i - c)^{2b\psi}}} \exp\left[-\frac{\{q_i - e^{\alpha_0 + \alpha_1 b + \epsilon}(w_i - c)^b\}^2}{2\tau^2(w_i - c)^{2b\psi}}\right].$$

The prior distribution for the parameter vector $(\epsilon, b, c, \psi, \tau^2)$ is formed by assuming that the five parameters are independent. Let $\pi(\epsilon)$, $\pi(b)$, $\pi(c)$, $\pi(\psi)$ and $\pi(\tau^2)$ denote the independent prior distributions of ϵ, b, c, ψ and τ^2, respectively. The exact form of these prior distributions is given in Chapter 3 and they are utilized in the data analysis in Chapter 4. The posterior distribution of $(\epsilon, b, c, \psi, \tau^2)$ is given by

$$\pi(\epsilon, b, c, \psi, \tau^2 | q, w) \propto f(q|\epsilon, b, c, \psi, \tau^2, w)\pi(\epsilon)\pi(b)\pi(c)\pi(\psi)\pi(\tau^2).$$

To generate a sample from the posterior distribution of $(\epsilon, b, c, \psi, \tau^2)$, the following Gibbs sampler is used to iterate from the following conditional distributions.

$$\begin{aligned}
\pi(\epsilon|b, c, \psi, \tau^2, q, w) &\propto f(q|\epsilon, b, c, \psi, \tau^2, w)\pi(\epsilon) \\
\pi(b|\epsilon, c, \psi, \tau^2, q, w) &\propto f(q|\epsilon, b, c, \psi, \tau^2, w)\pi(b) \\
\pi(c|\epsilon, b, \psi, \tau^2, q, w) &\propto f(q|\epsilon, b, c, \psi, \tau^2, w)\pi(c) \\
\pi(\psi|\epsilon, b, c, \tau^2, q, w) &\propto f(q|\epsilon, b, c, \psi, \tau^2, w)\pi(\psi) \\
\pi(\tau^2|\epsilon, b, c, \psi, q, w) &\propto f(q|\epsilon, b, c, \psi, \tau^2, w)\pi(\tau^2)
\end{aligned}$$

In the above Gibbs sampler Metropolis–Hastings steps were needed for all parameter except for τ^2. The components of the Gibbs sampler as well as the Metropolis–Hastings steps are derived in A.3.

To ensure robustness of the method, the model was extensively tested on generated data with known parameters. Three data sets were generated and then the point estimates were compared to the real parameters. Two of the data sets were chosen to test extreme values and the third was chosen to represent ordinary data.

2.3.2 Prediction Intervals for the Discharge Measurements

Assuming that the data follows the normal model described in (2.3), an estimate of a $100(1-\alpha)\%$ prediction interval for discharge measurements given that the water level is equal to w', is given by

$$\exp(\alpha_0 + \alpha_1\hat{b} + \hat{\epsilon})(w' - \hat{c})^{\hat{b}} \pm z_{\alpha/2}\hat{\tau}(w' - \hat{c})^{\hat{b}\hat{\psi}}$$

where $\hat{\epsilon}$, $\hat{b}$, $\hat{c}$, $\hat{\psi}$ and $\hat{\tau}$ are the posterior means of ϵ, b, c, ψ and τ, respectively, and $z_{\alpha/2}$ is the $100(1 - \alpha/2)\%$ percentile of the standard normal distribution.

2.3.3 Credible Regions for the Rating Curve

To eliminate autocorrelation from the posterior distribution and to decrease program run time, the posterior distribution is sampled once every 100 values. As the generated posterior distribution consists of 5 series of 50.000 values, this results in a subset posterior distribution of 2500 values. An estimated credible region for the rating curve is then created by sampling all the parameters over their whole respective subset posterior distribution. This is done over the whole range of the measured water levels, i.e., from $W_{\min}$ through $W_{\max}$ in 1 cm intervals, generating a distribution of 2500 discharge values for each water level. From those discharge distributions the 2.5%, 25%, 50%, 75% and 97,5% percentiles and a 95% credible regions, are easily estimated.

2.3.4 Credible Regions for the Mean Discharge

A similar approach as in Section 2.3.3 is used to estimate credible regions for the annual mean discharge. A water level time series contains N values, in this case, daily average values for one year, so N equals 365. For each water level value, a discharge value is generated by sampling all the parameters over their respective subset posterior distribution. This, in turn, results in a distribution of 2500 discharge values for each water level. The average for each water level is then calculated and gathered into a distribution of mean discharge values corresponding to the water levels in the time series. A sample mean and percentiles are then calculated from that posterior sample, resulting in a point estimate (the posterior mean) and credible region for the annual mean discharge.

2.3.5 Credible Regions for the Maximum and Minimum Discharge

In case of the annual maximum and minimum discharge a similar approach as in Sections 2.3.3 and 2.3.4 is applied. The maximum (minimum) water level is found within each annual time series and posterior samples of the corresponding discharge are computed. A sample mean and percentiles are then calculated from that posterior sample, resulting in a point estimate (the posterior mean) and credible region for the annual maximum (minimum) discharge.

Chapter 3

The Data and a priori Estimates

The proposed Bayesian model is based on prior information adapted from pure academic studies, experience and standard practice. The model parameters, are the previously discussed, (see Section 1.3.2), a, b and c (see Section 1.3, and the parameters ψ and τ^2 that are introduced in Section 2.3.

For all rating curves, the values of a, b and c, are kept in flat files in the HS database. All data, however, was converted into cm from m before any comparisons began. Only single segment rating curves were considered to keep model complexity under control. The method should, however, be relatively easy to modify in order to deal with more complex rating curves.

In order to use the best data available, only the most recent rating curve estimate for each monitoring station was used. Finally some rating curves were dropped due to data abnormalities. The collection of rating curve estimates given by the vector $(\widehat{a}, \widehat{b}, \widehat{c})$ is shown in histograms and scatter plots in Figure 3.1.

In Figure 3.2 normal probability plots of $\ln(\widehat{a})$, $\widehat{b}$ and $\widehat{c}$ are shown. The estimates for $\ln(\widehat{a})$ appear to be normally distributed while $\widehat{b}$ and $\widehat{c}$ show some deviation from normality, especially in the tails.

3.1 The Prior Distributions

While the data sets may seem rather noninformative, an obvious bell shaped curvature can be seen in all cases. A strong negative correlation between $\ln(a)$ and b is also observed. This can be expected, if b increases, a must decrease in order to keep the same scale. Furthermore, there is little indication of a long tail, typically associated with gamma or log normal distributions.

3.1.1 The Prior Distribution of the Parameter a

The data for the parameter a needs to be transformed with the natural logarithm to obtain a distinct bell shape and normality. The proposed prior distribution for $\ln(a)$ is a normal distribution with mean $\mu_{\ln(a)} = -6.60$ and standard deviation $\sigma_{\ln(a)} = 4.10$. These values are based on the data on $\widehat{a}$ described above, that is,

$$
\begin{aligned}
\pi(\ln(a)) &= \mathbf{N}(\mu_{\ln(a)}, \sigma^2_{\ln(a)}), \\
\mu_{\ln(a)} &= -6.60, \\
\sigma_{\ln(a)} &= 4.10.
\end{aligned}
$$
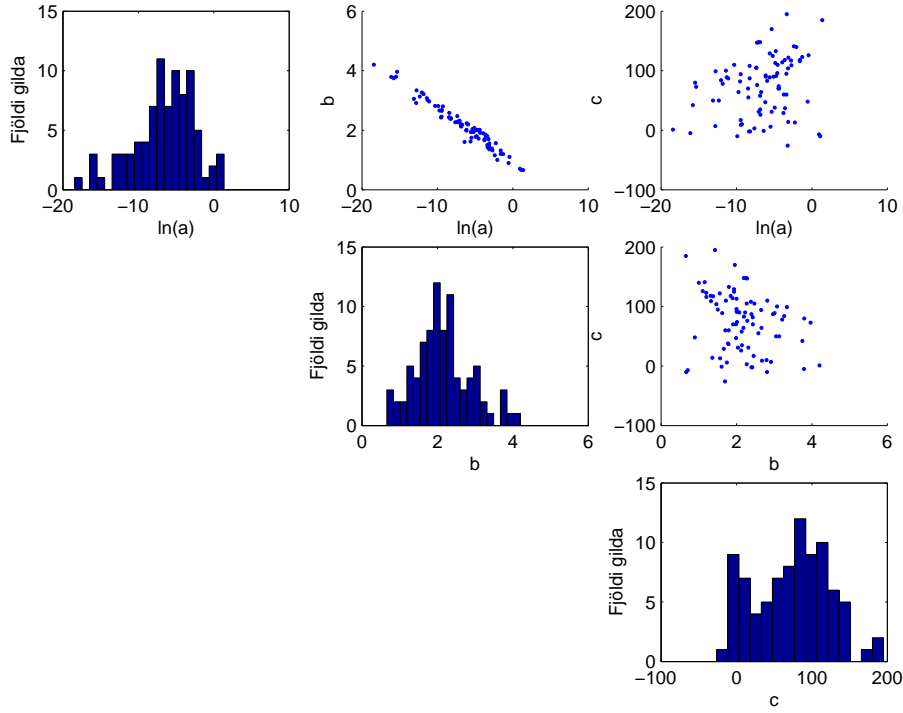
Figure 3.1: The collection of parameter estimates from the HS database. On the diagonal are the histograms of the parameter estimates, for each parameter $\ln(a)$, b and c. The off-diagonal graphs show scatter plots of the parameter estimates, revealing their dependence. It can be seen that the only parameters that are dependent are b and $\ln(a)$, which seem to have a strong linear dependency.

3.1.2   The Prior Distribution of the Parameter b

The data for the parameter b has a sharp top at a value centered around 2 as would be expected based on channel shape arguments, (see Section 1.3.2). The parameter b must be positive and it is known that values above 3 and below 1 occur very rarely. Experience also shows that higher values found in the data, in some cases up to 16, are almost without exception wrong and always unusable for prediction. Large values of b have, therefore, been omitted from the prior distribution by capping it at b value of 5. The values of 0.5 and 5 are chosen so as not to disregard the possibility of b values as small as 0.5 or as large as 5, however unlikely they may be.

Based on the above arguments and data on $\widehat{b}$, the prior distribution for b is proposed to be a normal distribution with the sample mean $\mu_b = 2.15$ and standard deviation $\sigma_b = 0.75$ and with cut-off values are at 0.5 and 5, that is,

$$
\begin{aligned}
\pi(b) &= \mathbf{N}(\mu_b, \sigma_b^2), \ 0.5 < b < 5, \\
\mu_b &= 2.15, \\
\sigma_b &= 0.75.
\end{aligned}
$$
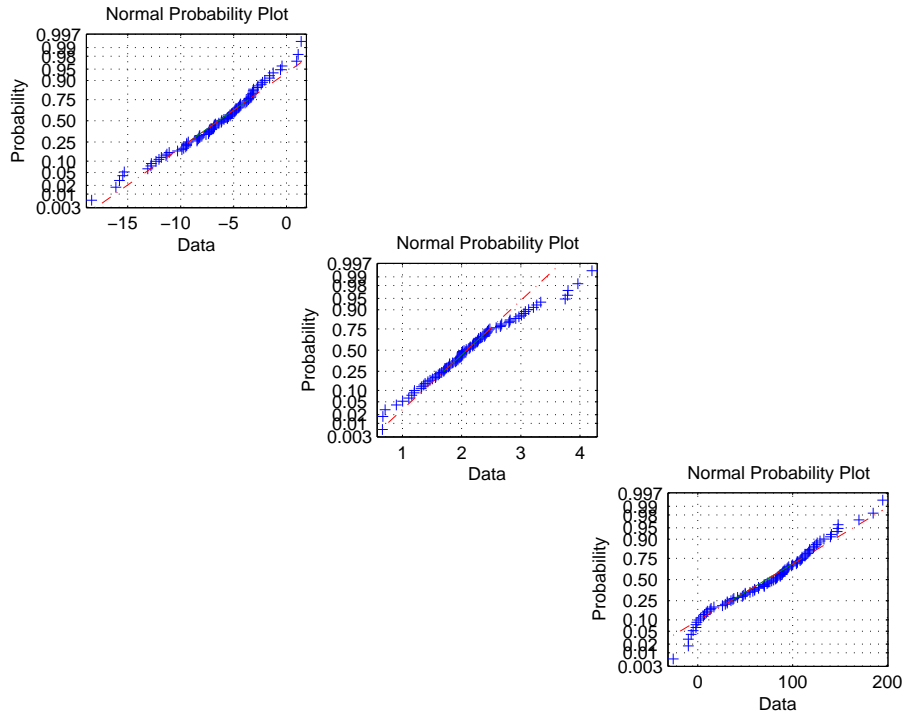
Figure 3.2: Normal probability plots of the data, parameters $\ln(a)$, b and c.
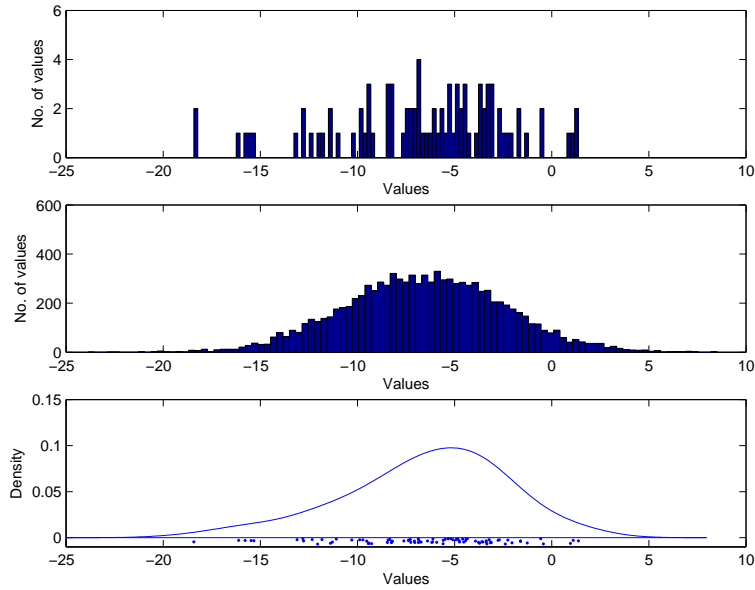
Figure 3.3: **Top**: A histogram of the estimates of a. **Center**: Normally distributed random samples based on the proposed prior distribution of a. **Bottom**: A smooth representation of the Gaussian kernel density of the estimates of a.

27
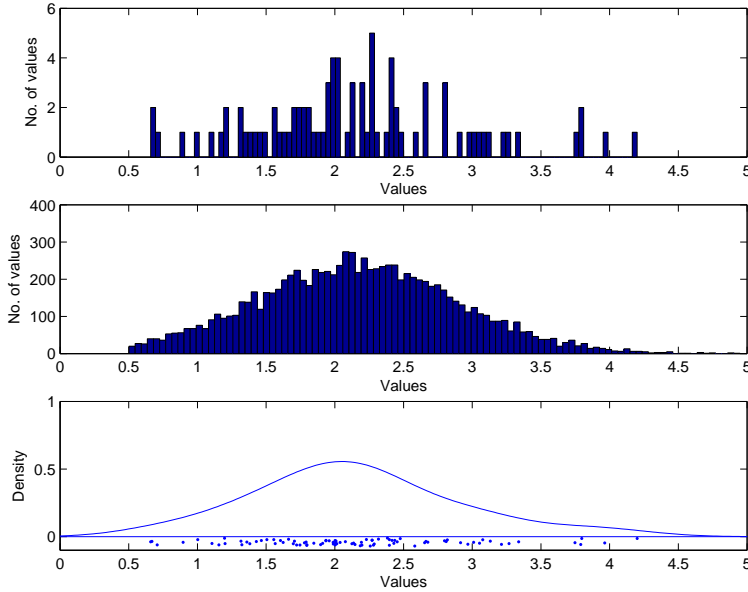
Figure 3.4: **Top**: A histogram of the estimates of b. **Center**: Normally distributed random samples based on the proposed prior distribution of b. **Bottom**: A smooth representation of the Gaussian kernel density of the estimates of b.

The Relationship of $\ln(a)$ and b

If the rating curve equation is log transformed, the following is valid,

$$\ln(Q) = \ln(a) + b\ln(w - c)$$

revealing that $\ln(a)$ and b would have a strong negative linear correlation. This is due to the fact that in simple linear regression, the estimator for the intercept, $(\ln(\widehat{a}))$, is negatively correlated with the estimator for the slope, $(\widehat{b})$ when the center of the variable, $(\ln(w - c))$, is positive. The correlation between the parameter estimates, denoted by $\rho_{\ln(a),b}$, is estimated as -0.979 based on the collection of $(\ln(\widehat{a}),\widehat{b})$ values, (see Figure 3.5).

It is, therefore, proposed that $\ln(a)$ and b have the following joint normal distribution.

$$
\begin{aligned}
\pi(\ln(a), b) &= \mathbf{N}_2(\mu, \Sigma) \\
&= \frac{1}{\sqrt{(2\pi)^2|\Sigma|}} \exp\{-\frac{1}{2}(x - \mu)'\Sigma^{-1}(x - \mu)\} \\
x &= [\ln(a); b] \\
\mu &= [\mu_{\ln(a)}; \mu_b] \\
\Sigma &= [\sigma^2_{\log(a)}, \sigma_{\log(a)}\sigma_b\rho_{\ln(a),b}; \sigma_{\log(a)}\sigma_b\rho_{\ln(a),b}, \sigma^2_b]
\end{aligned}
$$

This on the other hand causes some problems regarding proper distribution sampling, mainly due to dependencies. The dual nature of a has not been addressed, yet it has to be taken into consideration. One aspect of a is to properly scale the equation to fit the measured discharge and the other is to properly balance the equation with regard to the parameter b. By using

28
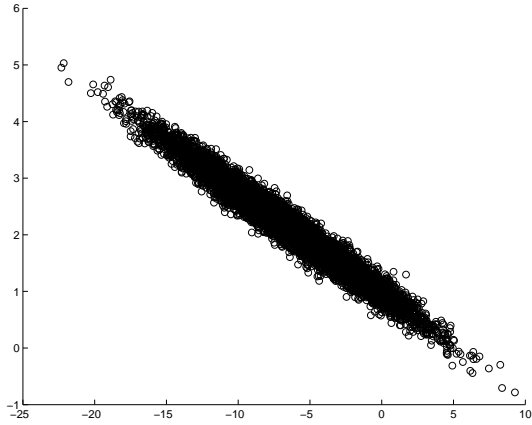
Figure 3.5: The estimated joint distribution of $\ln(a)$ and b.

the following parametrization, based on the linear correlation of the two parameters, this dual nature is easily observed. This has many advantages, simplifying the correlation of a and b while portraying the two meanings of a in understandable terms, *scale* and *balance*. The reparameterization is given by

$$
\begin{aligned}
\ln(a) &= \alpha_0 + \alpha_1 b + \epsilon \\
\epsilon &= \mathbf{N}(\mu_\epsilon, \sigma_\epsilon^2) \\
a &= \exp(\alpha_0 + \alpha_1 b) \exp(\epsilon)
\end{aligned}
$$

where ϵ is the parameter to be estimated, instead of the parameter a. The parameter ϵ can be considered as the scale term of $\ln(a)$ while $\alpha_0 + \alpha_1 b$ as the balance term. The parameters α_0 and α_1 are constants, and are estimated from the collection of $(\widehat{a}, \widehat{b})$ estimates as

$$
\begin{aligned}
\alpha_0 &= 4.9468, \\
\alpha_1 &= -5.3726.
\end{aligned}
$$

This reparameterization of a is used in the extended reparametrized model (see Section 2.3).

As could be expected, the ϵ parameter appears to be normally distributed around a mean of zero, although considerable deviation from normality near in tails is observed. The proposed prior distribution of ϵ is

$$
\begin{aligned}
\pi(\epsilon) &= \mathbf{N}(\mu_\epsilon, \sigma_\epsilon^2), \\
\mu_\epsilon &= -0.2, \\
\sigma_\epsilon^2 &= 3.829 \cdot 10^{-7}.
\end{aligned}
$$

and shown in Figure 3.7. Using this reparameterization, the model is composed of approximately independent components, making the Gibbs sampler more efficient (see Section 2.2.2) [16].

29
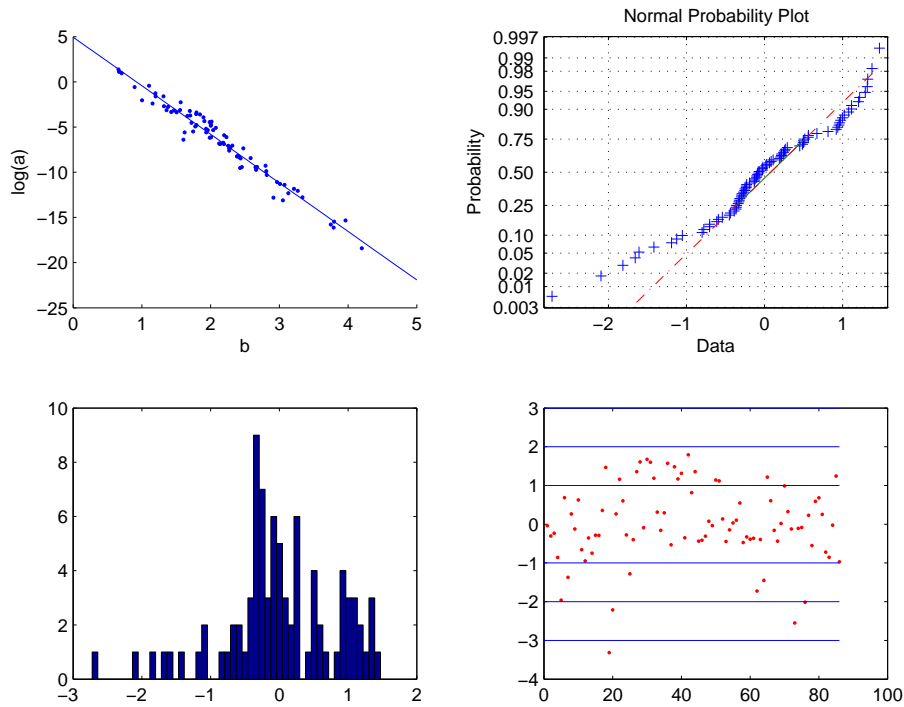
Figure 3.6: Results from the linear fit of $\ln(a)$ and b data. **Upper left:** The linear fit of $\ln(a)$ and b **Upper right:** A normal probability plot of the residuals. **Lower left:** A histogram of the residuals. **Lower left:** The standardized residuals and three standard deviation intervals.
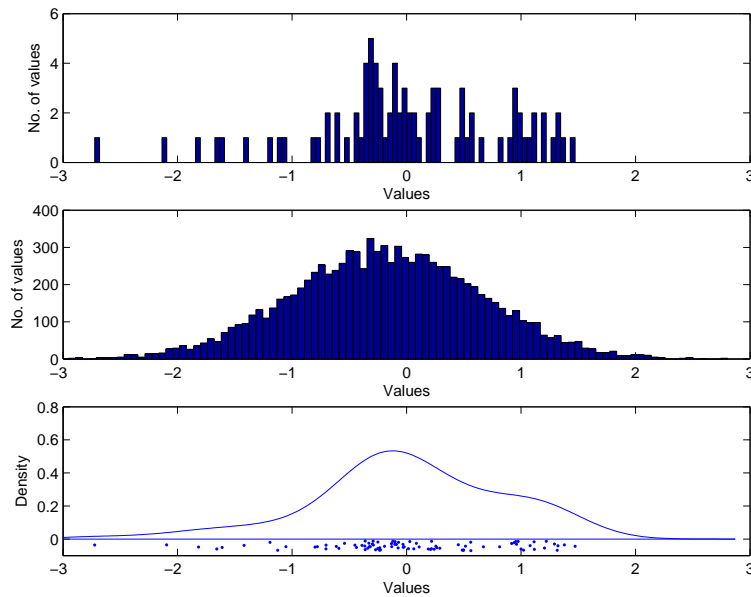
Figure 3.7: **Top**: A histogram of the estimates of ϵ. **Center**: Normally distributed random samples based on the proposed prior distribution of ϵ. **Bottom**: A smooth representation of the Gaussian kernel density of the estimates of ϵ.

3.1.3 The Prior Distribution of the Parameter c

The parameter c is a fully dependent on the choice of the coordinate system. Simply, it is at a relative height to 100 cm in the case of the HS. The depth gauge and coordinate system

should be calibrated so that c is never less than 100 cm, which means the depth sensor is always immersed. This is always attempted, though, almost never achieved. As can be seen from Figure 3.8, the c value is usually between 0 an 100 cm but other values do occur. The c value can quite possibly be less than zero, in that case, the bottom is at a negative height in the given coordinate system.

The estimation of the distribution of the c data was not straight forward. When the data is examined a large spike of c values is discovered at exactly zero. If that was true, each of those gauges were placed precisely at 1 meter above the river bottom. This explanation is of course not feasible. When examined thoroughly, each of these rating curves was indifferent to the actual value of c. This, in turn, is hypothesized to be a human element, to choose zero before other values when the opportunity presents itself. The theory is that the optimization algorithm used at the HS, in some cases, submits a very flat solution space. The user proposes a c value and linear regression based on least squares is applied to $\ln(q)$ and $\ln(w - c)$, to find optimal a and b values. In these cases, the optimal a and b values are, therefore, indifferent to the actual proposed value of c. This enables the user to prefer the lowest value parameter that satisfies the optimization conditions. In conclusion, all these zero values were estimated to be values in the vicinity of zero rather than precisely zero.

Given the arguments above and the collection of estimates of c (see Figure 3.8), the proposed prior distribution for c is a normal distribution with mean $\mu_c = 73.95$ and standard deviation $\sigma_c = 49.77$, that is,

$$
\begin{aligned}
\pi(c) &= \mathbf{N}(\mu_c, \sigma_c^2), \\
\mu_c &= 73.95, \\
\sigma_c &= 49.77.
\end{aligned}
$$

For a given data set (q,w) the prior of c is affected by $w_{\min}$, since in theory, c can never be greater than $w_{\min}$. Thus, for each data set (q,w), the prior of c is the above normal prior of c for values of c below $w_{\min}$ but equal to zero for values of c above $w_{\min}$.

3.1.4 The Prior Distribution of the Parameter ψ

The parameter ψ is a measure of how the errors behave as a function of the expected discharge which is proportional to $(w - c)^b$. If ψ equals one, then the standard deviation of the errors is exactly proportional to the discharge. If ψ is less than one, the errors decrease relative to the expected discharge and if ψ is greater than one the errors increase relative to the expected discharge. This parameter is generally less than one [1] but no data is available to form the prior distribution of ψ. In order not to narrow the choices available, while keeping the value of ψ reasonable, the proposed prior distribution is a normal distribution with a mean of $\mu_\psi = 0.8$ and standard deviation $\sigma_\psi = 0.25$ with cut-off values at 0.1 and 1.2, that is,

$$
\begin{aligned}
\pi(\psi) &= \mathbf{N}(\mu_\psi, \sigma_\psi^2), \ 0.1 < \psi < 1.2, \\
\mu_\psi &= 0.8, \\
\sigma_\psi &= 0.25.
\end{aligned}
$$
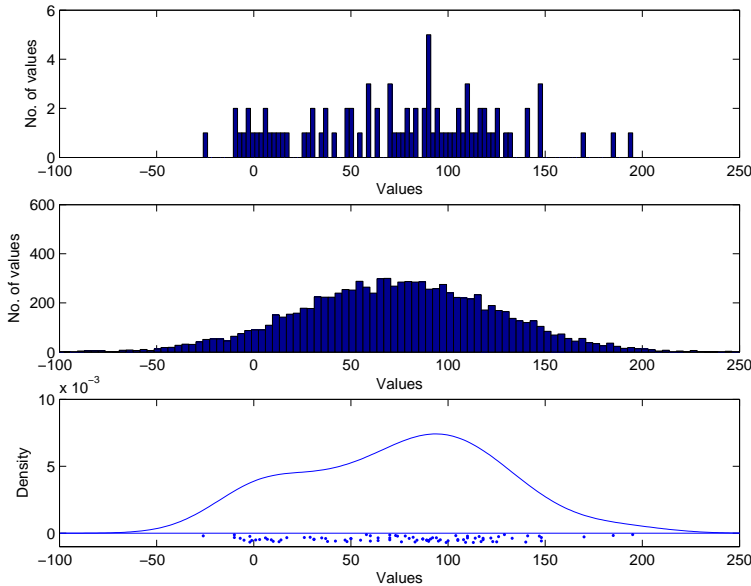
Figure 3.8: **Top**: A histogram of the estimates of c. **Center**: Normally distributed random samples based on the proposed prior distribution of c. **Bottom**: A smooth representation of the Gaussian kernel density of the estimates of c.

3.1.5 The Prior Distribution of the Parameter τ^2

The parameter τ^2, a function of a and ψ, is a measure of the variance of the errors, relative to $(w - c)^{2b\psi}$. This parameter is fundamentally based on the data set itself and hard to generalize with a prior distribution. It is not desired to predetermine the variance in the data set by establishing an informative prior distribution. Therefore, an improper (non-informative) inverse gamma distribution is proposed. Its conjugacy with the normal distribution makes this the only parameter that can be sampled directly from a proper distribution, eliminating the need for a Metropolis–Hastings step (see Section 2.2.2). The prior distribution of τ^2 is, therefore, given by,

$$
\begin{aligned}
\pi(\tau^2) &= \textbf{IGam}(\alpha_{\tau^2}, \beta_{\tau^2}), \\
\alpha_{\tau^2} &= -1, \\
\beta_{\tau^2} &= 10^{20}.
\end{aligned}
$$

An improper inverse gamma prior with the α parameter equal to -1 was used in [22], but they set the β parameter equal to 100. In this thesis, a very large value of β was needed since the scale of τ^2 can be very small.

Chapter 4

Case studies

4.1 Nordic Cooperation

The Nordic countries have a formal agreement of cooperation under the acronym CHIN (Chiefs of The Hydrological Institutes in the Nordic countries).

The Nordic hydrological institutes have worked together on various issues for a long time. This cooperation has, for example, taken form in workshops that are scheduled to investigate various issues concerning hydrological research. Leading experts from each institute are assigned to these work groups. In the late 1990's, a working group on rating curves was founded. The group published a paper on the uncertainties in the rating curve estimation process in August 2002, [2].

4.2 The CHIN Rating Curve Work Group

The experiment described in the CHIN paper, [2], was an attempt to estimate the methodological and personal uncertainties involved in establishing rating curves. Two gauging stations in each of the five Nordic countries were chosen for the experiment and discharge measurement data, water level and discharge, were sent to the other countries. Each country then estimated a rating curve for each of the ten data sets using the particular methodology used in that country. Average daily water level data from three years of record at each station (dry year, normal year and wet year), along with the highest and lowest annual water level for the entire recording period at each station, were also sent to each of the other countries so the rating curves could be applied to the water level data for comparison. Regrettably, the Swedish data were later found to be erroneous and were, therefore, not used in this research.

Table 4.1 shows some of the characteristics of the different stations, where the last column shows the ratio between the highest measured discharge Q_{max} and the discharge $Q_{W_{\max}}$, corresponding to the highest water level, $W_{\max}$ (see Section 1.3.2). A low value of this ratio means that the rating curve is extrapolated and one would expect to have some differences in the rating curves for high discharge. The rivers are of several types with very different watershed areas and the discharge data includes quite a variation in the ratio $Q_{max}/Q_{W_{\max}}$. The stations are also mapped in Figure 4.1.

Each country established rating curves for each of the ten stations using the discharge measurements and converted all the water level data to discharge. The resulting discharge data were then compared and analyzed. This comparison was carried out for average values and for

Table 4.1: The rivers that were chosen for extensive study by the CHIN group. Each river is defined by the size of its watershed area and the makeup of its runoff. Q_{max} is the highest discharge measured in an actual current meter measurement and $Q_{W_{max}}$ is the highest discharge as calculated from the highest recorded water level at the particular station [2].

Case	Station	Name	Area (km^2)	Description	Ratio $(\frac{Q_{max}}{Q_{W_{max}}})$
Case 1	DK_1	Skjern å	1055	Spring fed, natural, 1% lakes	0.41
Case 2	DK_2	Odense å	302	Mixed runoff, natural, 2% lakes	0.38
Case 3	FI_1	Lake Lannevesi	291	Outcome of lake, natural, 11% lakes	0.45
Case 4	FI_2	Lake Vahvajarvi	3510	Outcome of lake, natural, 22% lakes	0.63
Case 5	IS_1	Skjálfandafljót	1863	Mixed runoff, natural, 7% glacier	0.61
Case 6	IS_2	Fnjóská	1132	Direct runoff, natural	0.33
Case 7	NO_1	Gudbrandsdalslågen	11087	Large inland river, somewhat regulated, partly mountains	0.65
Case 8	NO_2	Kjerring-åga	16	Direct runoff, natural, mountain river, 17% lakes	0.14
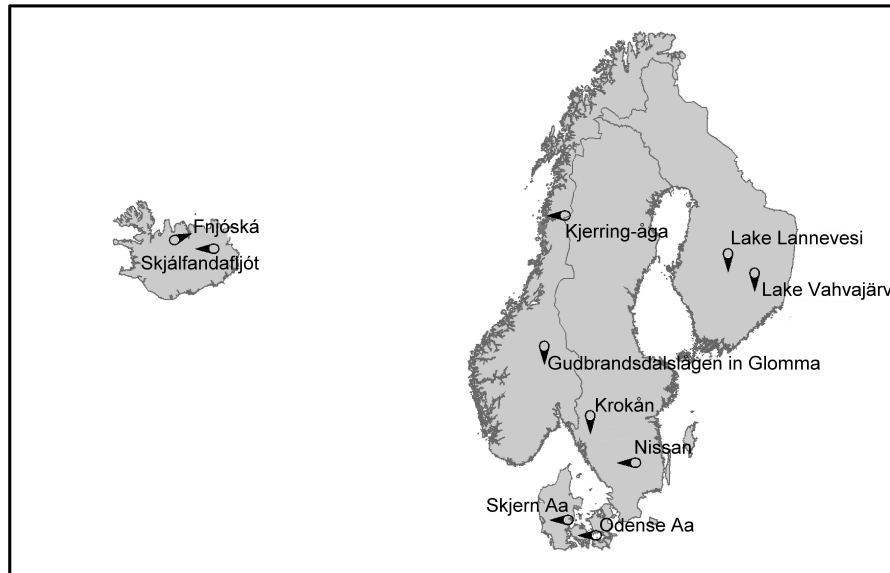
Figure 4.1: A map of the studied gauging stations, 2 stations in each country: Denmark, Finland, Iceland, Norway and Sweden [2].

high values of discharge [2]. Their results, that is the annual mean discharge values for seven stations and the estimates of highest and lowest discharge, are shown in Appendices C.2 and C.3.

4.3 Reenacting the CHIN Experiment using the Bayesian Approach

The data in the CHIN experiment as well as the results are essential for an effective comparison and were readily available and applicable. The focus of the original experiment was to create a varied sample of actual data, carefully selected by hydrological experts and the results are based on each country's standard method of rating curve construction. Therefore, the experiment was duplicated using the same data with the Bayesian approach model and the results compared and discussed. The importance and value of this comparison can not be emphasized strongly enough.

In this thesis, rating curves were constructed for each of the eight survey stations using the reparametrized model in (2.3) and the Bayesian approach, discharge measurement data and the maximum and the minimum recorded water level, (see Appendix C). Then, the rating curve is used to convert the three water level time series for each station to discharge time series. Finally, some key values are extracted from the discharge time series including annual mean values and maximum and minimum discharge.

One notable key difference between the Bayesian approach and classical statistics, is the ability of the Bayesian approach to provide accurate credible regions for any function of the parameters. A 95% credible region for each of the rating curves is constructed and exercised on the water level time series, resulting in credible regions on the discharge time series and the annual mean values. These credible regions are then compared to the results of the original experiment. Also, 95% prediction intervals for the discharge measurements are implemented and shown.

4.4 Detailed Case Studies

It is not possible to present all the results from each station in this chapter. However, some characteristic results have been chosen for presentation from each station. Therefore, one case is shown in its entirety and the results from all the others collected into Tables C.1 through C.21 and Figures C.1 through C.70. To conclude the chapter, all of these results are discussed thoroughly at the end of this section.

For the showcase scenario the Icelandic river Fnjóská, station IS_2, was chosen. The relative discharge measurement data set is shown in Figure 4.2. The rest of the CHIN data is shown in Figures B.1 through B.7 and other relative data is shown in Appendix B.

Table 4.2: The α, β values and the number of discharge measurements for Case 6

Station no. 2 in Iceland	
α value	0.6104
β value	0.8458
Number of discharge measurements	34

As noted in Chapter 2, the Bayesian approach allows two sources of information to be combined, namely, the data and prior knowledge. The result is the posterior distribution of the model parameters which contains the updated information about the parameters. From that posterior distribution, various quantities and the respective credible regions can be derived.
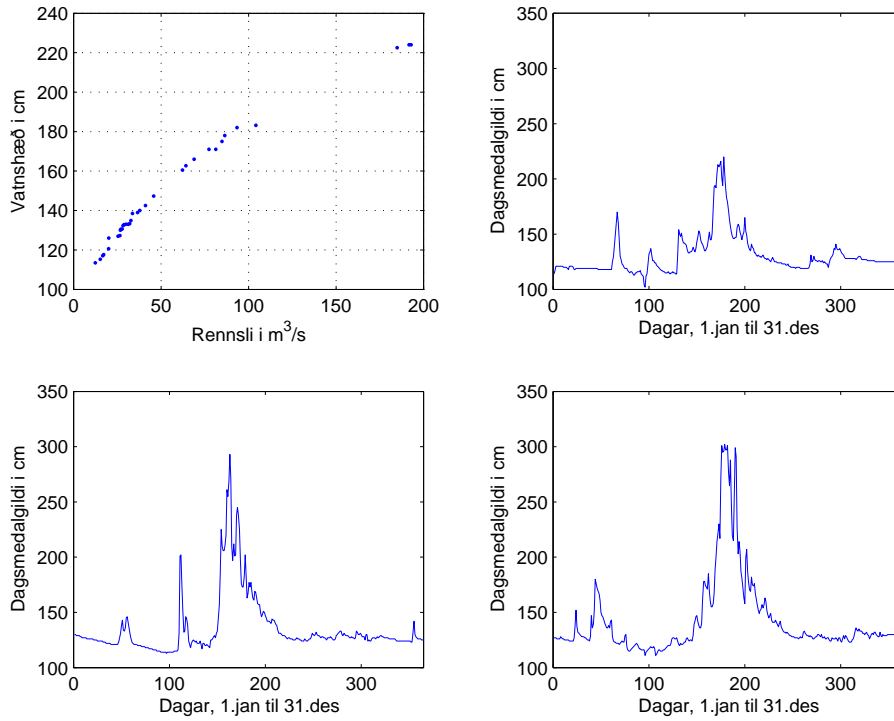
Figure 4.2: **Upper left:** The rating curve data for Fnjóská, station IS_1. **Upper right:** The dry year water level time series. **Lower left:** The normal year water level time series. **Lower right:** The wet year water level time series.

The first step in the Bayesian approach is to establish the following key distributions and functions

- The prior distributions (see Chapter 3 and Appendix A.1)

- The conditional distributions (see Appendix A.3)

- The likelihood function (see Appendix A.2)

Then, using nonlinear optimization on the discharge and water level data set, W_{Q_n} (see Section 1.3.2), optimal starting values for the parameters are obtained, usually referenced as θ_0. Also needed, are the absolute maximum and minimum water level measurements from the gauging station. These values are used to know how far up and down the rating curve needs to be extrapolated. Furthermore, the c parameter prior distribution depends on the minimum value, as c cannot be greater than $W_{\min}$.

The next step is to find the value of the tuning parameter that gives an acceptance ratio around 40% (see Section 2.2.2). This is done for all the parameters, one at time, while the other parameters are kept at their respective θ_0 value. Three Markov chains of length 10.000 each are generated over a large, decreasing interval of tuning parameters. This interval usually spanned from 1 to 10^{-10} in multiples of 10^{-1}. By graphing the acceptance ratio as a function of these proposed tuning parameters it is relatively easy to estimate the tuning parameter value that gives the desired acceptance ratio. When all the tuning parameters have been estimated, it is possible to run the MCMC algorithm for all of the model parameters simultaneously.

It was decided to generate 5 chains of length 200.000 values each, for the final estimate with the MCMC algorithm, using random values around θ_0 as initial values (see Figure 4.3).
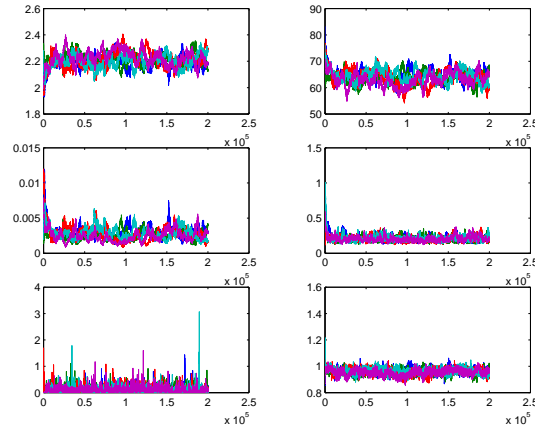
Figure 4.3: **From left to right:** b, c, $\ln(a)$, ψ, τ^2 and ϵ. The generated Markov chains for each parameter converging to the mode of the posterior distribution from their respective initial value.

For the Markov chains, a burn-in period was defined as 75%, due to the possible correlation of the parameters and relatively slow convergence. This means that the first 75% or 150.000 values, of the chains are removed and the last 25% or 50.000 values of each Markov chain (see Figure 4.4), are used and combined into a series of 250.000 values. These values are defined to be random samples of the target posterior distribution, if all requirements are met.
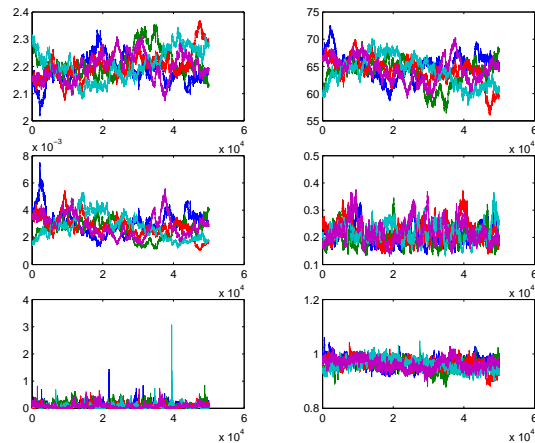
Figure 4.4: **From left to right:** b, c, $\ln(a)$, ψ, τ^2 and ϵ. The mixing of the Markov chains after the burn-in period.

Histograms of these series reveal the marginal posterior distributions of the parameters (see Figure 4.5).

Figures 4.6 and 4.7 show the comparison of the prior distribution to the marginal posterior distribution for b, c, ϵ and ψ. It is interesting to note how small the dispersion of the posterior distributions is. This points to the relative accuracy of these parameter estimates.
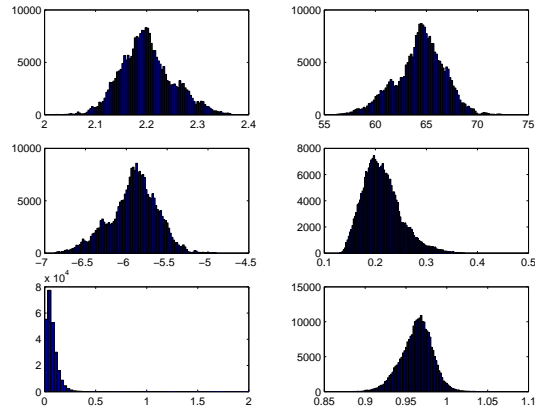
Figure 4.5: **From left to right:** b, c, $\ln(a)$, ψ, τ^2 and ϵ. The resulting posterior distributions for each parameter. On each figure the parameter estimates, the mean and the median are shown.
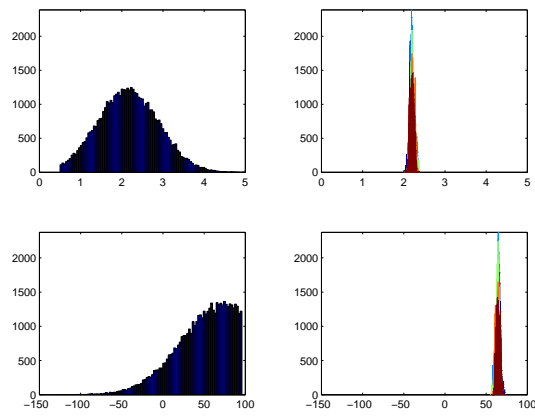
Figure 4.6: **Upper left:** The prior distribution for parameter b. **Upper right:** The posterior distribution of parameter b. **Lower left:** The prior distribution for parameter c. **Lower right:** The posterior distribution of parameter c.
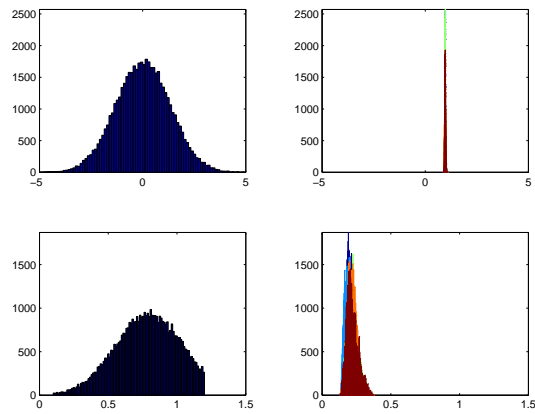
Figure 4.7: **Upper left:** The prior distribution for parameter ϵ. **Upper right:** The posterior distribution of parameter ϵ. **Lower left:** The prior distribution for parameter ψ. **Lower right:** The posterior distribution of parameter ψ.

A key requirement, is that the $\widehat{R}$ statistic (see 2.2.3) is less than 2 and as near to 1 as possible. One way to reach lower values of $\widehat{R}$ is to generate longer chains. Due to long computing times, each case requiring around 24 hours of run time using Matlab on a Unix server, 200.000 values were deemed to be sufficient to reach proper convergence with acceptable $\widehat{R}$ values (see Table 4.3).

Table 4.3: A compilation of the parameter estimates based on the Fnjóská data.

Station no. 2 in Iceland	ϵ	b	c	a	ψ	τ^2
Nonlinear estimate	0.990	2.023	71.587	7.2e-003	-	1.2e-007
Parameter estimate, mean	0.965	2.197	64.555	2.8e-003	0.208	5.9e-002
Parameter estimate, median	0.963	2.201	64.368	2.8e-003	0.213	7.2e-002
Acceptance ratio	0.45	0.44	0.40	-	0.53	-
$\widehat{R}$ ratio	1.26	1.38	1.38	-	1.14	1.08
Tuning parameter	7e-006	5e-007	1e-001	-	5e-005	-
2.5% percentile	0.922	2.108	59.236	1.4e-003	0.153	9.1e-003
25.0% percentile	0.951	2.166	62.987	2.3e-003	0.186	3.5e-002
50.0% percentile	0.965	2.197	64.555	2.8e-003	0.208	5.9e-002
75.0% percentile	0.976	2.231	65.958	3.3e-003	0.234	9.5e-002
97.5% percentile	0.998	2.311	68.690	4.6e-003	0.302	2.1e-001
Skewness	-0.263	0.311	-0.324	0.583	0.734	4.050
Kurtosis	3.53	3.06	3.14	3.93	3.65	3.65
Standard Deviation	1.9e-002	5.1e-002	2.4e+000	8.0e-004	3.7e-002	5.7e-002

In Table 4.3, the final acceptance ratios can be observed, as well as the shape parameters for the posterior distributions. From those shape parameters, skewness and kurtosis, deductions about the posterior distributions can be made. In most cases, the normal distribution form is observable, estimated with a kurtosis value around 3. The skewness of each distribution should be around 0 if it is approximately symmetrical around its mean (or median). In this case (actually, in all of the cases), all of the posterior distributions except the τ^2 distribution are approximately normal. As might have been expected (see Appendix A.3.5), the τ^2 distribution has the form of an inverse gamma distribution.

From these posterior distributions, the mean and median of each distribution, are estimated. The $2.5\%, 25\%, 75\%$ and 97.5% percentiles are also estimated. All of these estimates are shown in Table 4.3. It is obvious that the difference between using the mean or the median of the distributions, is negligible, except for τ^2.

The resulting rating curve, using the parameter estimates, is shown in Figures 4.8 and 4.9.

Figures 4.8 and 4.9 also show the approximate 95% prediction intervals for new discharge measurements and a 95% credible region for the rating curve. The discharge measurements are comfortably within the prediction interval, furthermore, it is worth noting that the ψ value in this case is very low, or around 0.2. This indicates that the variance is not directly relational to the discharge, rather that it seems to be equally distributed over the range of measurements, (see Figure 4.9).

This is confirmed by the residuals as, there are no apparent trends in the standardized residuals shown in Figure 4.10 and almost all of them fall within 2 standard deviations.

However, their normal behavior is further established by the normal probability plot in Figure 4.10 and the histogram of the residuals. It must be noted that sometimes, residual trends are
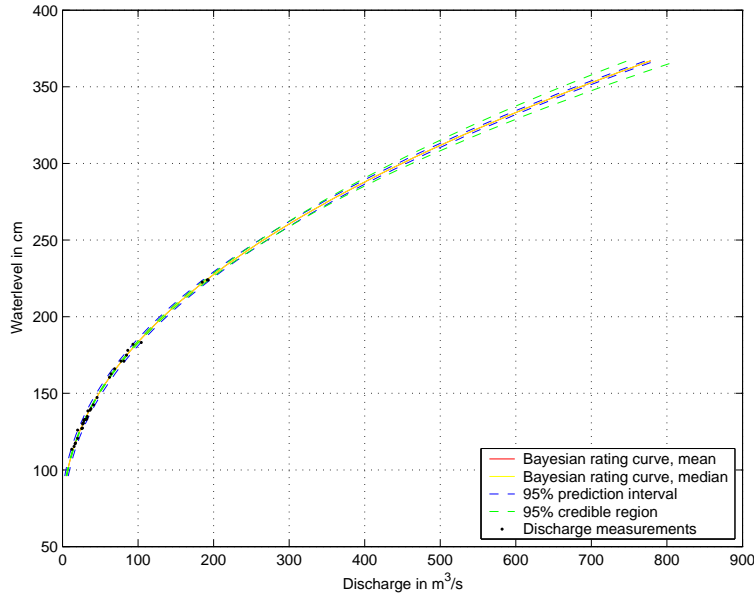
Figure 4.8: The estimated rating curve using the parameters a, b and c in Table 4.3. 95% prediction intervals for the discharge measurements are shown, as well as the 95% credible regions for the rating curve. Here, the whole range of water levels is shown, $W_{\min}$ through $W_{\max}$.
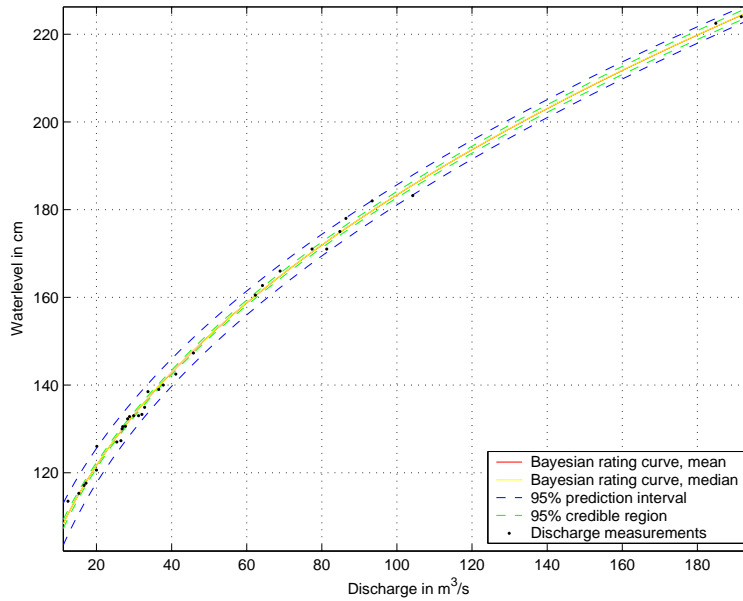
Figure 4.9: The estimated rating curve using the parameters a, b and c in Table 4.3. Approximate 95% prediction intervals for the discharge measurements are shown, as well as the 95% credible regions for the rating curve. Here, the range of water levels shown is, Q_{min} through Q_{max}.

only explained with, either, the lack of multiple segment rating curves or detailed shift analysis with respect to time.

In the case of the river Fnjóská, the rating curve model in (2.3) appears to fit the data

40

adequately well, judging by residual analysis and a subjective estimate of the rating curve itself.
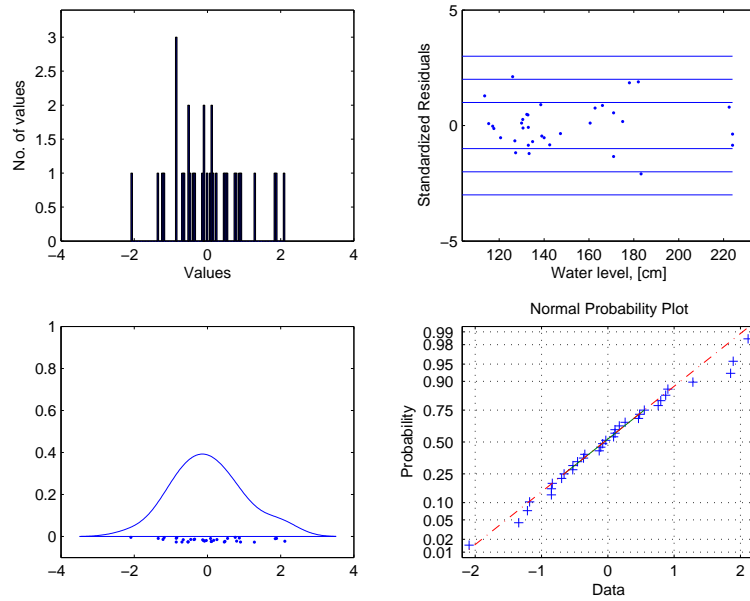
Figure 4.10: **Upper left:** A histogram of the standardized residuals. **Upper right:** Standardized residuals from the estimated rating curve as a function of water level. **Lower left:** A smooth representation of the residual density. **Lower right:** A normal probability plot of standardized residuals.

The mean annual discharge is calculated by generating the estimated discharge with 2500 samples from the posterior distributions. 95% credible regions for the mean annual discharge were estimated with 2.5% and 97.5% percentiles. This mean annual discharge value is compared to the results of the Nordic countries in Table 4.4 and in Figure 4.11.

These results, gathered with the results from the other stations, indicate that if the data set adequately covers the range of water level, the subjective differences of the countries' methods are reduced. This coverage can be judged by the proposed rating curve quality parameters α and β. Using the proposed γ value in conjunction with these parameters would have been optimal. Hence, as these values are relatively high in this case, the difference is small and the CHIN results fall comfortably within the 95% Bayesian credible regions.

Table 4.4: The estimated annual mean discharge based on the Fnjóská data.

Station no. 2 in Iceland	DK	FI	IS	NO	SE	2.5%	25%	50%	75%	97.5%
Dry year	30.3	30.6	30.8	30.3	30.0	29.86	30.28	30.39	30.50	30.89
Normal year	38.9	41.0	39.4	38.9	38.7	38.45	38.92	39.03	39.15	39.62
Wet year	51.4	57.7	51.4	51.3	51.4	50.96	51.56	51.72	51.89	52.51
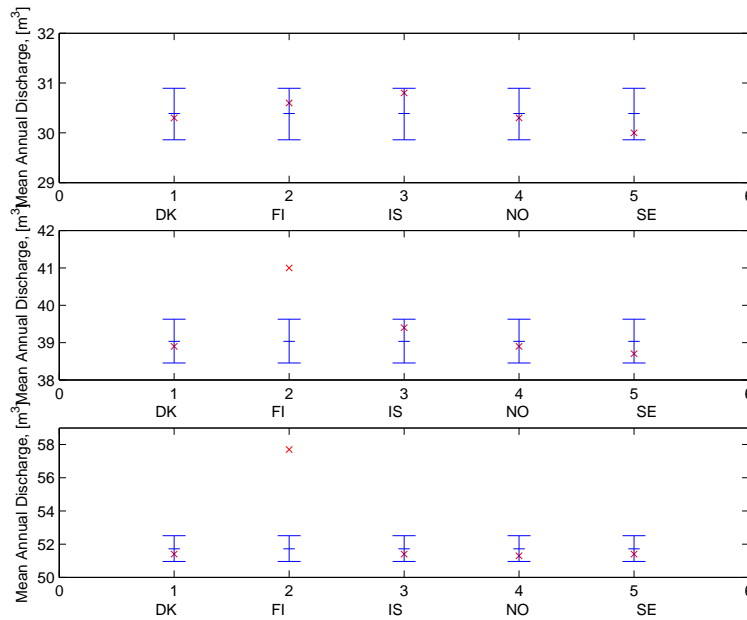
Figure 4.11: The CHIN results from each country, compared to the posterior mean and 95% credible regions for the annual mean discharge for three years. **Top** Dry year. **Middle** Average year. **Bottom** Wet year.

Finally, the maximum and minimum values were estimated with 95% credible regions and compared to the CHIN results. This is shown in Table 4.5 and Figure 4.12. Here, considerable differences are observed. Due to the low α value, extensive extrapolation of the rating curve is needed. Therefore, even apparently small differences between the various rating curves become quite large at the extreme value of $W_{\max}$. The Finnish results are far outside the credible regions. The Norwegian and Icelandic are of a similar value, yet outside the intervals. However, if similar intervals were to be estimated for these results, it is likely that the respective intervals would intersect.

In the case of the minimum values, however, all but the Finnish results fall within the Bayesian 95% credible regions.

Two conclusions may be made from these facts, the Finnish method differs substantially from the other methods in this case and the Bayesian method does not seem to give different results than the Nordic results.

Table 4.5: The estimated maximum and minimum discharge values based on the Fnjóská data.

Station no. 2 in Iceland	DK	FI	IS	NO	SE	2.5%	25%	50%	75%	97.5%
Highest calculated discharge	758.9	1371.1	697.0	701.6	780.0	747.99	768.36	778.27	790.09	814.70
Lowest calculated discharge	5.5	8.8	6.2	6.2	5.6	5.22	5.60	5.78	5.98	6.38
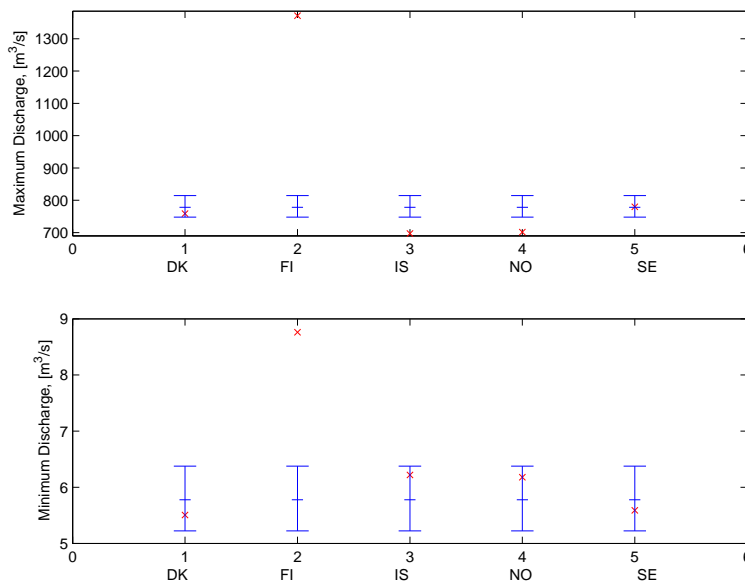
Figure 4.12: The CHIN results from each country, compared to the posterior mean and 95% credible regions for the maximum and minimum discharge. **Upper:** The maximum discharge. **Lower:** The minimum discharge.

4.5 General Discussion and Comparison of the Results of the Case Studies

The detailed analysis above is used, as a basis for a general analysis of all the case studies. Both, successful implementation and failures of the methodology are evaluated and points of interest are emphasized. For comparative purposes, the results are supported by respective figure types, e.g., rating curves, residuals, distributions and so on.

- **The discharge data** Overall, the data is relatively consistent in nature and a power function shape is observed. Also, variable data scatter and clustering behavior is noticeable.

- **The α and β values** These values were higher than one might expect, however, it is probable that the data was chosen in various ways and does not necessarily represent all data from the countries. A definite outlier is the Norwegian data, with extremely low α and β values, both less than 0.3. Both of the Danish data sets, on the other hand, are especially well bounded, with both values higher than 0.9. It should be noted that there is a positive linear correlation of high α and β values and the number of discharge measurements in the data set.

- **The water level time series** The time series are very similar for all the cases and the annual difference in daily discharge values can be compared to the runoff type of each river and the discussion in Section 1.2.3.

- **The prior distributions** For the parameters ϵ, b, ψ and τ^2, the prior distributions are the same for all the cases. The prior distribution for c depends on the respective $W_{\min}$ for each data set, for visualization of the prior of c, see Figure 4.6.

- **The Markov chains** All of these chains reach an obvious convergence. In some cases, however, the convergence is more apparent due to the difference of the posterior parameter estimate and the original nonlinear parameter estimate. These are sometimes very different and this difference can be observed in, e.g., Figures C.3 and C.11.

- **The Markov chain mix** It is hard to see any difference in these figures as the $\widehat{R}$ value has reached a value close to 1 in almost all of the cases.

- **The posterior distributions** For all the cases, the posterior distributions are very well defined and the dispersion is very small. In Case 2 (see Figure C.13), the posterior distributions have two peaks, indicating that the model is not modeling the data properly. One hypothesis might be that a shift in the rating curve manifests in this way and possibly that the data set might be split into two separate rating curves. This hypothesis, however, is not researched any further. It is also possible that longer chains are required in this case, as the $\widehat{R}$ values are still rather high.

  When the posteriors are coupled with their respective prior distributions, the difference is quite visible. The posteriors are well defined and do not seem to be overly influenced by the priors. I.e., the posteriors do not follow any predictable patterns such as converging consistently around the mean of the prior distribution, rather, are clearly defined subsets within the prior distribution boundaries.

Another abnormal behavior regarding the posterior distributions is seen in some of the τ^2 distributions. It seems that, instead of forming a bell shaped distribution, the density gathers around the zero boundary. This behavior is recognizable in Figures C.37 and C.53. This can, however, be explained with inadequate scaling in the figures.

- **The rating curves** The comparison of different rating curves is possibly the most subjective aspect of this discussion. Quite often, this subjective approach results from a hunch, based on the "feel" or the "look" of the rating curve. Does the rating curve "seem" to fit the data and so on.

  This thesis offers many ways of reducing this subjectivity, in the form of simple graphs and clearly defined credible regions and prediction intervals to aid in the decision making process. A closer look at the rating curves, supported by residual analysis, follows.

  - Rating Curve 1, Figures C.1 and C.2
    The rating curve seems to fit the data well, almost every single measurement falls within the prediction intervals. There are, however, outliers at both ends of the rating curve. Because the residuals are symmetrical around zero, this might be considered acceptable. However, these outliers, when standardized, exceed not only three standard deviations but four, (see Figure C.6). This reduces the validity of the model and it is further undermined by the normal probability plot. Strange trends are also observed in the standardized residual plot. All these clues point to the conclusion that this rating curve does not sufficiently model the data.

  - Rating Curve 2, Figures C.9 and C.10
    When this rating curve is observed, its obvious lack of fit is apparent. As before, the mass of discharge measurements falls within the prediction intervals. However, the higher the discharge, the further the measurements fall from the rating curve. In this case, the standardized residuals are not even symmetrical around zero. Coupled with the information derived from the normal probability plot and the aforementioned dual peak nature of the posterior distributions, this rating curve does not model the data in an acceptable way. It seems likely that another segment rating curve with an apparent break point around 8 m^3/s is needed.

  - Rating Curve 3, Figures C.17 and C.18
    Here, the rating curve fits the data acceptably, one measurement might be considered an outlier as its standardized residual exceeds two standard deviations. The residuals are symmetrical around zero mean and seem to be normally distributed. It must be noted, that, the standardized residual plot is a better estimator of normality than the normal probability plot when n (the number of measurements) is as low as in this case, $n=10$.

  - Rating Curve 4, Figures C.25 and C.26
    This rating curve fits all criteria, normally distributed residuals, all within the prediction intervals and clearly defined posterior distributions. If the largest observation is left out, a potential trend is observed.

  - Rating Curve 5, Figures C.33 and C.34
    Here, the rating curve fits the data acceptably, three measurements might be considered outliers as their standardized residuals barely exceed two standard deviations.

Even so, one in twenty measurements can be expected to be, on the average, outside the 95%interval. The residuals are symmetrical around zero mean and seem to be normally distributed.

– Rating Curve 6, Figures C.41 and C.42
This rating curve fits the data very well, two measurements might be considered outliers as their standardized residuals barely exceed two standard deviations. The residuals are symmetrical around zero mean and seem to be normally distributed.

– Rating Curve 7, Figures C.49 and C.50
This rating curve models the data successfully, only one measurement might be considered an outlier and due to the inherent properties of the 95% prediction interval, on average, 5 of every 100 measurements will not fit within the interval. Some trend in the standardized residuals is noticeable. On the other hand, the residuals seem to be normally distributed around zero mean and the model, therefore, deemed acceptable.

- **The annual mean discharge estimates** The CHIN results for annual mean discharge usually fall relatively close to and symmetrically around the 95% Bayesian credible regions or often within them. Even though, both of the Bayesian rating curves for the Danish data do not model the data efficiently, the annual mean estimates seem to fall, if not within the credible regions, symmetrically around them. It must be noted, that these intervals are very narrow and the fact that nearly all of these estimates fall within them is very important.
It can be hypothesized that almost any given rating curve that passes through the data set will fall within these intervals, as the difference between the various rating curves, would be very small for each daily value. The magnitude of the means, therefore, are always relatively similar.
The fact of the matter, however, is that the subjectivity of the various methods used by the different countries is negated with these Bayesian intervals. It is, therefore, possible to estimate the annual mean discharge objectively. This is the main result of this comparison and must be emphasized.

- **The maximum and minimum discharge estimates** In this case, the extreme values for each station are compared to Bayesian credible regions. It must be emphasized, that any notable difference in the parameter b value will result in vastly different discharge estimates if the rating curve needs to be extrapolated far. Furthermore, it is not optimal, to compare the single segment Bayesian rating curve used here, to the multiple segment rating curves that are used in some cases for the CHIN results, as the multiple segment rating curves can have very different b values for each segment. Though, for the arguments' sake, this comparison is carried out.
It must be emphasized, that the Bayesian rating curves differ from some (subjective) rating curves in a fundamental way. The highest discharge measurement does *not* control the shape or b value, as is often observed. Sometimes, by deliberately forcing the rating curve *through* the highest measurement (a human tendency) instead of appropriately *close to* it, the innate variance of the data set is negated. This fact, should also, explain some of the observable differences.
It is harder to make generalizations about the comparison of extreme values than about

the annual mean values. Suffice to say, the minimum values, as could be expected (the extrapolation needed is usually far less for the minimum values than the maximum values), were overall very close to and symmetrically around the Bayesian credible regions or simply within them. In one case (see Figure C.68), a systematic error is observed, as all the minimum values are higher than the Bayesian estimates. The maximum values, however, are much more varied.

- Case 1, Figure C.64
  The maximum value estimates fall symmetrically around the posterior mean and credible regions and no value is within them.

- Case 2, Figure C.65
  One value is within the interval and the other values are all less than the Bayesian estimate.

- Case 3, Figure C.66
  Those three values that are not within the intervals, are above the Bayesian estimate.

- Case 4, Figure C.67
  Two of these maximum values are within the credible regions and the other three are symmetrical around them. It seems very likely that the this maximum discharge estimate is acceptable.

- Case 5, Figure C.68
  Here, no values are within the intervals, however, they are symmetrically scattered around them. It is very possible that this is a good estimate of maximum discharge.

- Case 6, Figure C.69
  In this case, all values but the Finnish, fall within or very near the intervals and symmetrically. This is quite likely an acceptable estimate of maximum discharge.

- Case 7, Figure C.70
  A possible systematic error is encountered in this case, as all the maximum values are far from the Bayesian credible regions. The combination of an extreme extrapolation and the different handling of the maximum discharge measurement during the rating curve estimation, seems a likely explanation for this divergence.

In conclusion, 5 of the 7 rating curves are deemed acceptable in accordance with the rating curve and residual analysis. It must be noted, that without this objective scrutiny, it is possible that these rating curves might pass through a more subjective analysis. Even though this methodology is far less subjective than those that are used by the Nordic countries, it is obvious that this method is not fully automated in its estimation process and thus allows *and* needs a human element. To remove that element completely is neither the goal of this thesis nor the wish of the scientific community.

The annual mean values estimated with the Bayesian approach are comparable to the original CHIN results and, in fact for the most part, encompass them within the posterior mean and credible regions. As might be expected, the variance in estimated minimum values is low and the variance in the maximum values is relatively high. The Bayesian method based on a single segment, however, is successful in many cases, yet, is hampered by the lack of flexibility that multiple segment rating curves offer. The Bayesian method *can* be extended for multiple segment rating curves. That extension is an urgent and a valuable research topic.

Chapter 5

Conclusions

The Bayesian approach for estimating rating curves, implemented in this thesis, is very promising. Seven rating curves, of eight, with prediction intervals and credible regions, were successfully estimated, even though two of these were later discarded. A new statistical model, [1], is used with interesting results. Prior distributions for the rating curve parameters are researched extensively, using real parameter data from the Icelandic Hydrological Service. The results of the Bayesian approach, both the rating curve estimates and the derived data therefrom, are rigorously compared to the the respective CHIN results.

The results from the case studies are very promising when compared to the CHIN results. For almost all of the cases, the estimated annual means fall close to and symmetrically around the Bayesian 95% credible regions or within them. These annual mean values are as was mentioned before, calculated with different methods and either single or multiple segment rating curves. This indicates that the difference between the Nordic methods is not as drastic as was the initial concern. These findings, therefore, give appropriate reason to propose that the Bayesian method is a valid method with the potential to become a common methodology for the Nordic countries, even without a more advanced model, that is, one including shifts or multiple segment rating curves.

One of the proposed methods of estimating rating curve quality was experimented with and the results are promising. The future agenda calls for α, β and γ values to be implemented on the HS rating curves. These values can be monitored and used for organizing discharge measurement schedules, providing actual obtainable goals, e.g., "All HS γ values will be higher than 75% by the year 2010". Instead of wasting resources on discharge measurements that will not influence the quality values, other actions may be taken, such as, limiting trips to acquire exact discharge measurements for each rating curve/station. As the water level time series data used in the CHIN report did not portray a whole runoff series, e.g., only three years, no attempt was made to estimate the γ rating curve quality parameter. The proposal, however, stands and remains to be tested with sufficient data.

The advanced credible regions also open up possibilities in the joint calibration of other hydraulic such as a HEC model for example. By forming an iteration cycle with such a model, prior distributions can be redefined according to other inputs of information.

The method is also successful in estimating whether the actual measurements fall within the estimated 95% prediction intervals, as only a few of the measurements fall outside of the intervals. This can be expected. It is highly important to be able to know immediately whether a measurement is within this interval for the monitoring of each station and its rating curve.

Judging by an estimate of residual scatter and the varied values of the variance parameter ψ, the model introduced by Øverleir [1], deals efficiently with variance heteroscedasticity, establishing the functionality of that model even further. In no case, does the proposed parameter of ψ equal 1, as it does in the traditional model. This is a critical issue and needs to be further addressed in future research.

In no cases do the prior distributions influence the posterior distribution. Rather, the posterior distribution is a well defined subset distribution, well within the boundaries of the prior distribution. It is, therefore, proposed that the prior distributions efficiently simulate actual parameter values, and in no case inhibit the estimates in reaching the likeliest values.

When determining long term changes, as is the main focus of many current international projects, a measure of variability in long term means is invaluable. Practical benefits are also many. The Bayesian approach provides a simple way to measure the effect a single measurement has on rating curve quality. The prediction interval for discharge measurements will make it far easier to monitor changes or shifts in the control section. The actual calculation of the rating curve is simplified and free of tedious trial and error methods or depending on nonlinear regression algorithms.

The method proposed was unsuccessful in one case, the Norwegian station no. 2, in the river Kjerring åga. The discharge data is of a good quality, yet, a likely b is in the region of 9-11. This value, of course, lies far from the proposed prior distribution for b which was capped at value 5. It was stated that higher values of b were not suitable for extrapolation and that statement still holds true. Therefore, this method can not submit a solution as that would require extrapolation of the rating curve with b higher than 5. Therefore, no results are shown in the appendices. The solution to this dilemma is a multiple segment Bayesian rating curve. This extension of the Bayesian approach remains to be implemented and is certainly the next research agenda.

Bibliography

[1] Asgeir Petersen-Øverleir. Accounting for heteroscedasticity in rating curve estimates. *Journal of Hydrology*, pages 173 – 181, 2004.

[2] Páll Jónsson, Asgeir Petersen-Øverleir, Eva Nilsson, Magnus Edström, Hans Legard Iversen, and Hannu Sirvio. Methodological and personal uncertainties in the establishment of rating curves. In Anund Killingtveit, editor, *XXII Nordic Hydrological Conference, Nordic Hydrological Programme, NHP Report No 47*, volume I, pages 35, 35 – 44, 44, 2002.

[3] Jóna Finndís Jónsdóttir. Long term variability in Icelandic hydrological series and its relation to variability in atmospheric circulation over the North Atlantic Ocean. *Environmental and Ecological Statistics*, 10:179 – 200, 2003.

[4] The Nordic Coordination Committee for Hydrology. *Hydrometric monitoring and its development in the nordic countries*. Number 42. Finnish Environment Institute, 2002.

[5] International Organization for Standardization, Geneva, Switzerland. *International Standard IS0 4373. Measurement of liquid flow in open channels - Water-level measuring devices*, second edition, 1995.

[6] Árni Snorrason and Páll Jónsson. Error analysis of the rating curve for the glacial river, Jökulsá á Dal, Iceland. In Juha Kajander, editor, *XX Nordic Hydrological Conference, Nordic Hydrological Programme, NHP Report No 44*, volume II, pages 404 – 412, 1998.

[7] Snorri Árnason. Jökulsá á Fjöllum við Upptyppinga, vhm 162. Rating curves no. 5-16 14288 OS-2001/049 32. Technical report, The Hydrological Service, National Energy Authority, September 2001.

[8] Snorri Árnason. Hvítá, Hvítárvatnsbrú, vhm 57. Rating curves no. 3-15 14334 OS-2001/090 20. Technical report, The Hydrological Service, National Energy Authority, December 2001.

[9] Snorri Árnason. Djúpá, Fljótshverfi, vhm 150, V150. Rating curves no. 9-16 14401 OS-2002/049 38. Technical report, The Hydrological Service, National Energy Authority, October 2002.

[10] Áslaug Sóley Bjarnadóttir and Snorri Árnason. Jökulsá á Dal, Hjarðarhaga, vhm 110. Rating curve no. 8 14502 OS-2003/048. Technical report, The Hydrological Service, National Energy Authority, December 2003.

[11] Krishan P. Singh and Arni Snorrason. Sensitivity of outflow peaks and flood stages to the selection of dam breach parameters and simulation models. Technical report, Illinois Department of Energy and Natural Resources, June 1984.

[12] Krishan P. Singh and Arni Snorrason. Sensitivity of outflow peaks and flood stages to the selection of dam breach parameters and simulation models. *Journal of Hydrology*, 68:295 – 310, February 1984.

[13] Ven Te Chow. *Open-channel hydraulics*. McGraw-Hill Civil Engineering Series. McGraw-Hill, 1959.

[14] R.A. Moyeed and R.T. Clarke. The use of Bayesian methods for fitting rating curves, with case studies [article in press]. *Advances in Water Resources*, 2005.

[15] J. M. Bernardo and A. F. M. Smith. *Bayesian Theory*. Wiley, New York, 1994.

[16] Andrew Gelman, John B. Carlin, Hal S. Stern, and Donald B. Rubin. *Bayesian Data Analysis*. Chapman and Hall/CRC, second edition, 2004.

[17] B. P. Carlin and T. A. Louis. *Bayes and Empirical Bayes Methods for Data Analysis*. Chapman & Hall/CRC, London, second edition, 2000.

[18] A. Gelman and D. B. Rubin. Inference from iterative simulation using multiple sequences. *Statistical Science*, pages 457– 472, 1992.

[19] R.T. Clarke. Uncertainty in the estimation of mean annual flood due to rating-curve indefinition. *Journal of Hydrology*, pages 185– 190, 1999.

[20] R. W. Herschy. Hydrometry principles and practices. New York, 1999. Wiley.

[21] K.D. Gawne and S.P. Simonovic. A computer based system for modeling the stage-discharge relationship in steady-state conditions. *Hydrological Science Journal*, pages 487– 506, 1994.

[22] H.S. Stan and N. Cressie. Posterior predictive model checks for disease mapping models. *Statistics in Medicine*, 19:2377– 2397, 2000.

II

Appendix A

Appendices

A.1 The Prior Distributions

A.1.1 The Prior Distribution for the Parameter $\ln(a)$

$$\pi(\ln(a)) = \frac{1}{\sqrt{2\pi\sigma_{\ln(a)}^2}} \exp\left\{-\frac{1}{2\sigma_{\ln(a)}^2}(\ln(a) - \mu_{\ln(a)})^2\right\}.$$

The log transformation of $\pi(\ln(a))$ is given by

$$\ln(\pi(\ln(a))) = -\frac{1}{2}\ln(2\pi\sigma_{\ln(a)}^2) - \frac{1}{2\sigma_{\ln(a)}^2}\left\{\ln(a)^2 - 2\ln(a)\mu_{\ln(a)} + \mu_{\ln(a)}^2\right\}.$$

A.1.2 The Prior Distribution for the Parameter ϵ

$$\pi(\epsilon) = \frac{1}{\sqrt{2\pi\sigma_\epsilon^2}} \exp\left\{-\frac{1}{2\sigma_\epsilon^2}(\epsilon - \mu_\epsilon)^2\right\}.$$

The log transformation of $\pi(\epsilon)$ is given by

$$\ln(\pi(\epsilon)) = -\frac{1}{2}\ln(2\pi\sigma_\epsilon^2) - \frac{1}{2\sigma_\epsilon^2}(\epsilon^2 - 2\epsilon\mu_\epsilon + \mu_\epsilon^2).$$

A.1.3 The Prior Distribution for the Parameter b

$$\pi(b) \propto \frac{1}{\sqrt{2\pi\sigma_b^2}} \exp\left\{-\frac{1}{2\sigma_b^2}(b - \mu_b)^2\right\} I(0.5 < b < 5).$$

The log transformation of $\pi(b)$ is given by

$$\ln(\pi(b)) \propto -\frac{1}{2}\ln(2\pi\sigma_b^2) - \frac{1}{2\sigma_b^2}(b^2 - 2b\mu_b + \mu_b^2)I(0.5 < b < 5).$$

A.1.4 The Prior Distribution for the Parameter c

$$\pi(c) = \frac{1}{\sqrt{2\pi\sigma_c^2}} \exp\left\{-\frac{1}{2\sigma_c^2}(c - \mu_c)^2\right\}.$$

The log transformation of $\pi(c)$ is given by

$$\ln(\pi(c)) = -\frac{1}{2}\ln(2\pi\sigma_c^2) - \frac{1}{2\sigma_c^2}(c^2 - 2c\mu_c + \mu_c^2).$$

A.1.5 The Prior Distribution for the Parameter ψ

$$\pi(\psi) = \frac{1}{\sqrt{2\pi\sigma_\psi^2}} \exp\left\{-\frac{1}{2\sigma_\psi^2}(\psi - \mu_\psi)^2\right\} I(0.1 < \psi < 1.2).$$

The log transformation of $\pi(\psi)$ is given by

$$\ln(\pi(\psi)) = -\frac{1}{2}\ln(2\pi\sigma_\psi^2) - \frac{1}{2\sigma_\psi^2}(\psi^2 - 2\psi\mu_\psi + \mu_\psi^2)I(0.1 < \psi < 1.2).$$

A.1.6 The Prior Distribution for the Parameter τ^2

$$\pi(\tau^2) \propto (\tau^2)^{-(\alpha_{\tau^2}+1)} \exp\left(\frac{-1}{\beta_{\tau^2}\tau^2}\right).$$

The log transformation of $\pi(\tau^2)$ is given by

$$\ln\pi(\tau^2) \propto -(\alpha_{\tau^2} + 1)\ln(\tau^2) - \frac{1}{\beta_{\tau^2}\tau^2}.$$

A.2 The Likelihood Function for the Rating Curve Model

We have

$$f(q_i|\epsilon, b, c, \psi, \tau^2, w_i) = \frac{1}{\sqrt{2\pi\tau^2(w_i - c)^{2b\psi}}} \exp\left[-\frac{\{q_i - \exp(\alpha_0 + \alpha_1 b + \epsilon)(w_i - c)^b\}^2}{2\tau^2(w_i - c)^{2b\psi}}\right]$$

$$f(q|\epsilon, b, c, \psi, \tau^2, w) = \prod_{i=1}^{n} \frac{1}{\sqrt{2\pi\tau^2(w_i - c)^{2b\psi}}} \exp\left[-\frac{\{q_i - \exp(\alpha_0 + \alpha_1 b + \epsilon)(w_i - c)^b\}^2}{2\tau^2(w_i - c)^{2b\psi}}\right]$$

$$= \mathbf{N}(\exp(\alpha_0 + \alpha_1 b + \epsilon)(w_i - c)^b, \tau^2(w_i - c)^{2b\psi})$$

The log transformation is given by

$$\ln(f(q_i|\epsilon, b, c, \psi, \tau^2, w_i)) \;=\; f_1 + f_2$$

$$f_1 \;=\; \sum_{i=1}^{n} \ln\left(\frac{1}{\sqrt{2\pi\tau^2(w_i - c)^{2b\psi}}}\right)$$

$$\;=\; -\frac{n}{2}\ln(2\pi) - \frac{n}{2}\ln(\tau^2) - b\psi\sum_{i=1}^{n}\ln(w_i - c)$$

$$f_2 \;=\; -\frac{1}{2\tau^2}\sum_{i=1}^{n}(w_i - c)^{-2b\psi}\left\{q_i - \exp(\alpha_0 + \alpha_1 b + \epsilon)(w_i - c)^b\right\}^2$$

A.3   The Conditional Distributions

A.3.1   The Conditional Distribution of the Parameter ϵ

We have

$$\pi(\epsilon|b, c, \psi, \tau^2, w, q) \propto f(q|\epsilon, b, c, \psi, \tau^2, w)\pi(\epsilon).$$

The log transformation of $\pi(\epsilon|b, c, \psi, \tau^2, w, q)$ is proportional to

$$\;=\; -\frac{1}{\tau^2}\sum_{i=1}^{n}\frac{\left\{q_i - \exp(\alpha_0 + \alpha_1 b + \epsilon)(w_i - c)^b\right\}^2}{(w_i - c)^{2b\psi}} - \frac{1}{2\sigma_\epsilon^2}(\epsilon^2 - 2\epsilon\mu_\epsilon + \mu_\epsilon^2).$$

A.3.2   The Conditional Distribution of the Parameter b

We have We have

$$\pi(b|\epsilon, c, \psi, \tau^2, w, q) \propto f(q|\epsilon, b, c, \psi, \tau^2, w)\pi(b)I(0 < b0 < 5).$$

The log transformation of $\pi(b|\epsilon, c, \psi, \tau^2, w, q)$ is proportional to

$$\;=\; -b\psi\sum_{i=1}^{n}\ln(w_i - c) - \frac{1}{\tau^2}\sum_{i=1}^{n}\frac{\left\{q_i - \exp(\alpha_0 + \alpha_1 b + \epsilon)(w_i - c)^b\right\}^2}{(w_i - c)^{2b\psi}}$$

$$\;-\; \frac{1}{2\sigma_b^2}(b^2 - 2b\mu_b + \mu_b^2).$$

V

A.3.3 The Conditional Distribution of the Parameter c

We have We have

$$\pi(c|\epsilon, b, \psi, \tau^2, w, q) \propto f(q|\epsilon, b, c, \psi, \tau^2, w)\pi(c).$$

The log transformation of $\pi(c|\epsilon, b, \psi, \tau^2, w, q)$ is proportional to

$$
\begin{aligned}
= \quad & -b\psi \sum_{i=1}^{n} \ln(w_i - c) - \frac{1}{\tau^2} \sum_{i=1}^{n} \frac{\left\{ q_i - \exp(\alpha_0 + \alpha_1 b + \epsilon)(w_i - c)^b \right\}^2}{(w_i - c)^{2b\psi}} \\
& - -\frac{1}{2\sigma_c^2}(c^2 - 2c\mu_c + \mu_c^2).
\end{aligned}
$$

A.3.4 The Conditional Distribution of the Parameter ψ

We have We have

$$\pi(\psi|\epsilon, b, c, \tau^2, \psi, w, q) \propto f(q|\epsilon, b, c, \psi, \tau^2, w)\pi(\psi).$$

The log transformation of $\pi(\psi|\epsilon, b, c, \tau^2, \psi, w, q)$ is proportional to

$$
\begin{aligned}
= \quad & -b\psi \sum_{i=1}^{n} \ln(w_i - c) - \frac{1}{\tau^2} \sum_{i=1}^{n} \frac{\left\{ q_i - \exp(\alpha_0 + \alpha_1 b + \epsilon)(w_i - c)^b \right\}^2}{(w_i - c)^{2b\psi}} \\
& - -\frac{1}{2\sigma_\psi^2}(\psi^2 - 2\psi\mu_\psi + \mu_\psi^2)
\end{aligned}
$$

A.3.5 The Conditional Distribution of the Parameter τ^2

We have

$$\pi(\tau^2|\epsilon, c, b, \psi, w, q) \propto f(q|\epsilon, b, c, \psi, \tau^2, w)\pi(\tau^2).$$

The log transformation of $\pi(\tau^2|\epsilon, c, b, \psi, w, q)$ is proportional to

$$
\begin{aligned}
& - \frac{n}{2}\ln(\tau^2) - \frac{1}{\tau^2} \sum_{i=1}^{n} \frac{\left\{ q_i - \exp(\alpha_0 + \alpha_1 b + \epsilon)(w_i - c)^b \right\}^2}{(w_i - c)^{2b\psi}} \\
& - (\alpha_{\tau^2})\ln(\tau^2) - \frac{1}{\beta_{\tau^2}\tau^2} \\
= \quad & \mathbf{IGam}\left(\frac{n}{2} + \alpha_{\tau^2}, \left[\frac{1}{2} \sum_{i=1}^{n} \frac{\left\{ q_i - \exp(\alpha_0 + \alpha_1 b + \epsilon)(w_i - c)^b \right\}^2}{(w_i - c)^{2b\psi}} + \frac{1}{\beta_{\tau^2}} \right]^{-1} \right)
\end{aligned}
$$

VI

Appendix B

The CHIN Data
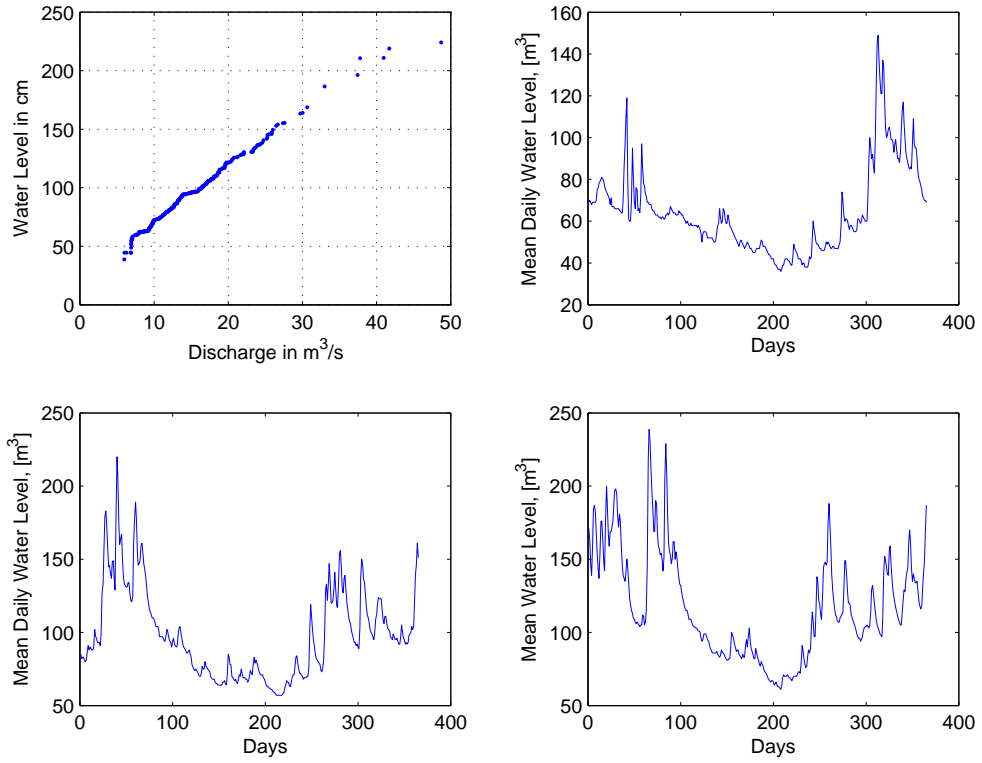
Figure B.1: **Upper left:** The rating curve data for Skjern å, Station DK_1. **Upper right:** The dry year water level time series. **Lower left:** The normal year water level time series. **Lower right:** The wet year water level time series.

Table B.1: The α, β values and the number of discharge measurements for Case 1

Station no. 1 in Denmark	
α value	0.8525
β value	0.9044
Number of discharge measurements	284
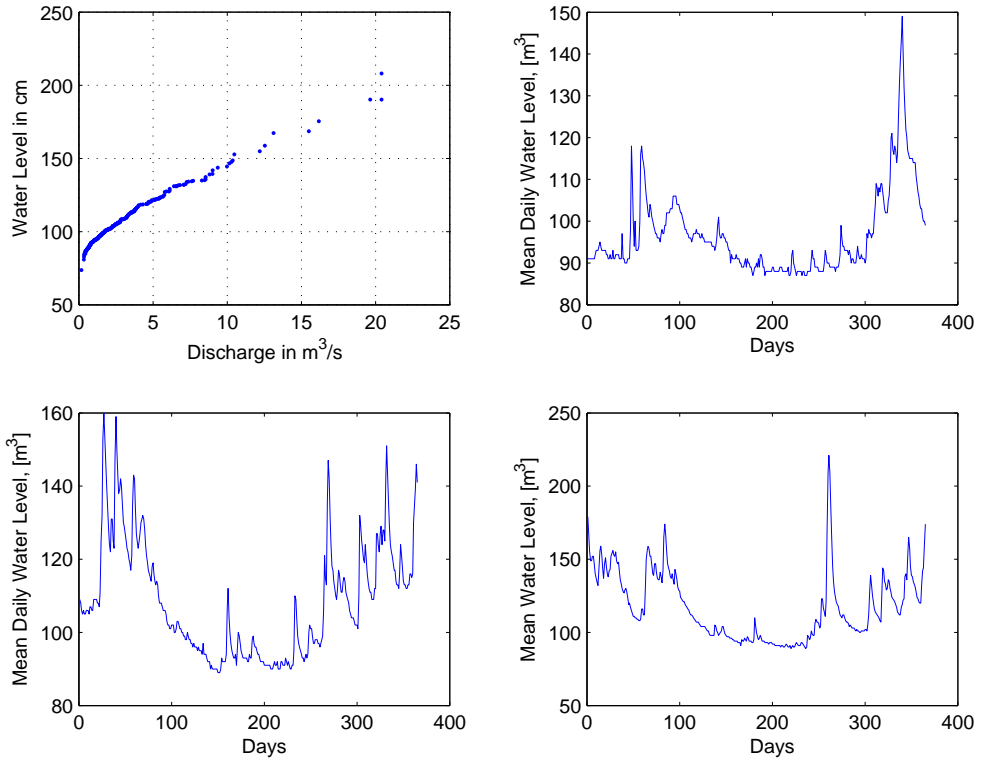
Figure B.2: **Upper left:** The rating curve data for Odense å, Station DK_2. **Upper right:** The dry year water level time series. **Lower left:** The normal year water level time series. **Lower right:** The wet year water level time series.

Table B.2: The α, β values and the number of discharge measurements for Case 2

Station no. 2 in Denmark	
α value	0.9416
β value	1
Number of discharge measurements	360
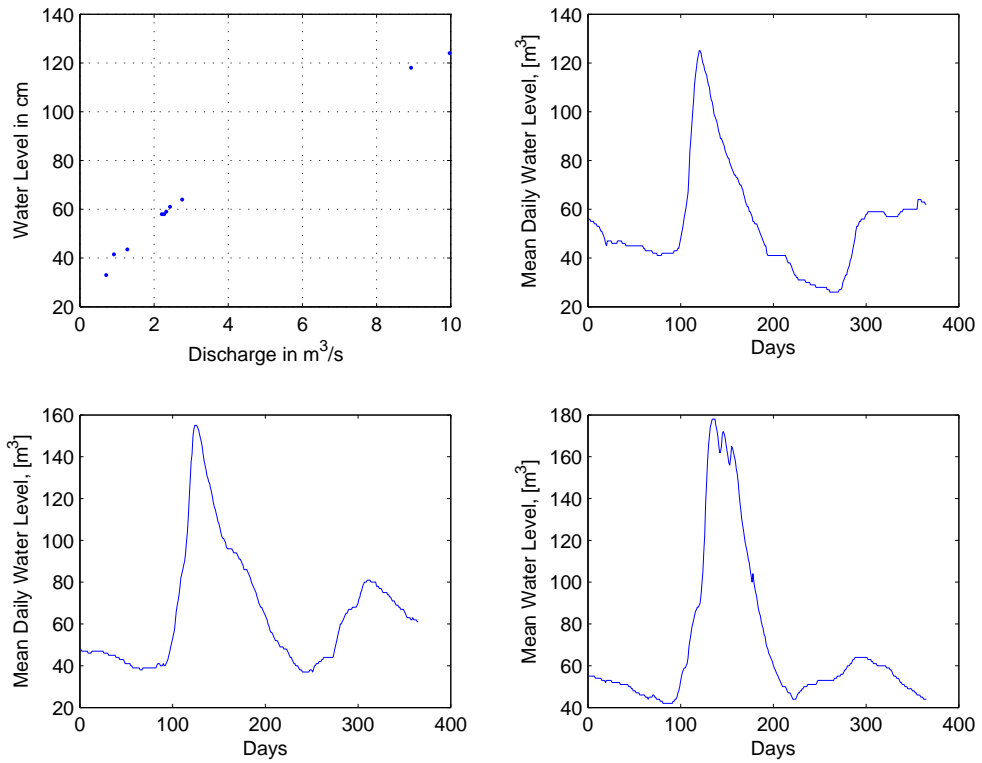
Figure B.3: **Upper left:** The rating curve data for Lake Lannevesi, Station FI_1. **Upper right:** The dry year water level time series. **Lower left:** The normal year water level time series. **Lower right:** The wet year water level time series.

Table B.3: The α, β values and the number of discharge measurements for Case 3

| Station no. 1 in Finland	
α value	0.6966
β value	0.7576
Number of discharge measurements	10
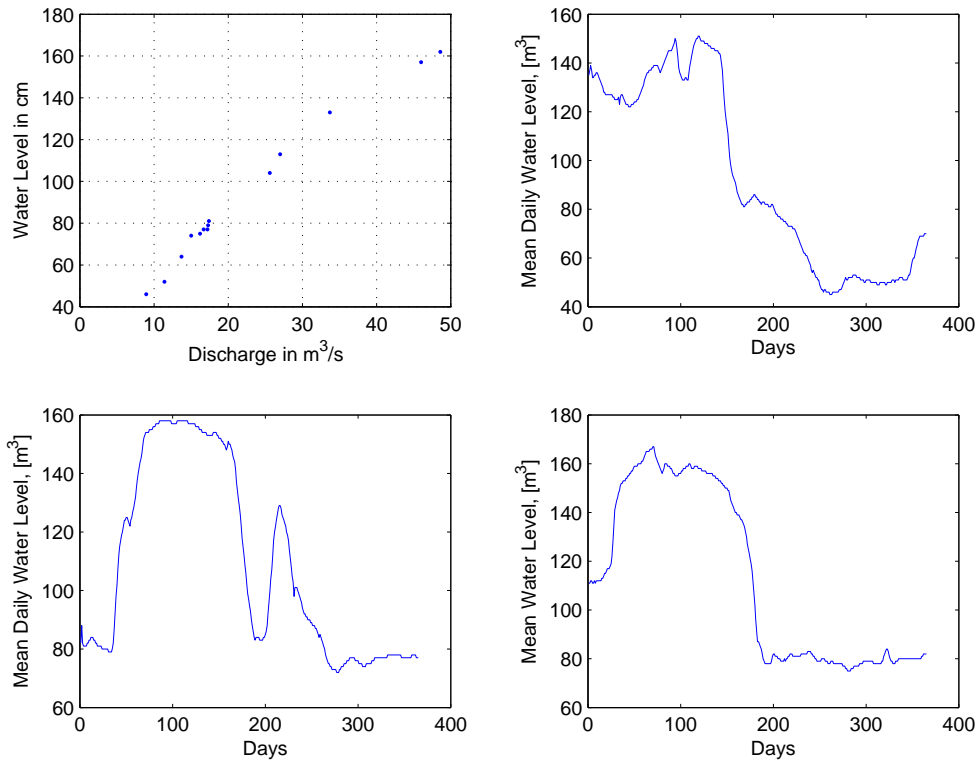
Figure B.4: **Upper left:** The rating curve data for Lake Vahvajarvi, Station FI_2. **Upper right:** The dry year water level time series. **Lower left:** The normal year water level time series. **Lower right:** The wet year water level time series.

Table B.4: The α, β values and the number of discharge measurements for Case 4

| Station no. 2 in Finland	
α value	0.9701
β value	0.9565
Number of discharge measurements	14
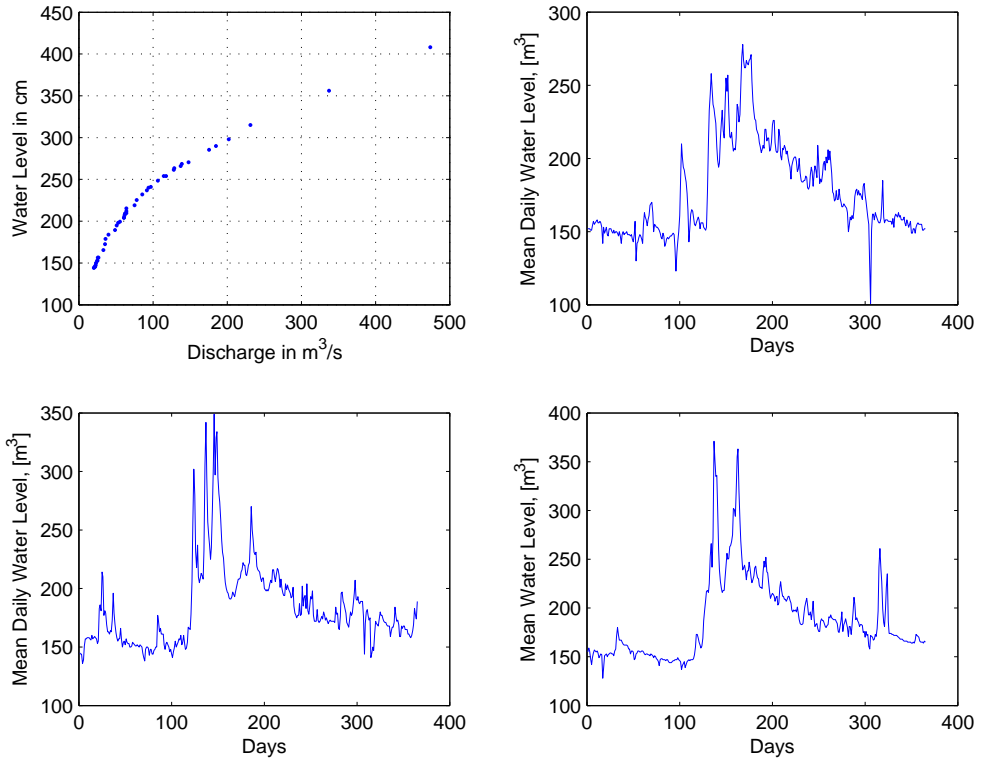
Figure B.5: **Upper left:** The rating curve data for Skjálfandafljót, Station IS_1. **Upper right:** The dry year water level time series. **Lower left:** The normal year water level time series. **Lower right:** The wet year water level time series.

Table B.5: The α, β values and the number of discharge measurements for Case 5

| Station no. 1 in Iceland	
α value	0.7953
β value	0.3056
Number of discharge measurements	46
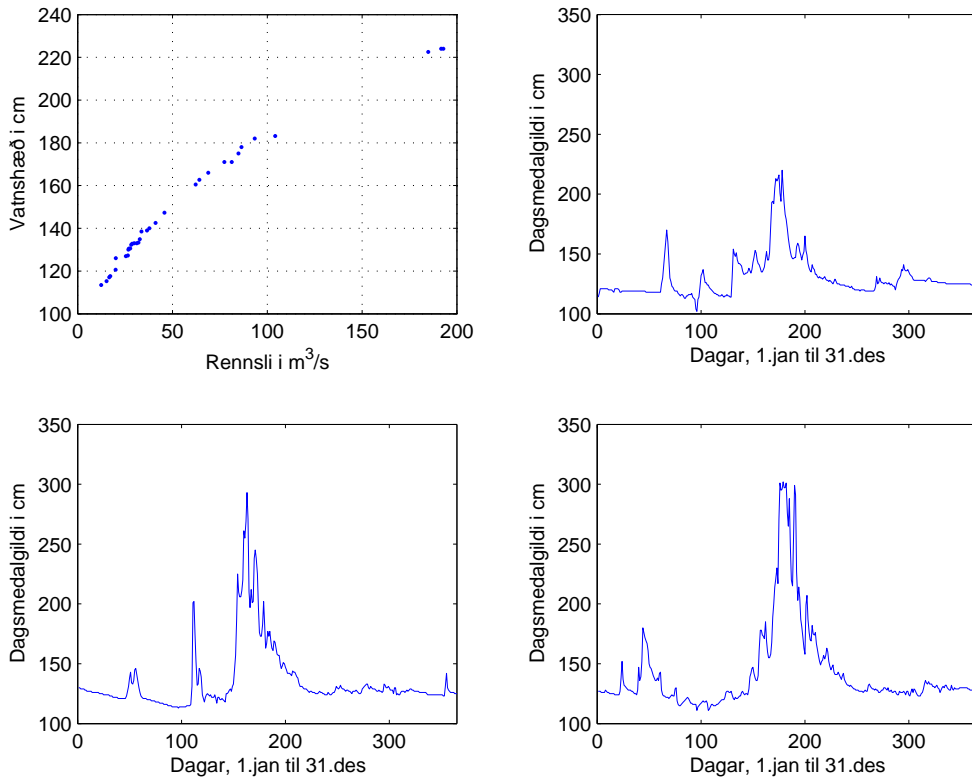
Figure B.6: **Upper left:** The rating curve data for Fnjóská, Station IS_2. **Upper right:** The dry year water level time series. **Lower left:** The normal year water level time series. **Lower right:** The wet year water level time series.

Table B.6: The α, β values and the number of discharge measurements for Case 6

| Station no. 2 in Iceland	
α value	0.6104
β value	0.8458
Number of discharge measurements	34

XIII
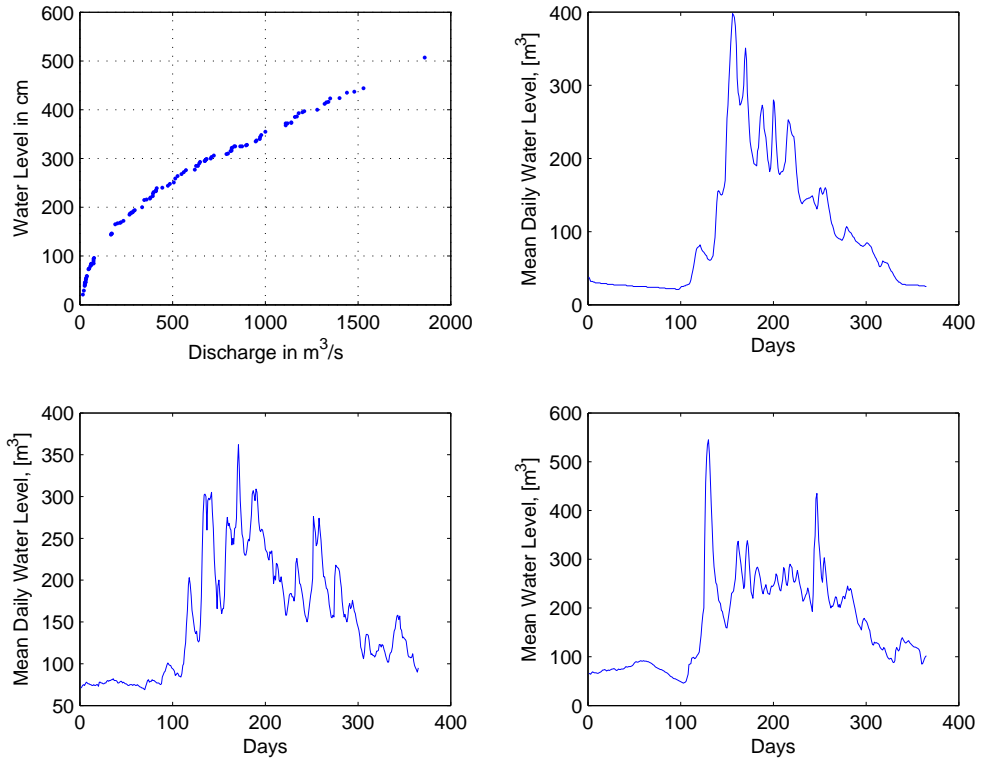
Figure B.7: **Upper left:** The rating curve data for Gudbrandsdalslågen, Station NO_1. **Upper right:** The dry year water level time series. **Lower left:** The normal year water level time series. **Lower right:** The wet year water level time series.

Table B.7: The α, β values and the number of discharge measurements for Case 7

Station no. 1 in Norway	
α value	0.2726
β value	0.0435
Number of discharge measurements	122

B.1 The Numerical Data

B.1.1 The Estimated Annual Mean Values

Table B.8: A compilation of the annual mean discharge from the CHIN report [2].

Station: DK_1	DK	FI	IS	NO	SE	max relative difference(%)
Dry year	9.6	9.2	9.9	10.6	9.7	14.7
Normal year	15.7	15.9	16.4	15.2	16.1	7.6
Wet year	19.7	19.7	20.6	19.0	20.0	8.3
Station: DK_2	DK	FI	IS	NO	SE	max relative difference(%)
Dry year	1.5	1.5	1.5	1.2	1.5	18.1
Normal year	3.1	3.3	3.2	3.2	3.2	8.3
Wet year	4.9	4.7	5.0	4.4	4.9	12.2
Station: FI_1	DK	FI	IS	NO	SE	max relative difference(%)
Dry year	2.2	2.3	2.3	2.2	2.2	4.8
Normal year	3.3	3.4	3.4	3.3	3.3	3.2
Wet year	4.0	4.1	4.0	4.0	3.9	3.2
Station: FI_2	DK	FI	IS	NO	SE	max relative difference (%)
Dry year	22.9	22.9	22.9	22.9	23.0	0.5
Normal year	27.5	27.5	27.6	27.6	27.6	0.5
Wet year	29.0	29.1	29.1	29.1	29.2	0.7
Station: IS_1	DK	FI	IS	NO	SE	max relative difference (%)
Dry year	43.3	43.2	43.0	43.1	43.0	0.6
Normal year	49.2	48.8	48.8	48.8	48.8	0.8
Wet year	54.7	54.3	54.3	54.3	54.3	0.7
Station: IS_2	DK	FI	IS	NO	SE	max relative difference(%)
Dry year	30.3	30.6	30.8	30.3	30.0	2.8
Normal year	38.9	41.0	39.4	38.9	38.7	5.9
Wet year	51.4	57.7	51.4	51.3	51.4	12.2
Station: NO_1	DK	FI	IS	NO	SE	max relative difference (%)
Dry year	151.4	157.5	154.5	152.4	151.2	4.1
Normal year	229.8	250.5	222.9	228.1	229.1	11.9
Wet year	296.9	309.6	299.8	306.3	296.0	4.5
Station: NO_2	DK	FI	IS	NO	SE	max relative difference (%)
Dry year	1.2	1.2	1.1	1.3	1.2	12.8
Normal year	2.1	2.1	2.0	2.1	2.1	7.6
Wet year	3.2	3.5	3.1	3.6	3.5	15.4
Station: SE_1	DK	FI	IS	NO	SE	max relative difference (%)
Dry year	6.1	5.7	5.6	5.7	6.4	12.4
Normal year	10.5	10.1	9.9	10.0	10.9	9.5
Wet year	15.3	15.2	14.6	14.9	16.6	13.0
Station: SE_2	DK	FI	IS	NO	SE	max relative difference (%)
Dry year	1.6	1.2	1.6	1.6	1.6	30.8
Normal year	3.9	4.0	4.0	3.9	3.9	3.4
Wet year	7.0	7.6	7.2	7.0	7.1	8.1

Appendix C

Bayesian Results

C.1 Parameter Estimates with Relevant Data

C.1.1 Case 1, Station DK_1, Skjern å

Table C.1: Parameter estimates based on the Skjern å data and other relevant data.

| Station no. 1 in Denmark	ϵ	b	c	a	ψ	τ^2
Nonlinear estimate	-1.245	1.451	-12.286	1.7e-002	-	3.9e-007
Parameter estimate, mean	-1.208	1.304	-1.823	3.8e-002	0.431	1.4e-003
Parameter estimate, median	-1.208	1.304	-1.820	3.8e-002	0.431	1.4e-003
Acceptance ratio	0.24	0.32	0.35	-	0.51	-
$\widehat{R}$ ratio	1.35	1.43	1.45	-	1.25	1.22
Tuning parameter	1e-007	1e-007	1e-002	-	1e-006	-
2.5% percentile	-1.210	1.298	-2.303	3.7e-002	0.405	9.9e-004
25.0% percentile	-1.208	1.302	-1.994	3.8e-002	0.422	1.3e-003
50.0% percentile	-1.208	1.304	-1.823	3.8e-002	0.431	1.4e-003
75.0% percentile	-1.207	1.306	-1.642	3.9e-002	0.440	1.6e-003
97.5% percentile	-1.206	1.311	-1.338	4.0e-002	0.457	2.1e-003
Skewness	-0.045	0.016	-0.008	0.028	-0.033	0.554
Kurtosis	2.70	2.53	2.50	2.53	2.70	2.70
Standard Deviation	1.1e-003	3.4e-003	2.6e-001	7.3e-004	1.3e-002	2.8e-004
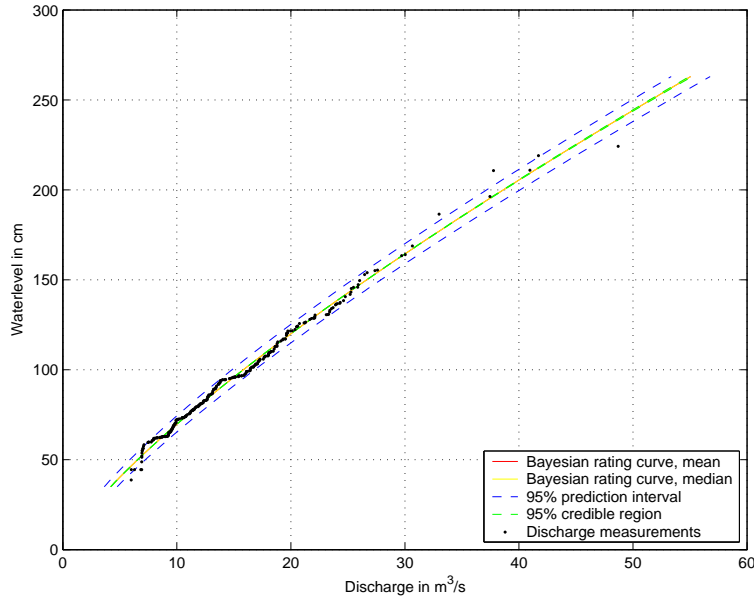
Figure C.1: The estimated rating curve using the parameters a, b and c in Table C.1. 95% prediction intervals for the discharge measurements are shown, as well as the 95% credible regions for the rating curve. Here, the whole range of water levels is shown, $W_{\min}$ through $W_{\max}$.
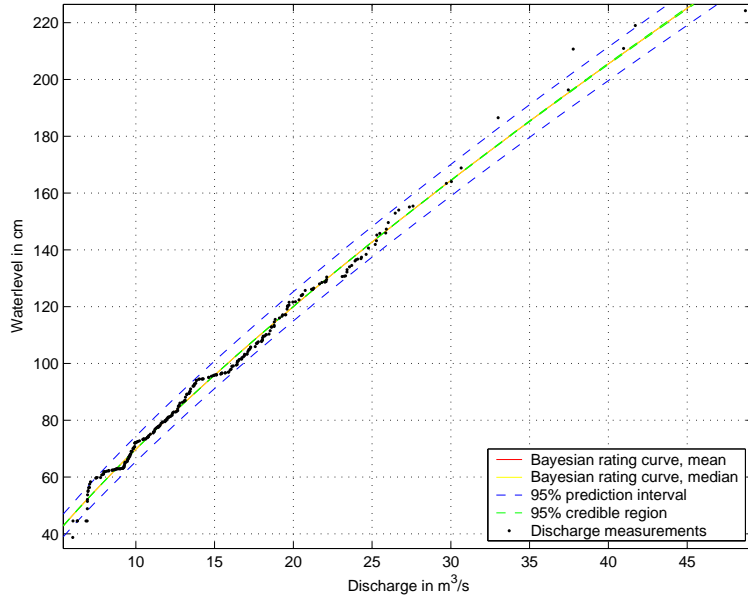
Figure C.2: The estimated rating curve using the parameters a, b and c in Table C.1. 95% prediction intervals for the discharge measurements are shown, as well as the 95% credible regions for the rating curve. Here, the range of water levels shown is, Q_{min} through Q_{max}.
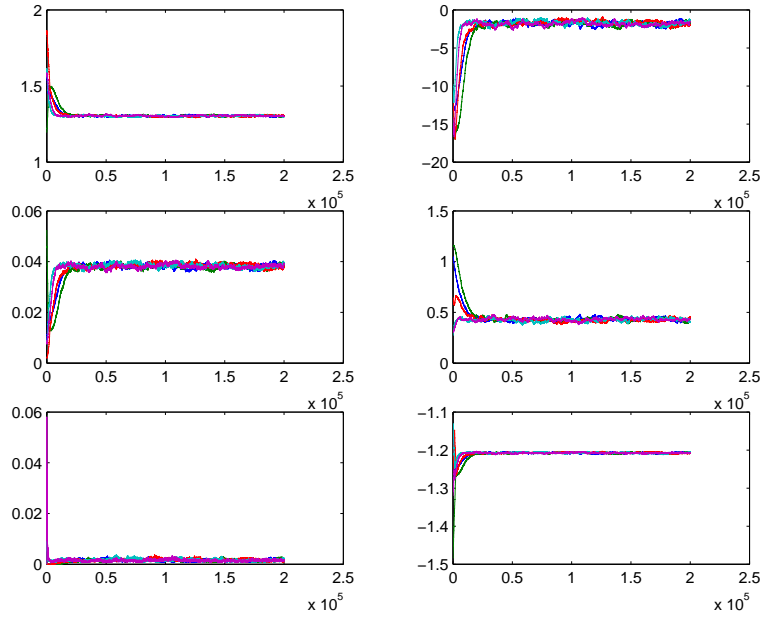

Figure C.3: **From left to right:** b, c, $\ln(a)$, ψ, τ^2 and ϵ. The generated Markov chains for each parameter converging to the mode of the posterior distribution from their respective initial value.
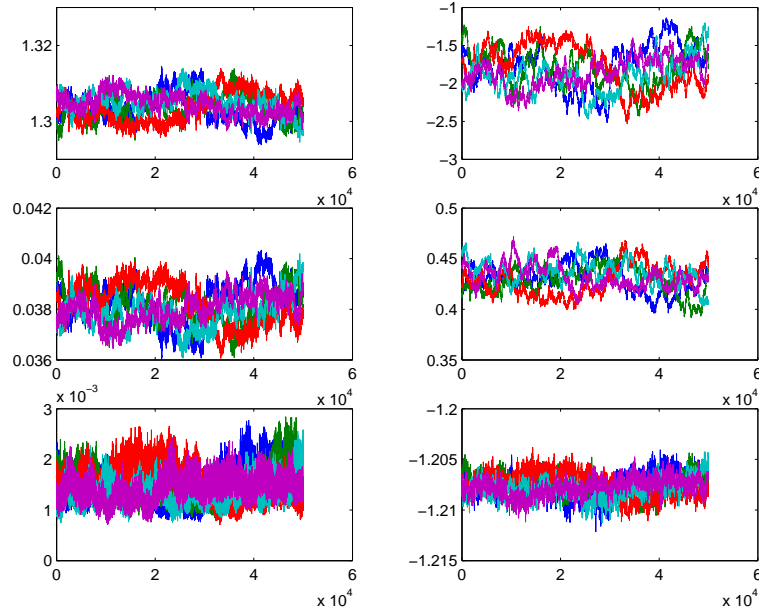
Figure C.4: **From left to right:** b, c, $\ln(a)$, ψ, τ^2 and ϵ. The mixing of the Markov chains after the burn-in period.
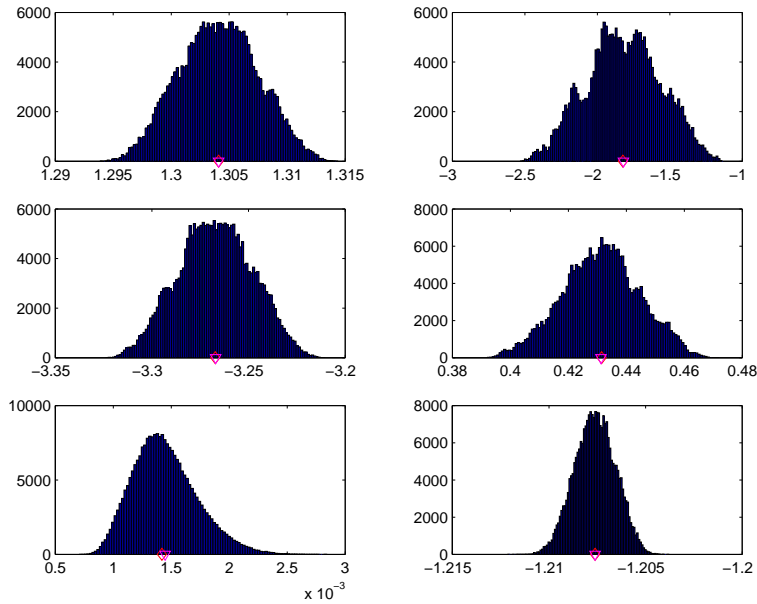
Figure C.5: **From left to right:** b, c, $\ln(a)$, ψ, τ^2 and ϵ. The resulting posterior distributions for each parameter. On each figure the parameter estimates, the mean and the median, are shown.
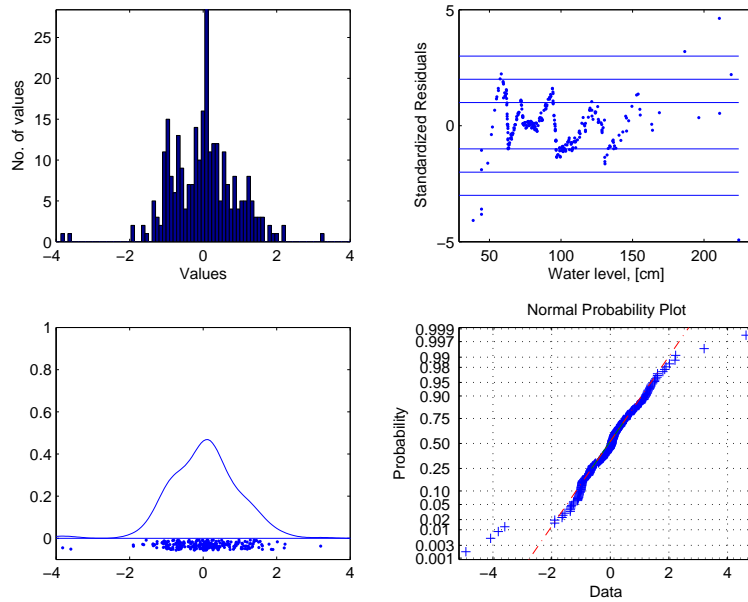
Figure C.6: **Upper left:** A histogram of the standardized residuals. **Upper right:** Standardized residuals from the estimated rating curve as a function of water level. **Lower left:** A smooth representation of the residual density. **Lower right:** A normal probability plot of standardized residuals.

Figure C.7: **Upper left:** The prior distribution for parameter ϵ. **Upper right:** The posterior distribution of parameter ϵ. **Lower left:** The prior distribution for parameter ψ. **Lower right:** The posterior distribution of parameter ψ.
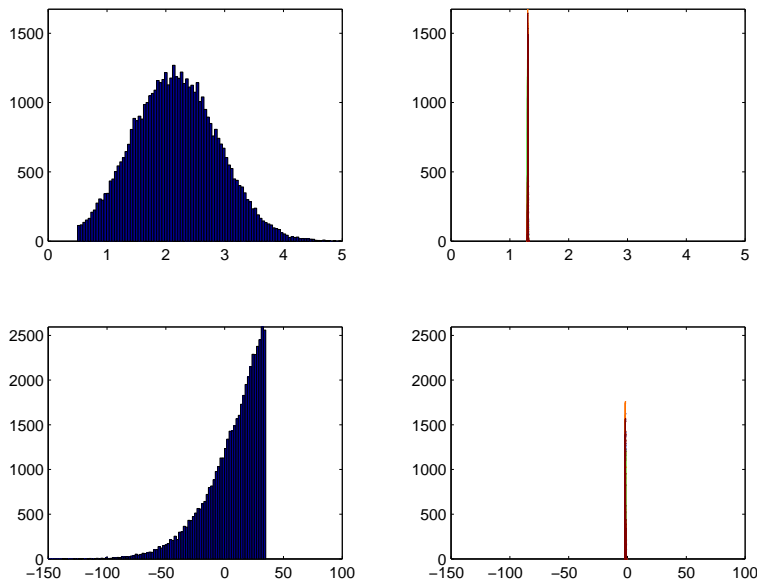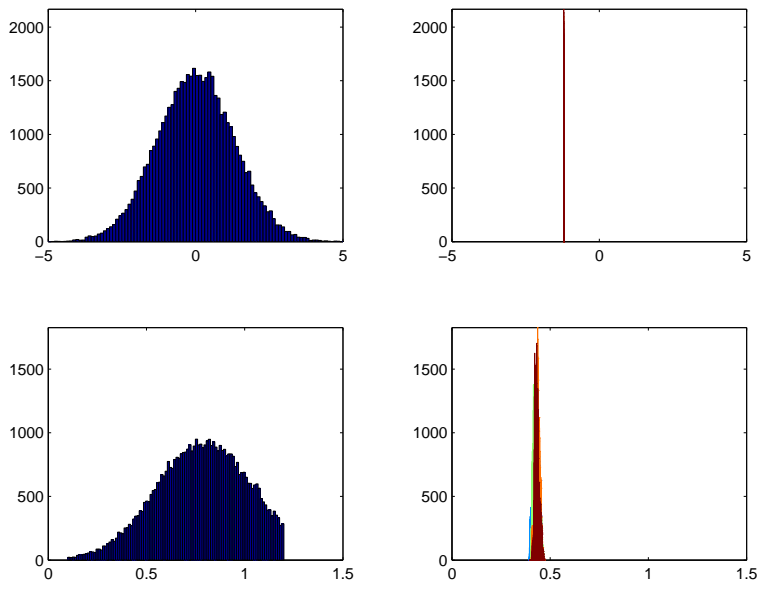
Figure C.8: **Upper left:** The prior distribution for parameter b. **Upper right:** The posterior distribution of parameter b. **Lower left:** The prior distribution for parameter c. **Lower right:** The posterior distribution of parameter c.

C.1.2 Case 2, Station DK_2, Odense å

Table C.2: Parameter estimates based on the Odense å data and other relevant data.

| Station no. 2 in Denmark	ϵ	b	c	a	ψ	τ^2
Nonlinear estimate	-0.378	2.195	66.223	7.3e-004	-	6.6e-009
Parameter estimate, mean	-0.608	1.989	68.329	1.7e-003	0.718	2.0e-006
Parameter estimate, median	-0.608	1.990	68.321	1.8e-003	0.719	2.1e-006
Acceptance ratio	0.32	0.45	0.43	-	0.54	-
$\widehat{R}$ ratio	1.65	1.70	1.67	-	1.52	1.56
Tuning parameter	5e-006	5e-008	1e-002	-	5e-006	-
2.5% percentile	-0.642	1.953	67.725	1.5e-003	0.685	8.8e-007
25.0% percentile	-0.622	1.973	68.096	1.6e-003	0.704	1.4e-006
50.0% percentile	-0.608	1.989	68.329	1.7e-003	0.718	2.0e-006
75.0% percentile	-0.594	2.005	68.561	1.9e-003	0.732	2.6e-006
97.5% percentile	-0.571	2.031	68.856	2.1e-003	0.756	3.9e-006
Skewness	0.110	0.127	-0.128	0.080	0.099	0.853
Kurtosis	2.61	2.52	2.55	2.51	2.66	2.66
Standard Deviation	1.9e-002	2.1e-002	3.1e-001	1.6e-004	1.9e-002	8.2e-007
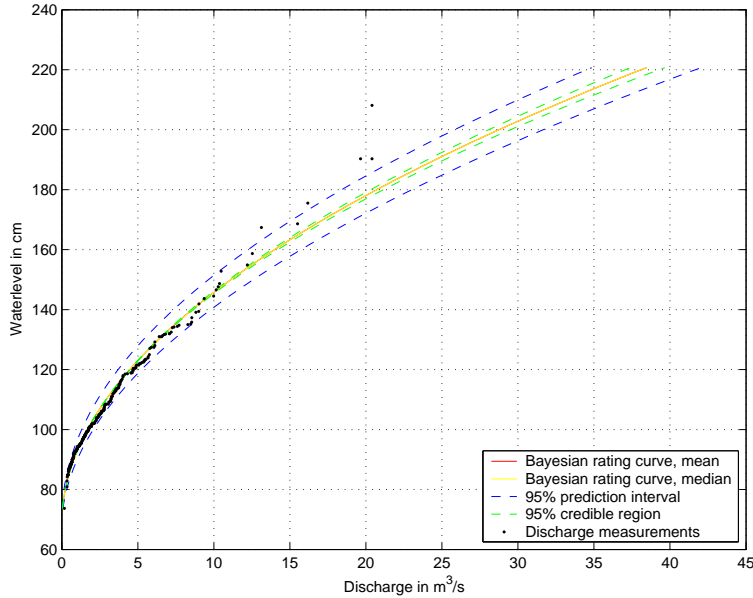
Figure C.9: The estimated rating curve using the parameters a, b and c in Table C.2. 95% prediction intervals for the discharge measurements are shown, as well as the 95% credible regions for the rating curve. Here, the whole range of water levels is shown, $W_{\min}$ through $W_{\max}$.
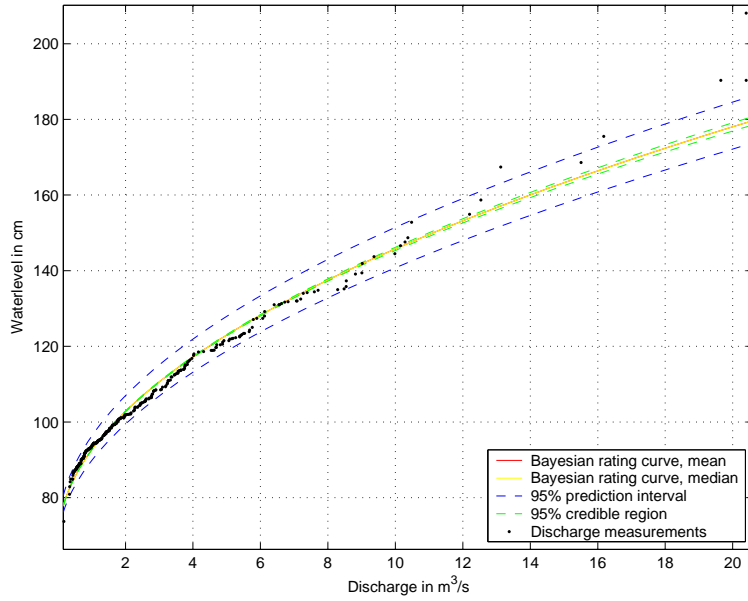
XXIII

Figure C.10: The estimated rating curve using the parameters a, b and c in Table C.2. 95% prediction intervals for the discharge measurements are shown, as well as the 95% credible regions for the rating curve. Here, the range of water levels shown is, Q_{min} through Q_{max}.
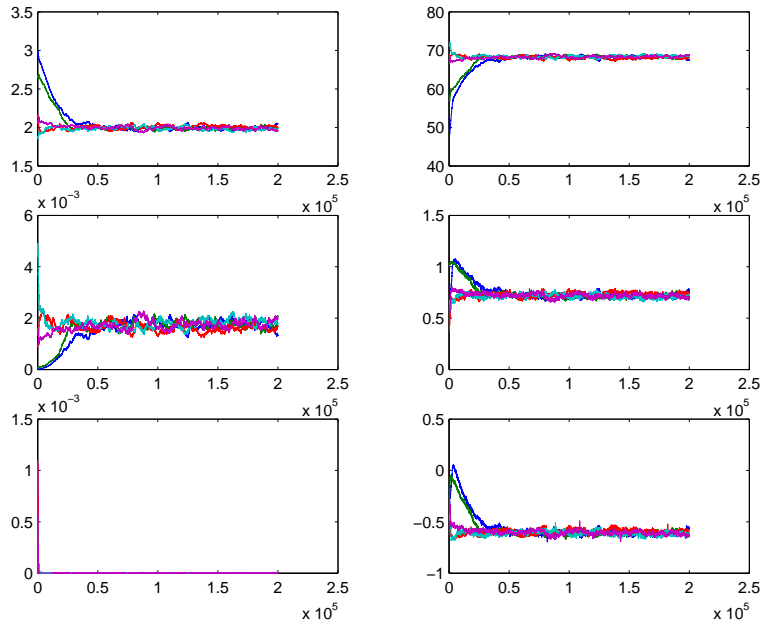

Figure C.11: **From left to right:** b, c, $\ln(a)$, ψ, τ^2 and ϵ. The generated Markov chains for each parameter converging to the mode of the posterior distribution from their respective initial value.
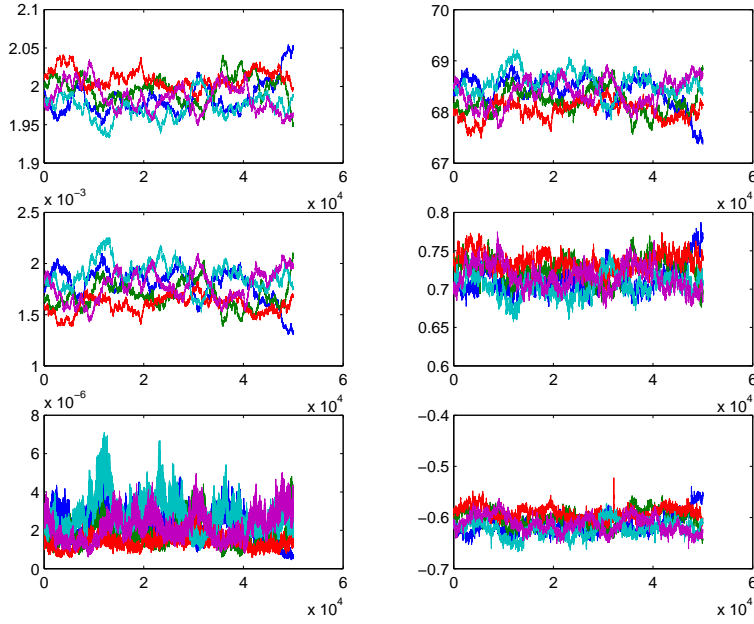
Figure C.12: **From left to right:** b, c, $\ln(a)$, ψ, τ^2 and ϵ. The mixing of the Markov chains after the burn-in period.
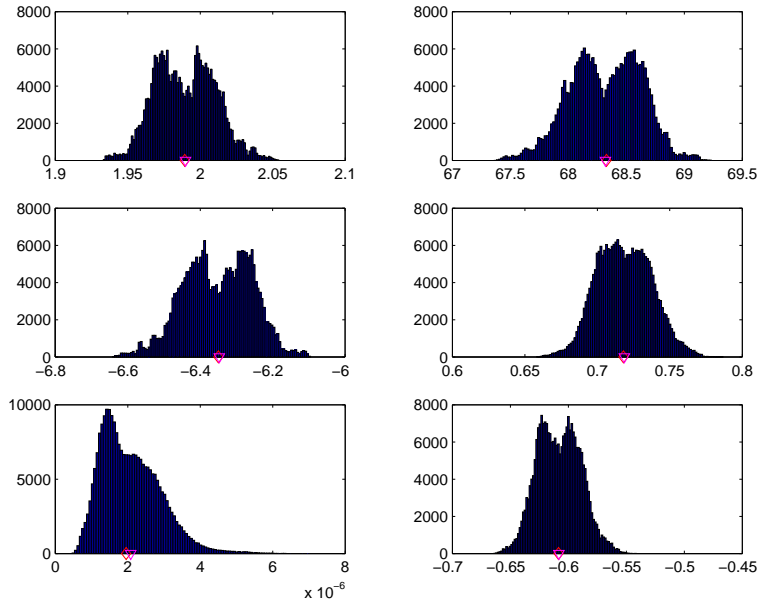
Figure C.13: **From left to right:** b, c, $\ln(a)$, ψ, τ^2 and ϵ. The resulting posterior distributions for each parameter. On each figure the parameter estimates, the mean and the median, are shown.
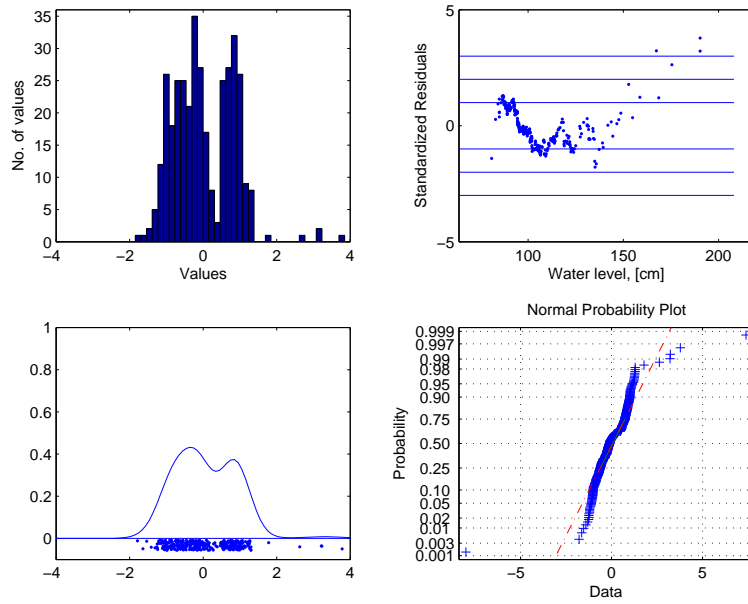
Figure C.14: **Upper left:** A histogram of the standardized residuals. **Upper right:** Standardized residuals from the estimated rating curve as a function of water level. **Lower left:** A smooth representation of the residual density. **Lower right:** A normal probability plot of standardized residuals.

Figure C.15: **Upper left:** The prior distribution for parameter ϵ. **Upper right:** The posterior distribution of parameter ϵ. **Lower left:** The prior distribution for parameter ψ. **Lower right:** The posterior distribution of parameter ψ.
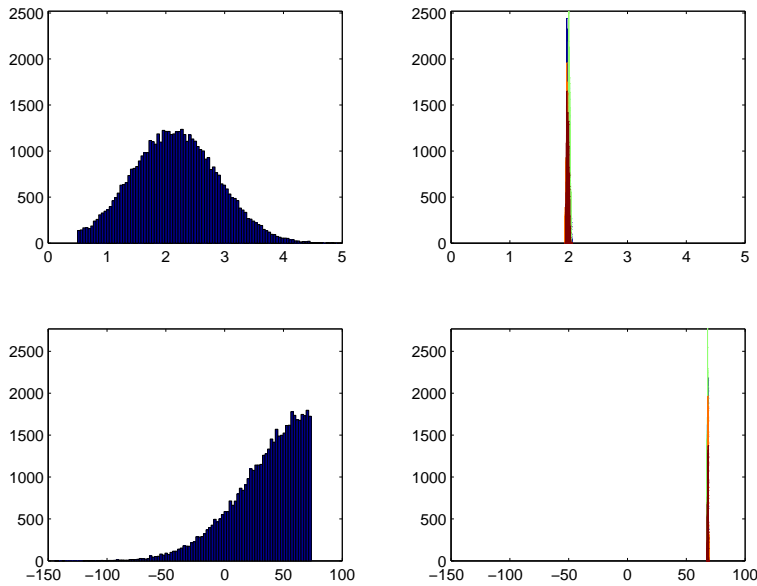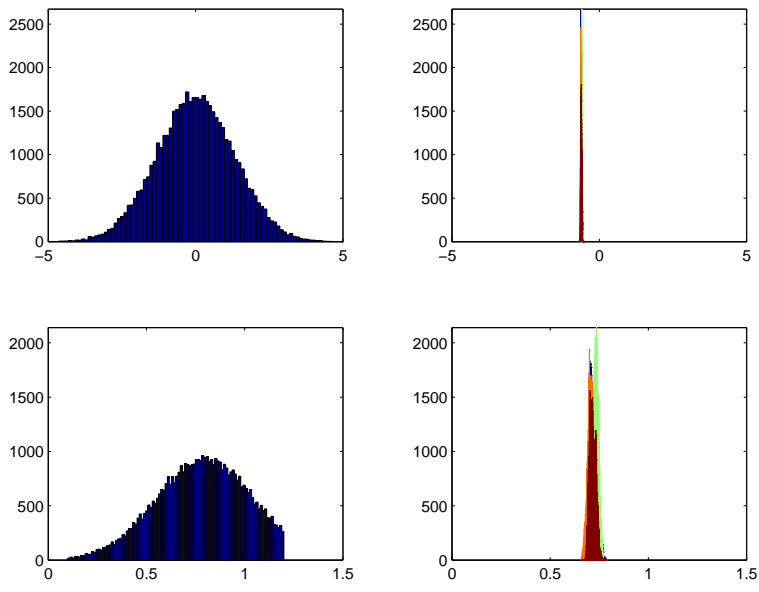
Figure C.16: **Upper left:** The prior distribution for parameter b. **Upper right:** The posterior distribution of parameter b. **Lower left:** The prior distribution for parameter c. **Lower right:** The posterior distribution of parameter c.

C.1.3 Case 3, Station FI_1, Lake Lannevesi

Table C.3: Parameter estimates based on the Lake Lannevesi data and other relevant data.

Station no. 1 in Finland	ϵ	b	c	a	ψ	τ^2
Nonlinear estimate	-1.532	1.878	4.717	1.3e-03	-	9.1e-09
Parameter estimate, mean	-1.555	1.800	6.960	1.9e-03	0.185	6.7e-04
Parameter estimate, median	-1.556	1.804	6.813	1.9e-03	0.185	8.4e-04
Acceptance ratio	0.37	0.45	0.36	-	0.50	-
$\widehat{R}$ ratio	1.02	2.05	1.94	-	1.08	1.01
Tuning parameter	4e-06	5e-08	2e-01	-	1e-05	-
2.5% percentile	-1.571	1.738	3.723	1.2e-03	0.167	2.6e-04
25.0% percentile	-1.560	1.775	5.628	1.6e-03	0.178	4.7e-04
50.0% percentile	-1.555	1.800	6.960	1.9e-03	0.185	6.7e-04
75.0% percentile	-1.551	1.834	7.999	2.1e-03	0.192	1.0e-03
97.5% percentile	-1.541	1.879	9.573	2.6e-03	0.205	2.4e-03
Skewness	-0.164	0.194	-0.180	0.202	0.189	5.843
Kurtosis	5.07	2.30	2.40	2.44	2.97	2.97
Standard Deviation	7.4e-03	3.9e-02	1.6e+00	3.8e-04	9.7e-03	6.5e-04

Figure C.17: The estimated rating curve using the parameters a, b and c in Table C.3. 95% prediction intervals for the discharge measurements are shown, as well as the 95% credible regions for the rating curve. Here, the whole range of water levels is shown, $W_{\min}$ through $W_{\max}$.
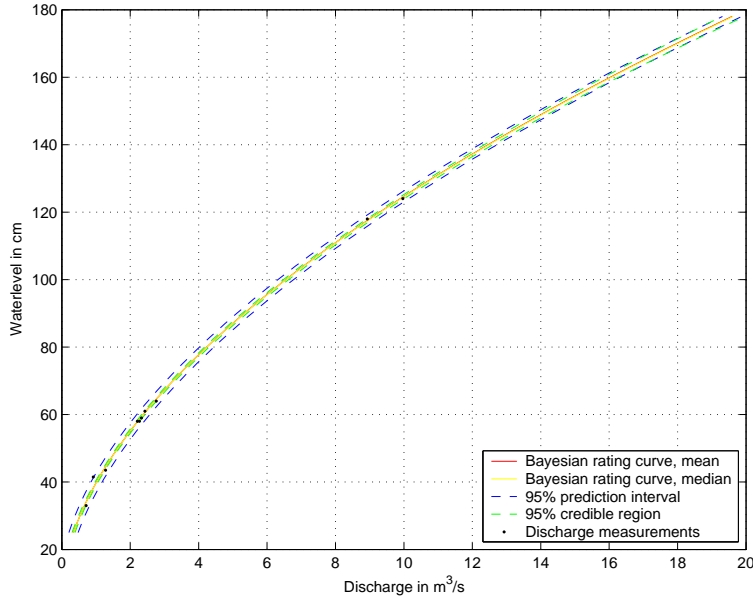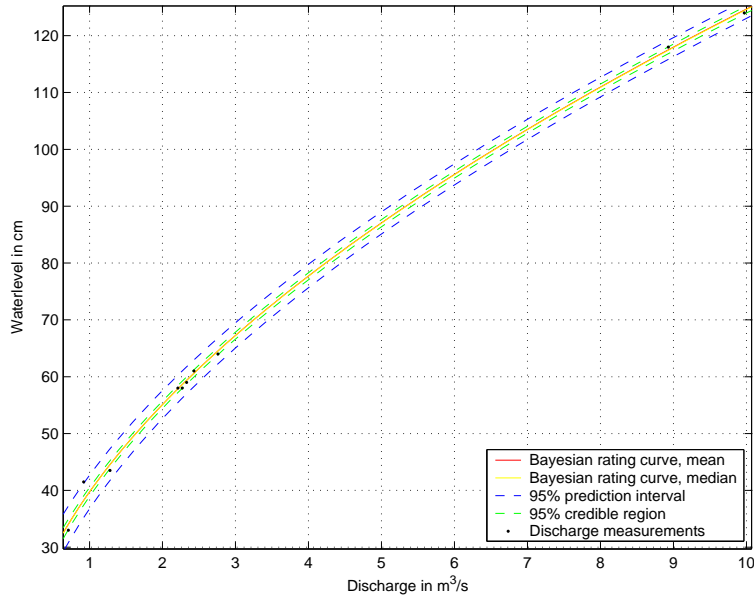
Figure C.18: The estimated rating curve using the parameters a, b and c in Table C.3. 95% prediction intervals for the discharge measurements are shown, as well as the 95% credible regions for the rating curve. Here, the range of water levels shown is, Q_{min} through Q_{max}.
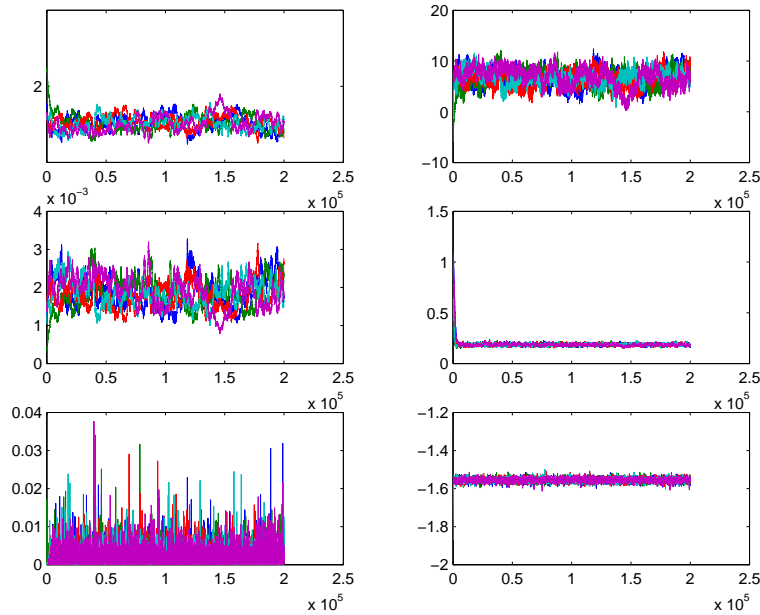

Figure C.19: **From left to right:** b, c, $\ln(a)$, ψ, τ^2 and ϵ. The generated Markov chains for each parameter converging to the mode of the posterior distribution from their respective initial value.

XXIX
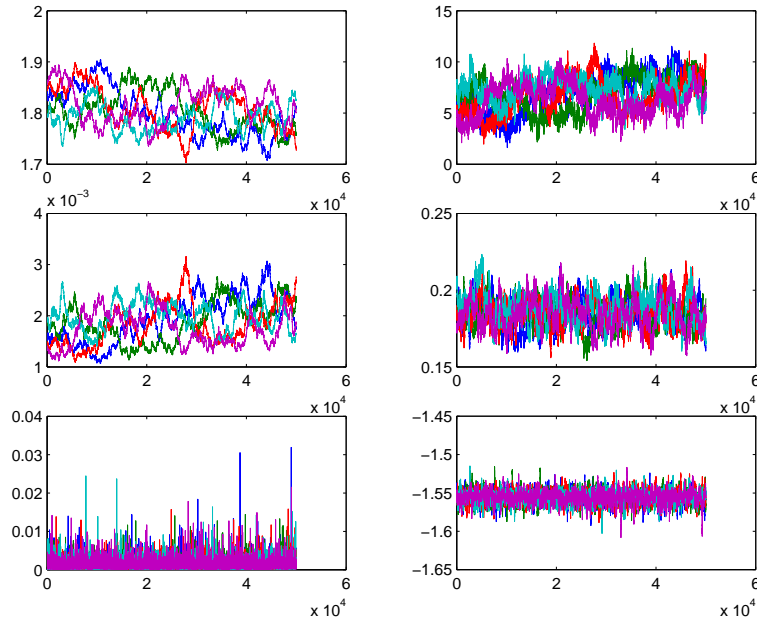
Figure C.20: **From left to right:** b, c, $\ln(a)$, ψ, τ^2 and ϵ. The mixing of the Markov chains after the burn-in period.
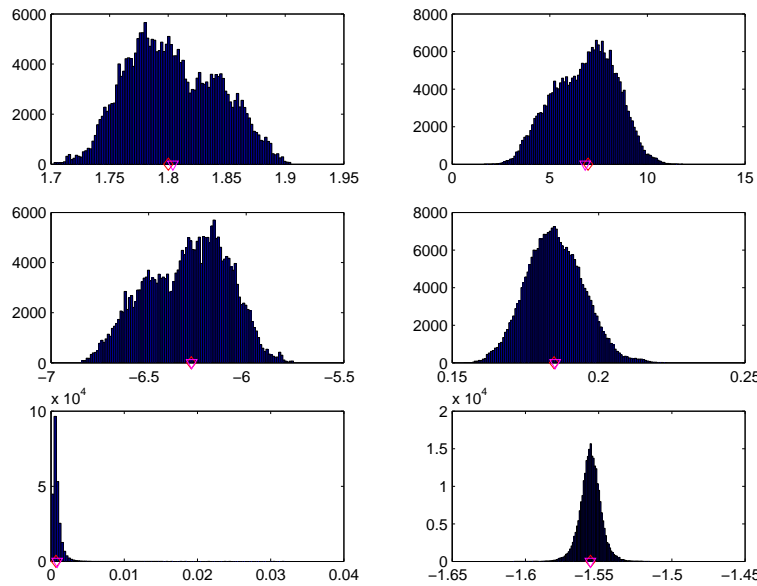
Figure C.21: **From left to right:** b, c, $\ln(a)$, ψ, τ^2 and ϵ. The resulting posterior distributions for each parameter. On each figure the parameter estimates, the mean and the median, are shown.
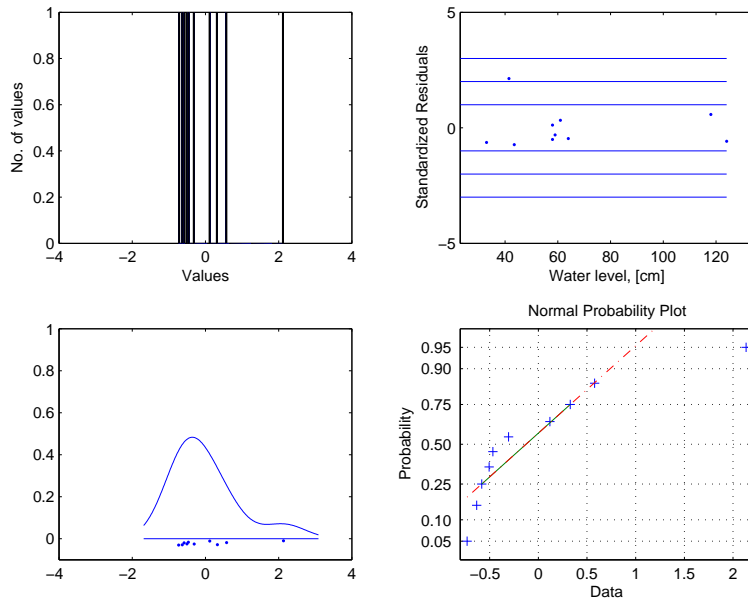
Figure C.22: **Upper left:** A histogram of the standardized residuals. **Upper right:** Standardized residuals from the estimated rating curve as a function of water level. **Lower left:** A smooth representation of the residual density. **Lower right:** A normal probability plot of standardized residuals.

Figure C.23: **Upper left:** The prior distribution for parameter ϵ. **Upper right:** The posterior distribution of parameter ϵ. **Lower left:** The prior distribution for parameter ψ. **Lower right:** The posterior distribution of parameter ψ.

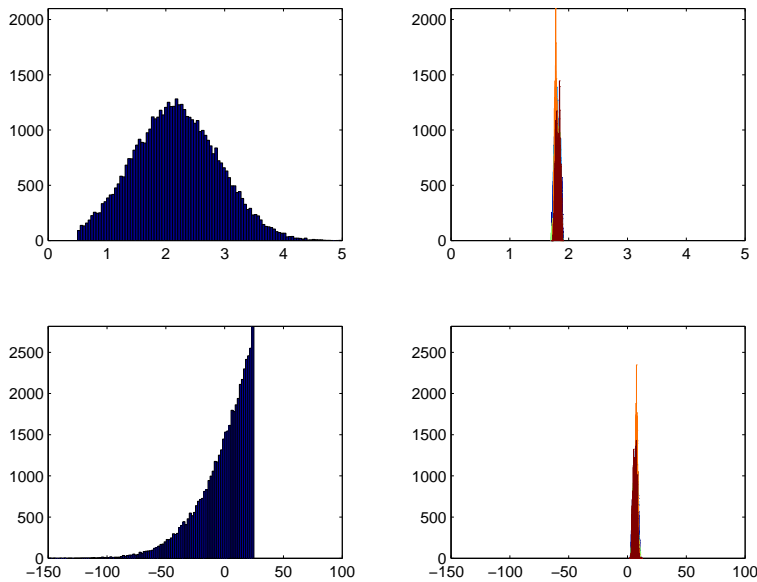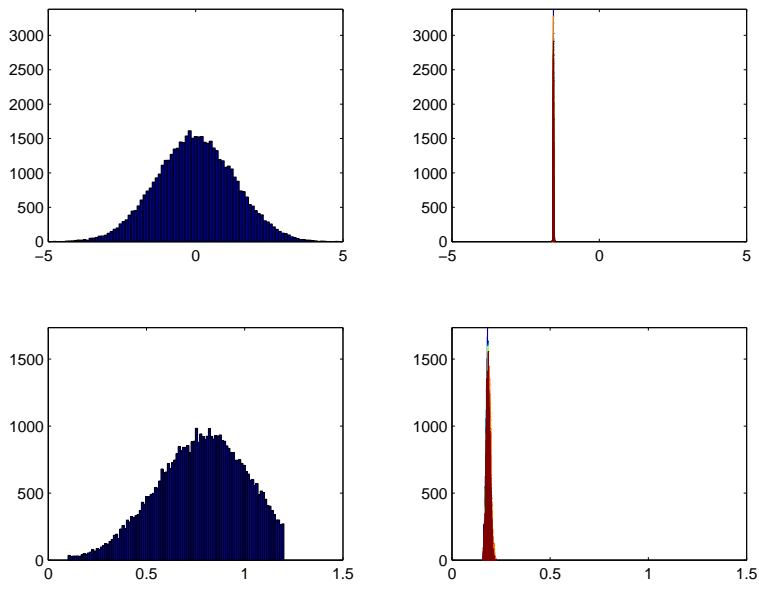Figure C.24: **Upper left:** The prior distribution for parameter b. **Upper right:** The posterior distribution of parameter b. **Lower left:** The prior distribution for parameter c. **Lower right:** The posterior distribution of parameter c.

C.1.4 Case 4, Station FI_2, Lake Vahvajarvi

Table C.4: Parameter estimates based on the Lake Vahvajarvi data and other relevant data.

Station no. 2 in Finland	ϵ	b	c	a	ψ	τ^2
Nonlinear estimate	-1.076	2.082	-52.720	6.6e-04	-	6.8e-10
Parameter estimate, mean	-0.901	1.835	-33.121	3.0e-03	0.191	2.3e-02
Parameter estimate, median	-0.902	1.836	-33.179	3.0e-03	0.193	2.6e-02
Acceptance ratio	0.18	0.47	0.19	-	0.51	-
$\widehat{R}$ ratio	1.49	1.49	1.50	-	1.20	1.08
Tuning parameter	4e-06	5e-08	2e-01	-	1e-05	-
2.5% percentile	-0.935	1.785	-37.395	2.1e-03	0.167	8.7e-03
25.0% percentile	-0.912	1.818	-34.547	2.7e-03	0.181	1.6e-02
50.0% percentile	-0.901	1.835	-33.121	3.0e-03	0.191	2.3e-02
75.0% percentile	-0.891	1.854	-31.794	3.3e-03	0.202	3.2e-02
97.5% percentile	-0.872	1.893	-29.340	4.0e-03	0.226	6.6e-02
Skewness	-0.199	0.152	-0.147	0.255	0.539	2.646
Kurtosis	2.86	2.83	2.82	2.78	3.52	3.52
Standard Deviation	1.6e-02	2.6e-02	2.0e+00	4.7e-04	1.5e-02	1.5e-02

Figure C.25: The estimated rating curve using the parameters a, b and c in Table C.4. 95% prediction intervals for the discharge measurements are shown, as well as the 95% credible regions for the rating curve. Here, the whole range of water levels is shown, $W_{\min}$ through $W_{\max}$.
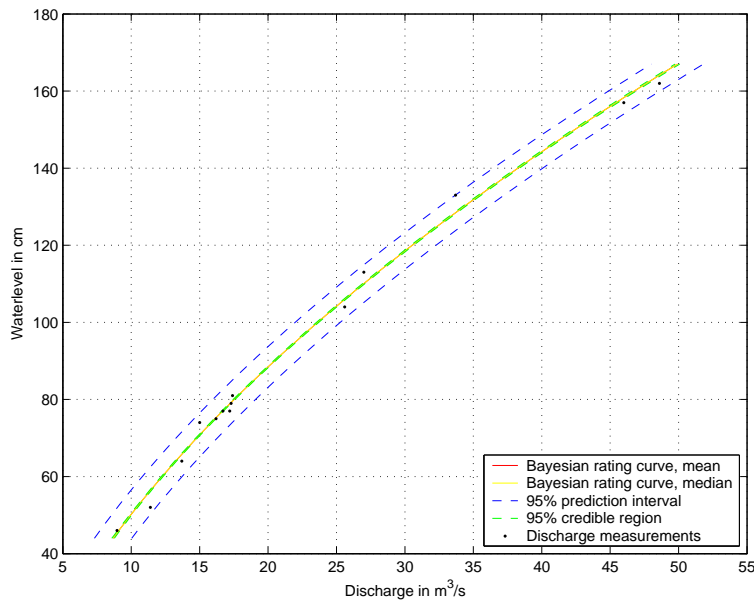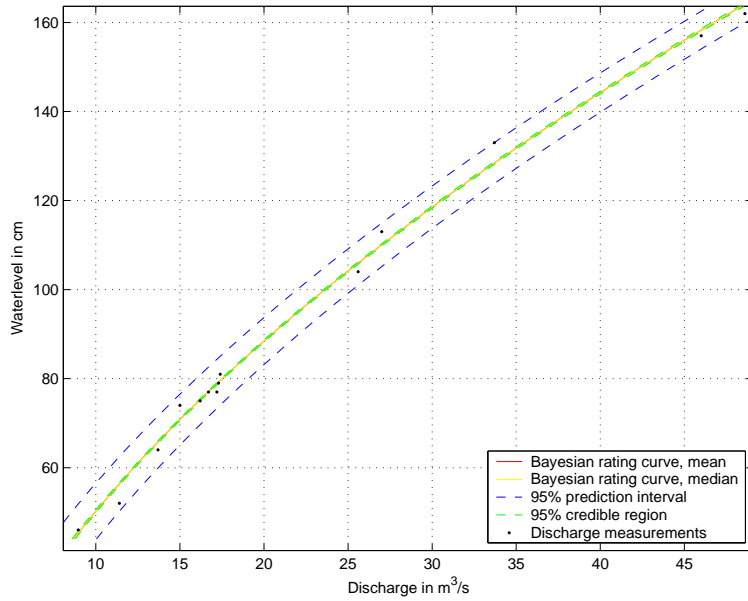
Figure C.26: The estimated rating curve using the parameters a, b and c in Table C.4. 95% prediction intervals for the discharge measurements are shown, as well as the 95% credible regions for the rating curve. Here, the range of water levels shown is, Q_{min} through Q_{max}.
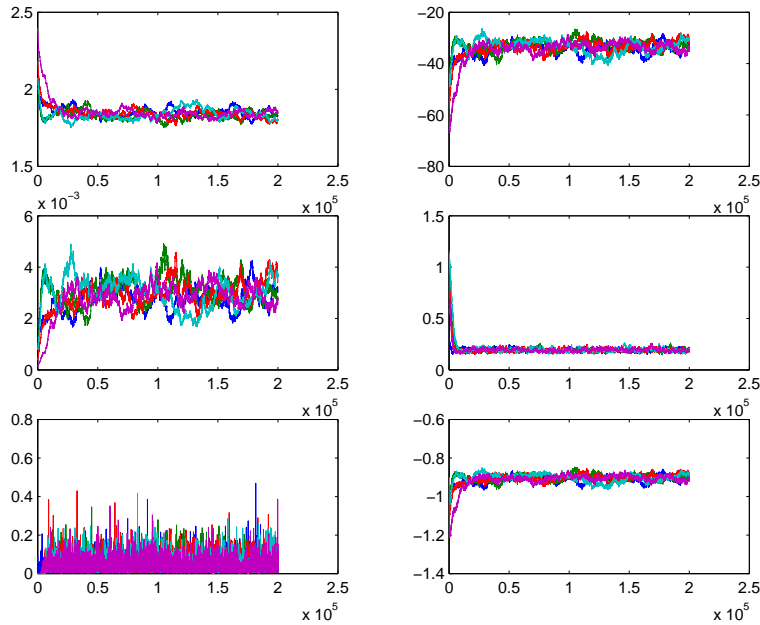

Figure C.27: **From left to right:** b, c, $\ln(a)$, ψ, τ^2 and ϵ. The generated Markov chains for each parameter converging to the mode of the posterior distribution from their respective initial value.
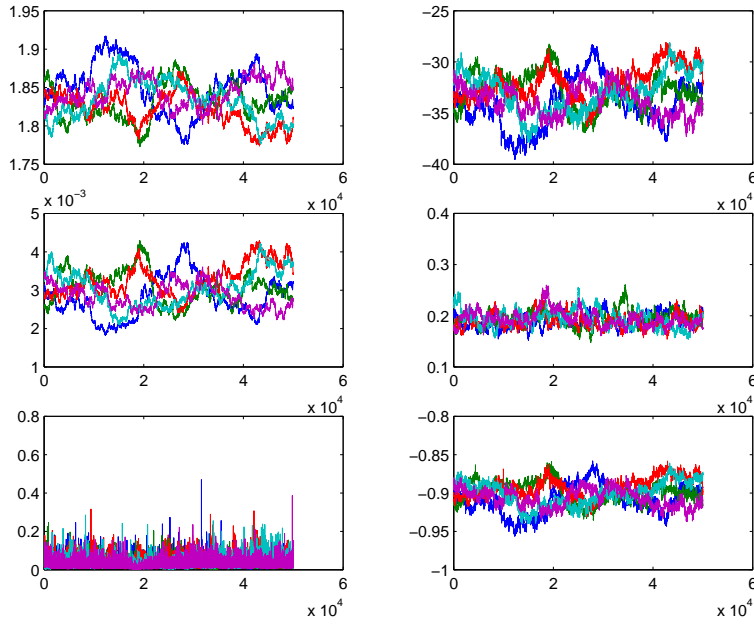
Figure C.28: **From left to right:** b, c, $\ln(a)$, ψ, τ^2 and ϵ. The mixing of the Markov chains after the burn-in period.
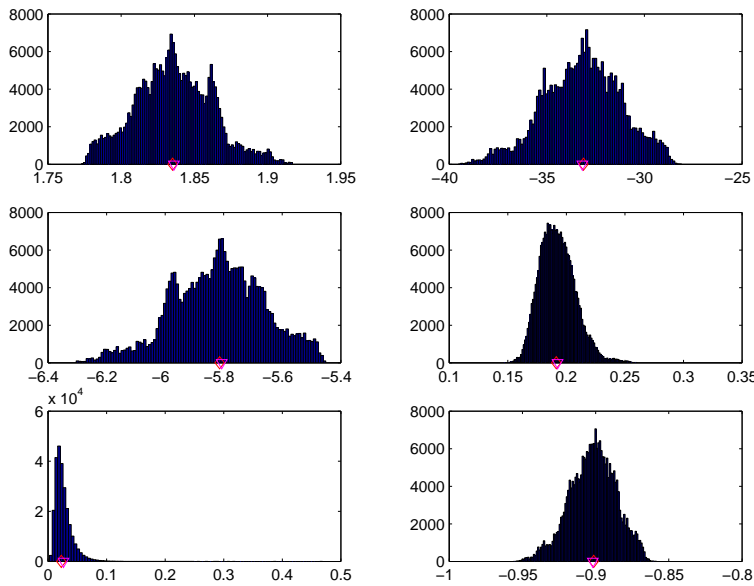
Figure C.29: **From left to right:** b, c, $\ln(a)$, ψ, τ^2 and ϵ. The resulting posterior distributions for each parameter. On each figure the parameter estimates, the mean and the median, are shown.

XXXV
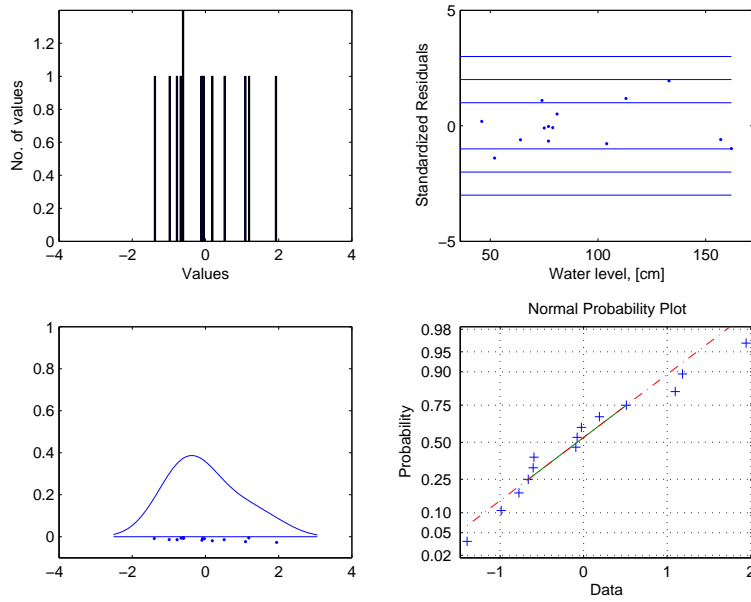
Figure C.30: **Upper left:** A histogram of the standardized residuals. **Upper right:** Standardized residuals from the estimated rating curve as a function of water level. **Lower left:** A smooth representation of the residual density. **Lower right:** A normal probability plot of standardized residuals.

Figure C.31: **Upper left:** The prior distribution for parameter ϵ. **Upper right:** The posterior distribution of parameter ϵ. **Lower left:** The prior distribution for parameter ψ. **Lower right:** The posterior distribution of parameter ψ.

Figure C.32: **Upper left:** The prior distribution for parameter b. **Upper right:** The posterior distribution of parameter b. **Lower left:** The prior distribution for parameter c. **Lower right:** The posterior distribution of parameter c.
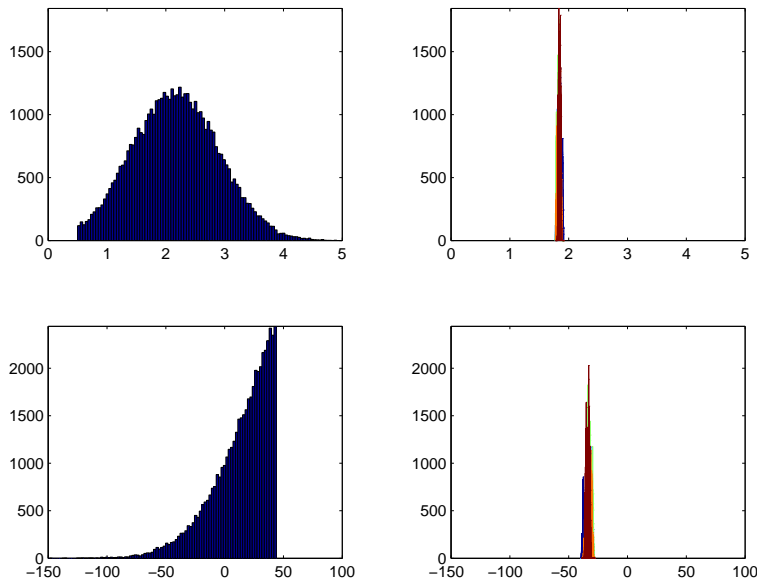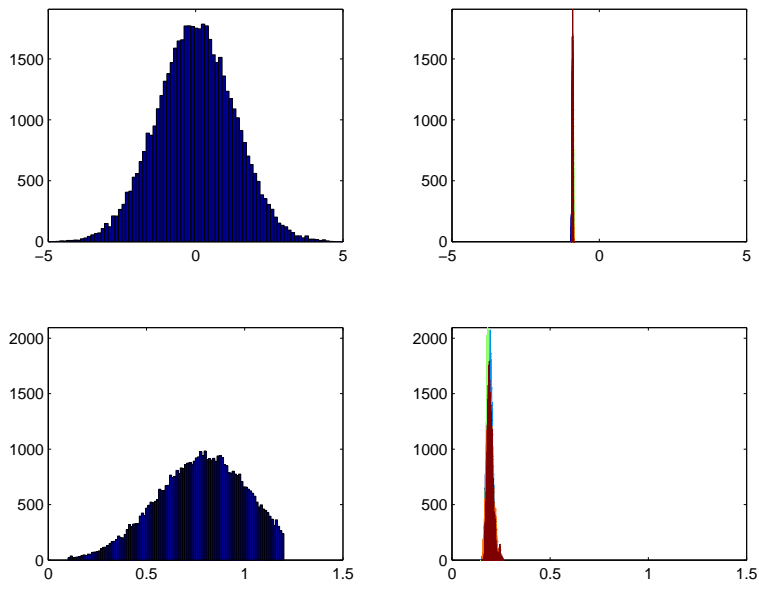
C.1.5   Case 5, Station IS_1, Skjálfandafljót

Table C.5: Parameter estimates based on the Skjálfandafljót data and other relevant data.

Station no. 1 in Iceland	ϵ	b	c	a	ψ	τ^2
Nonlinear estimate	-0.964	3.327	-17.455	9.3e-07	-	1.1e-15
Parameter estimate, mean	-0.342	2.759	25.337	3.7e-05	0.281	3.7e-03
Parameter estimate, median	-0.342	2.759	25.324	3.7e-05	0.283	7.6e-03
Acceptance ratio	0.31	0.49	0.32	-	0.53	-
$\widehat{R}$ ratio	2.52	2.55	2.50	-	2.03	2.00
Tuning parameter	4e-06	5e-08	2e-01	-	1e-05	-
2.5% percentile	-0.419	2.691	19.546	2.4e-05	0.205	1.3e-04
25.0% percentile	-0.370	2.735	23.195	3.1e-05	0.253	1.6e-03
50.0% percentile	-0.342	2.759	25.337	3.7e-05	0.281	3.7e-03
75.0% percentile	-0.315	2.783	27.419	4.3e-05	0.307	8.6e-03
97.5% percentile	-0.264	2.826	31.189	5.7e-05	0.385	4.0e-02
Skewness	0.022	-0.029	0.044	0.585	0.466	3.320
Kurtosis	2.59	2.59	2.60	3.13	3.16	3.16
Standard Deviation	4.0e-02	3.5e-02	3.0e+00	8.6e-06	4.5e-02	1.1e-02

Figure C.33: The estimated rating curve using the parameters a, b and c in Table C.5. 95% prediction intervals for the discharge measurements are shown, as well as the 95% credible regions for the rating curve. Here, the whole range of water levels is shown, $W_{\min}$ through $W_{\max}$.
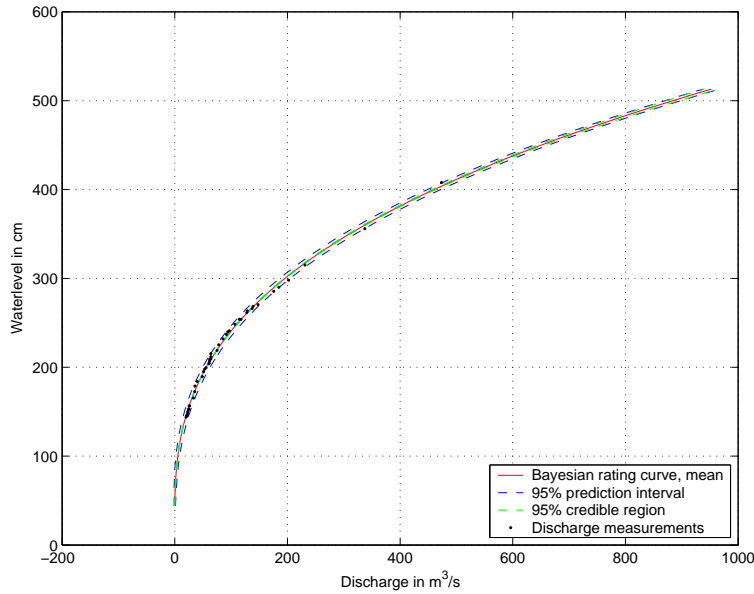
Figure C.34: The estimated rating curve using the parameters a, b and c in Table C.5. 95% prediction intervals for the discharge measurements are shown, as well as the 95% credible regions for the rating curve. Here, the range of water levels shown is, Q_{min} through Q_{max}.

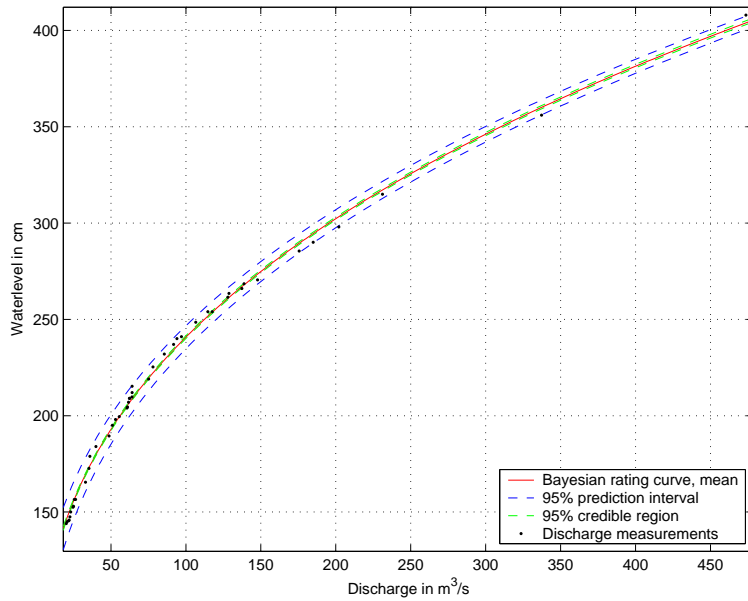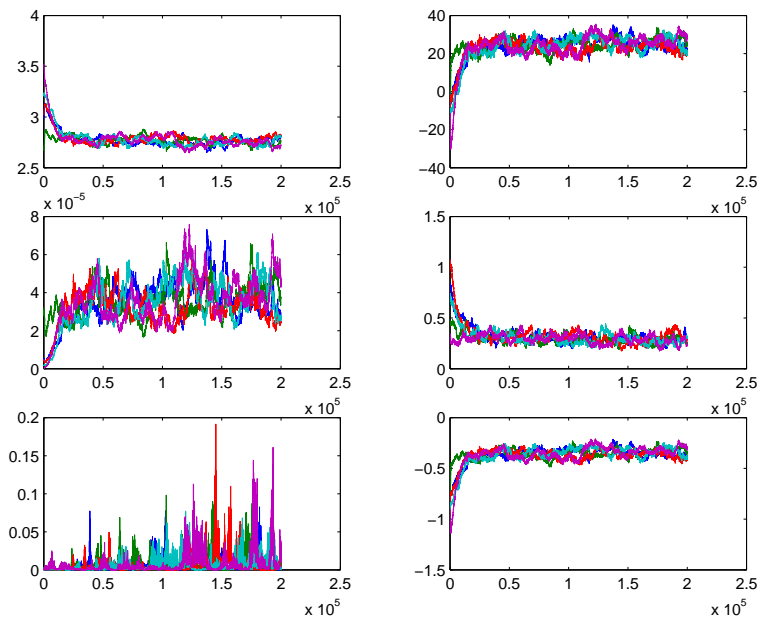Figure C.35: **From left to right:** b, c, $\ln(a)$, ψ, τ^2 and ϵ. The generated Markov chains for each parameter converging to the mode of the posterior distribution from their respective initial value.
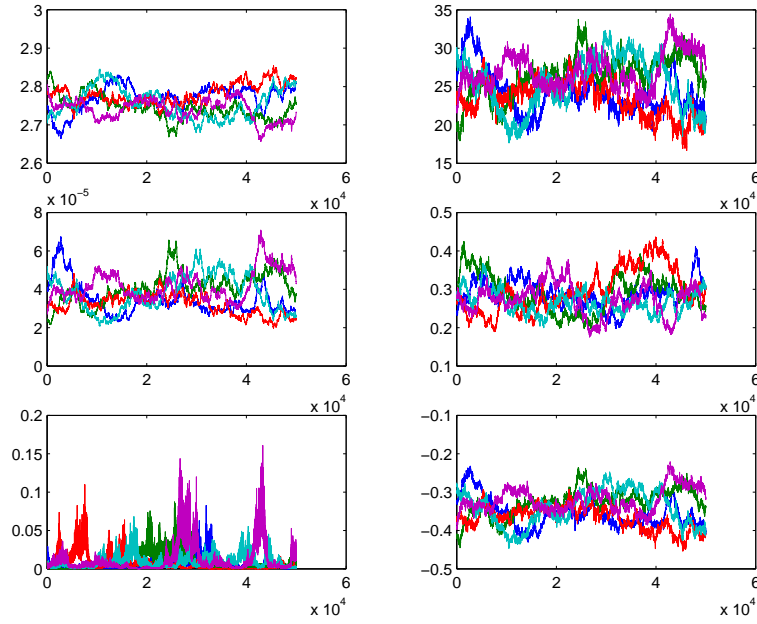
Figure C.36: **From left to right:** b, c, $\ln(a)$, ψ, τ^2 and ϵ. The mixing of the Markov chains after the burn-in period.
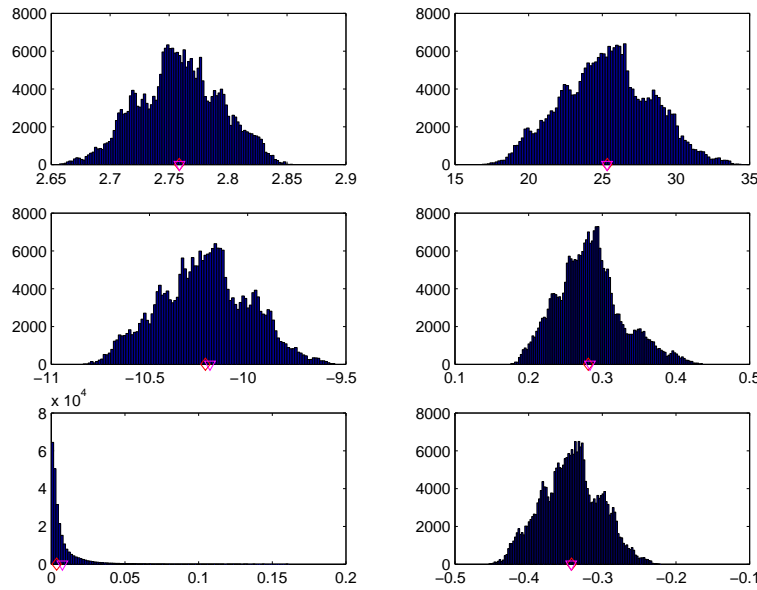
Figure C.37: **From left to right:** b, c, $\ln(a)$, ψ, τ^2 and ϵ. The resulting posterior distributions for each parameter. On each figure the parameter estimates, the mean and the median, are shown.

XL
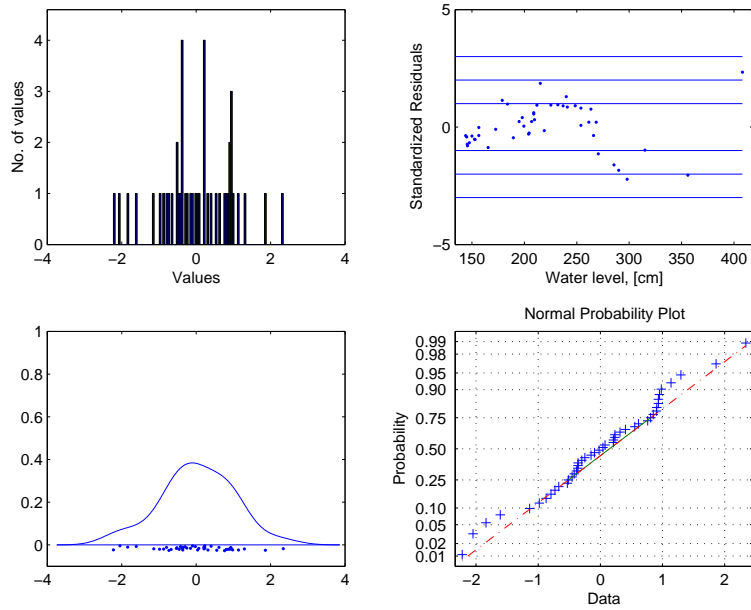
Figure C.38: **Upper left:** A histogram of the standardized residuals. **Upper right:** Standardized residuals from the estimated rating curve as a function of water level. **Lower left:** A smooth representation of the residual density. **Lower right:** A normal probability plot of standardized residuals.
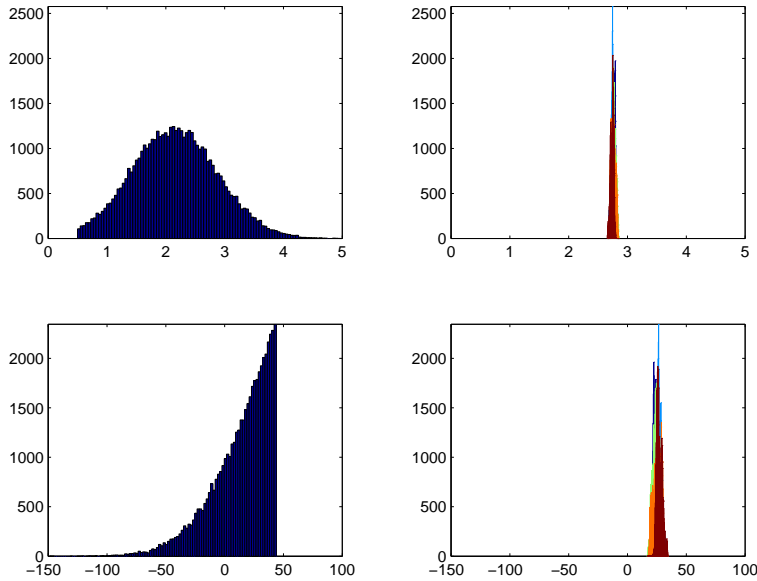
Figure C.39: **Upper left:** The prior distribution for parameter ϵ. **Upper right:** The posterior distribution of parameter ϵ. **Lower left:** The prior distribution for parameter ψ. **Lower right:** The posterior distribution of parameter ψ.

Figure C.40: **Upper left:** The prior distribution for parameter b. **Upper right:** The posterior distribution of parameter b. **Lower left:** The prior distribution for parameter c. **Lower right:** The posterior distribution of parameter c.

C.1.6 Case 6, Station IS_2, Fnjóská

Table C.6: Parameter estimates based on the Fnjóská data and other relevant data.
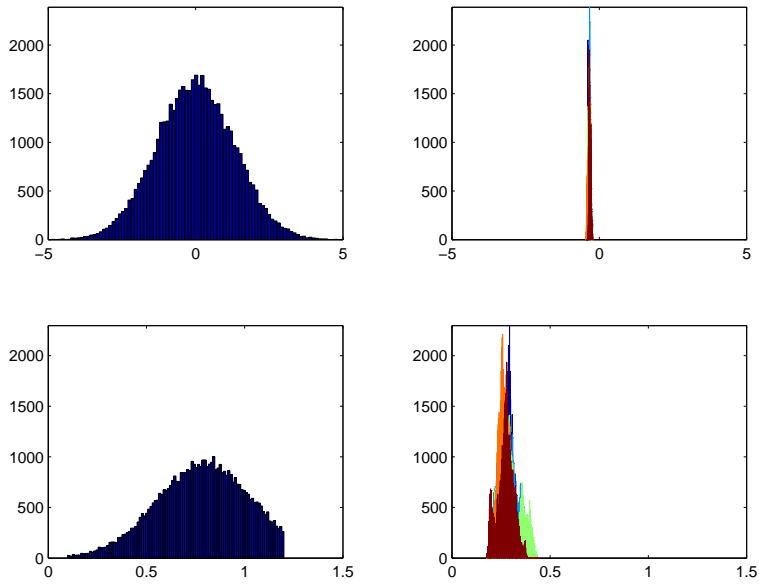
Station no. 2 in Iceland	ϵ	b	c	a	ψ	τ^2
Nonlinear estimate	0.990	2.023	71.587	7.2e-003	-	1.2e-007
Parameter estimate, mean	0.965	2.197	64.555	2.8e-003	0.208	5.9e-002
Parameter estimate, median	0.963	2.201	64.368	2.8e-003	0.213	7.2e-002
Acceptance ratio	0.45	0.44	0.40	-	0.53	-
$\widehat{R}$ ratio	1.26	1.38	1.38	-	1.14	1.08
Tuning parameter	7e-006	5e-007	1e-001	-	5e-005	-
2.5% percentile	0.922	2.108	59.236	1.4e-003	0.153	9.1e-003
25.0% percentile	0.951	2.166	62.987	2.3e-003	0.186	3.5e-002
50.0% percentile	0.965	2.197	64.555	2.8e-003	0.208	5.9e-002
75.0% percentile	0.976	2.231	65.958	3.3e-003	0.234	9.5e-002
97.5% percentile	0.998	2.311	68.690	4.6e-003	0.302	2.1e-001
Skewness	-0.263	0.311	-0.324	0.583	0.734	4.050
Kurtosis	3.53	3.06	3.14	3.93	3.65	3.65
Standard Deviation	1.9e-002	5.1e-002	2.4e+000	8.0e-004	3.7e-002	5.7e-002

Figure C.41: The estimated rating curve using the parameters a, b and c in Table C.6. 95% prediction intervals for the discharge measurements are shown, as well as the 95% credible regions for the rating curve. Here, the whole range of water levels is shown, $W_{\min}$ through $W_{\max}$.
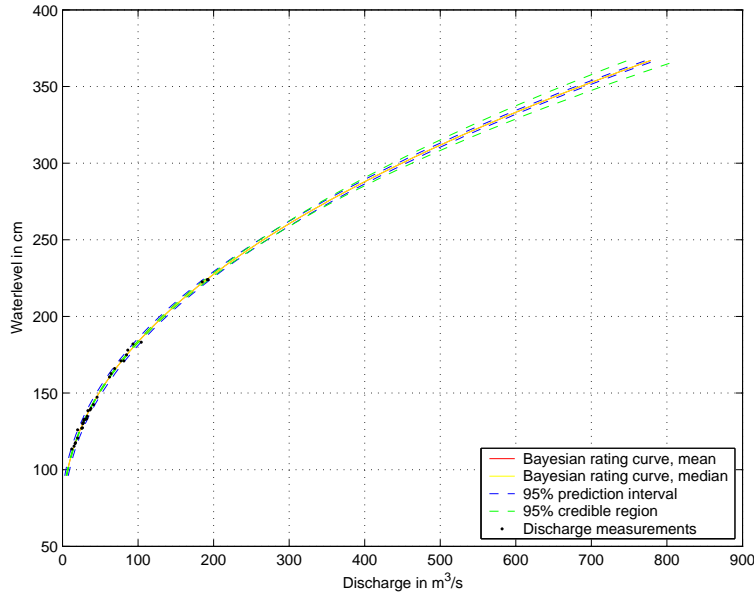
Figure C.42: The estimated rating curve using the parameters a, b and c in Table C.6. 95% prediction intervals for the discharge measurements are shown, as well as the 95% credible regions for the rating curve. Here, the range of water levels shown is, Q_{min} through Q_{max}.

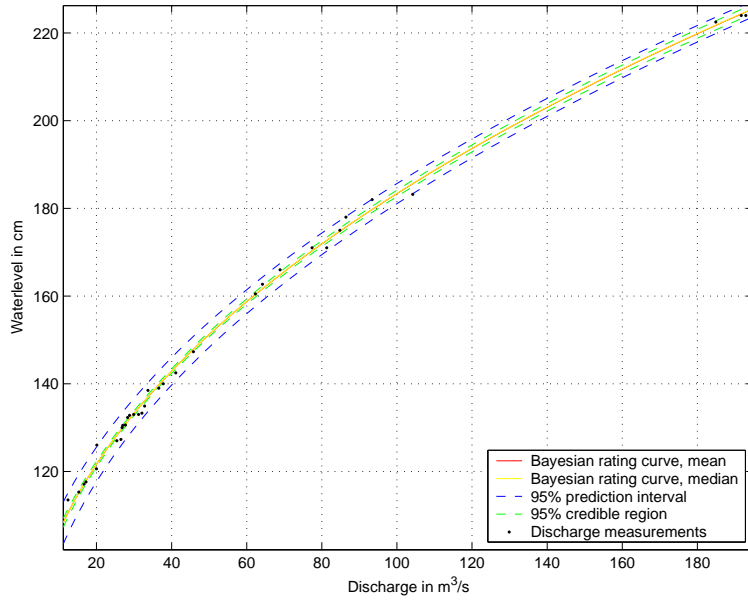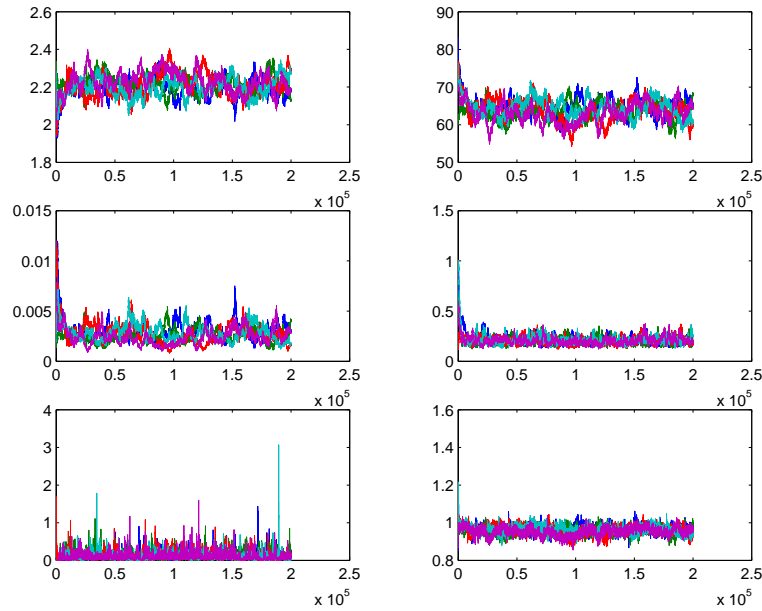Figure C.43: **From left to right:** b, c, $\ln(a)$, ψ, τ^2 and ϵ. The generated Markov chains for each parameter converging to the mode of the posterior distribution from their respective initial value.
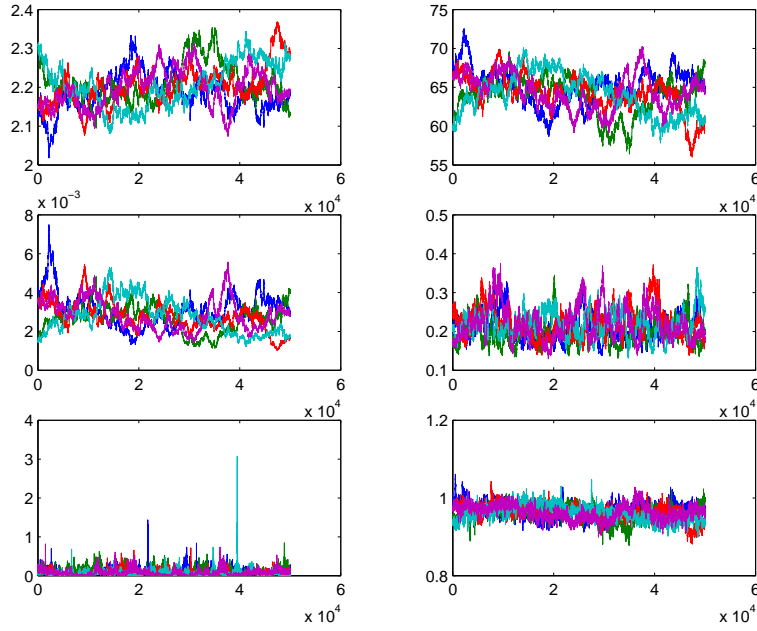
Figure C.44: **From left to right:** b, c, $\ln(a)$, ψ, τ^2 and ϵ. The mixing of the Markov chains after the burn-in period.
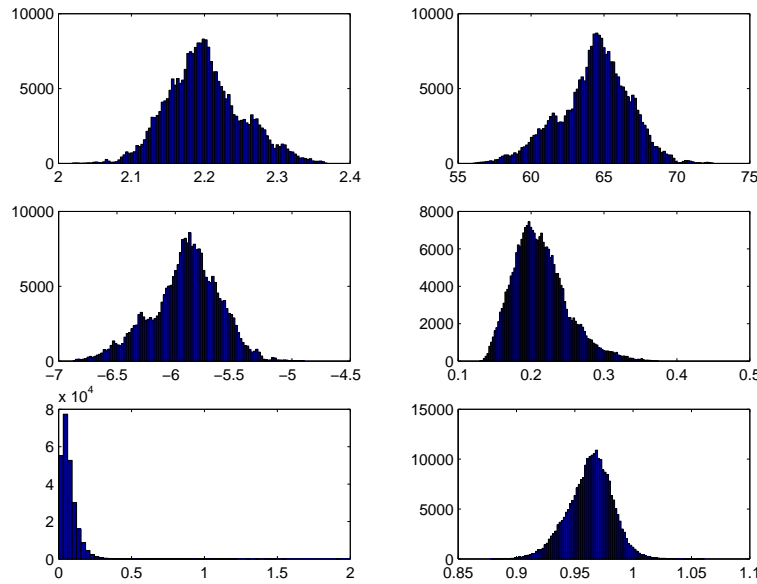
Figure C.45: **From left to right:** b, c, $\ln(a)$, ψ, τ^2 and ϵ. The resulting posterior distributions for each parameter. On each figure the parameter estimates, the mean and the median, are shown.
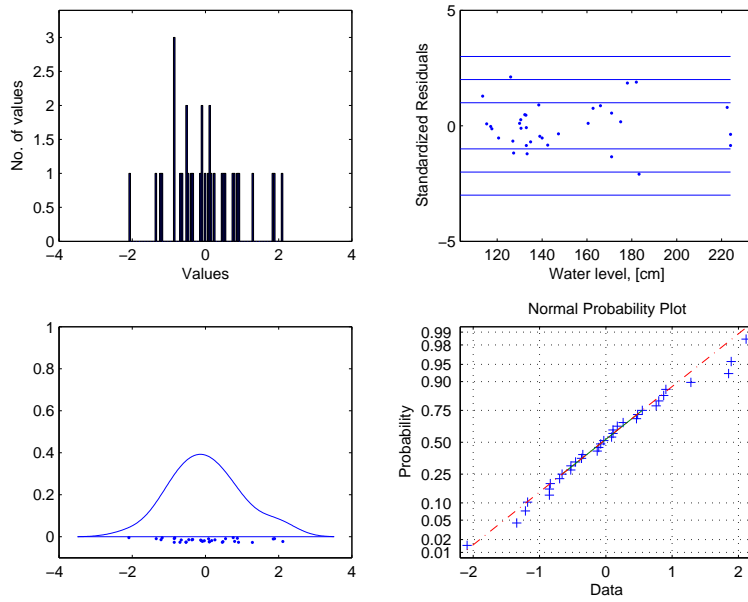
Figure C.46: **Upper left:** A histogram of the standardized residuals. **Upper right:** Standardized residuals from the estimated rating curve as a function of water level. **Lower left:** A smooth representation of the residual density. **Lower right:** A normal probability plot of standardized residuals.
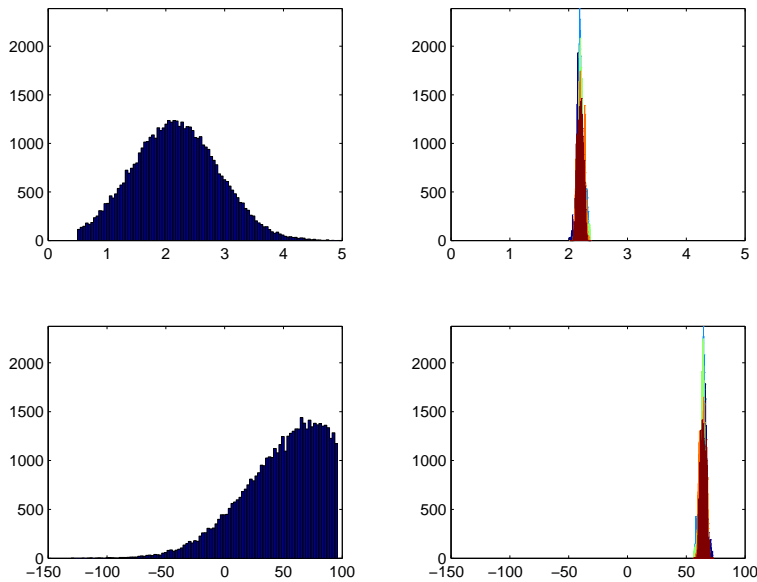
Figure C.47: **Upper left:** The prior distribution for parameter ϵ. **Upper right:** The posterior distribution of parameter ϵ. **Lower left:** The prior distribution for parameter ψ. **Lower right:** The posterior distribution of parameter ψ.

Figure C.48: **Upper left:** The prior distribution for parameter b. **Upper right:** The posterior distribution of parameter b. **Lower left:** The prior distribution for parameter c. **Lower right:** The posterior distribution of parameter c.

C.1.7 Case 7, Station NO_1, Gudbrandsdalslågen

Table C.7: Parameter estimates based on the Gudbrandsdalslågen data and other relevant data.

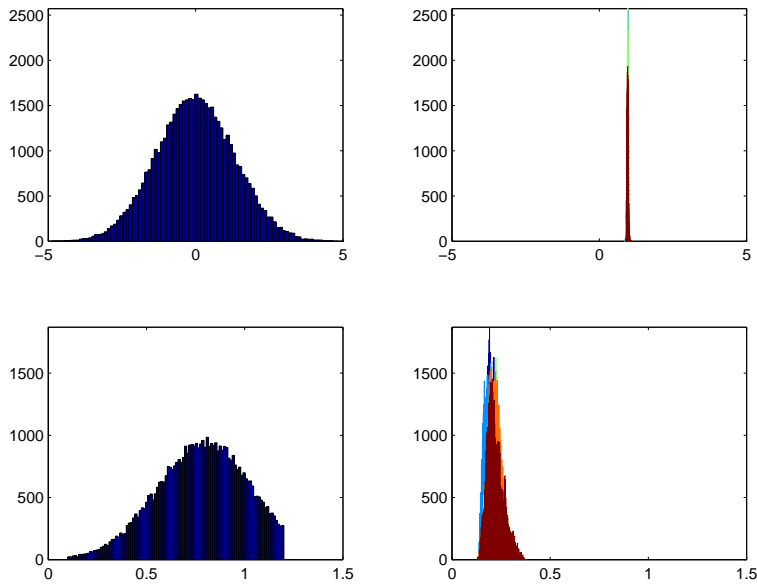| Station no. 1 in Norway	ϵ	b	c	a	ψ	τ^2
Nonlinear estimate	0.324	2.530	-56.648	2.4e-04	-	1.7e-10
Parameter estimate, mean	0.582	2.284	-37.068	1.2e-03	0.664	1.7e-05
Parameter estimate, median	0.582	2.284	-37.012	1.2e-03	0.663	4.1e-05
Acceptance ratio	0.26	0.47	0.30	-	0.55	-
$\widehat{R}$ ratio	1.40	1.41	1.39	-	1.30	1.05
Tuning parameter	1e-06	1e-07	1e-01	-	1e-05	-
2.5% percentile	0.532	2.240	-41.001	8.8e-04	0.576	1.6e-06
25.0% percentile	0.564	2.267	-38.472	1.1e-03	0.634	7.3e-06
50.0% percentile	0.582	2.284	-37.068	1.2e-03	0.664	1.7e-05
75.0% percentile	0.601	2.300	-35.526	1.3e-03	0.692	4.3e-05
97.5% percentile	0.631	2.330	-33.035	1.6e-03	0.740	2.2e-04
Skewness	0.028	-0.003	0.066	0.354	-0.165	6.623
Kurtosis	2.50	2.50	2.50	2.69	2.72	2.72
Standard Deviation	2.6e-02	2.4e-02	2.1e+00	1.8e-04	4.3e-02	7.3e-05
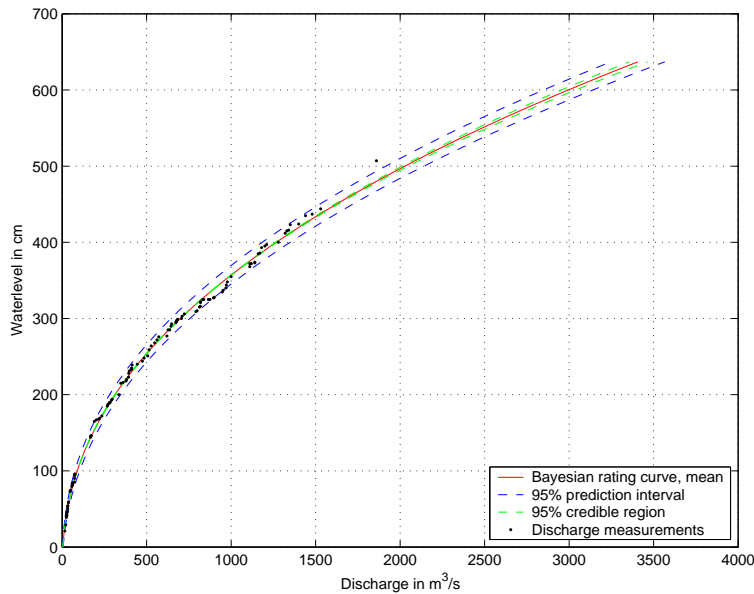
Figure C.49: The estimated rating curve using the parameters a, b and c in Table C.7. 95% prediction intervals for the discharge measurements are shown, as well as the 95% credible regions for the rating curve. Here, the whole range of water levels is shown, $W_{\min}$ through $W_{\max}$.
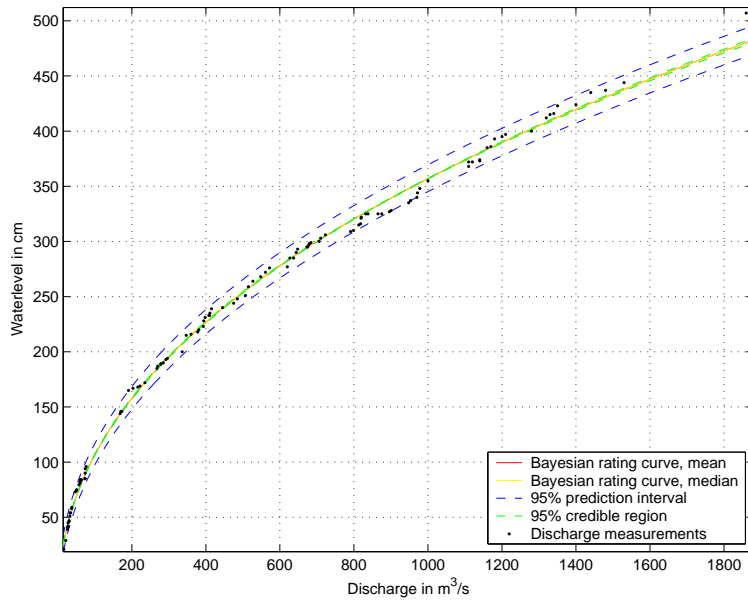
Figure C.50: The estimated rating curve using the parameters a, b and c in Table C.7. 95% prediction intervals for the discharge measurements are shown, as well as the 95% credible regions for the rating curve. Here, the range of water levels shown is, Q_{min} through Q_{max}.
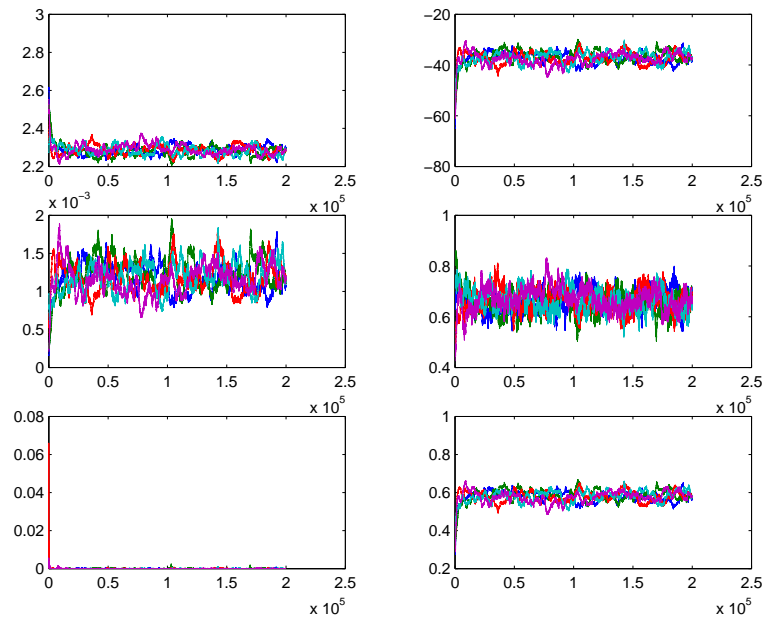
Figure C.51: **From left to right:** b, c, $\ln(a)$, ψ, τ^2 and ϵ. The generated Markov chains for each parameter converging to the mode of the posterior distribution from their respective initial value.
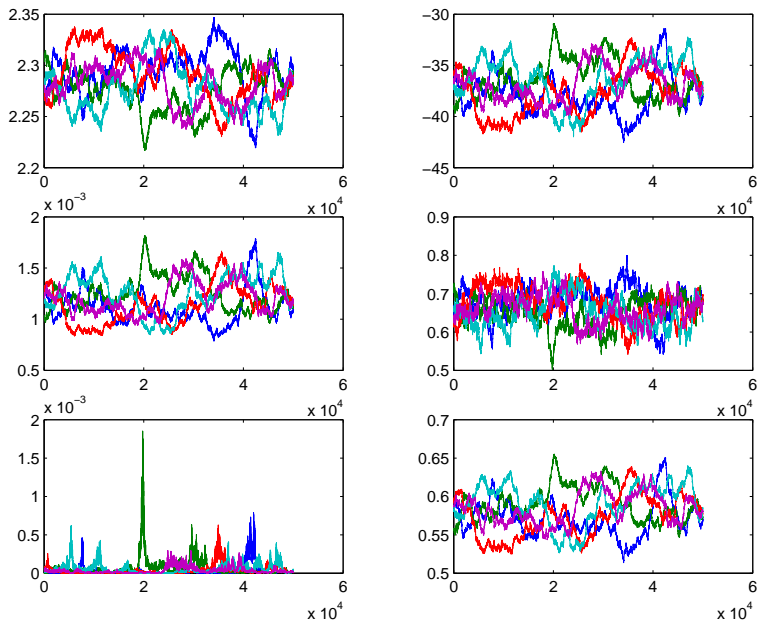
Figure C.52: **From left to right:** b, c, $\ln(a)$, ψ, τ^2 and ϵ. The mixing of the Markov chains after the burn-in period.
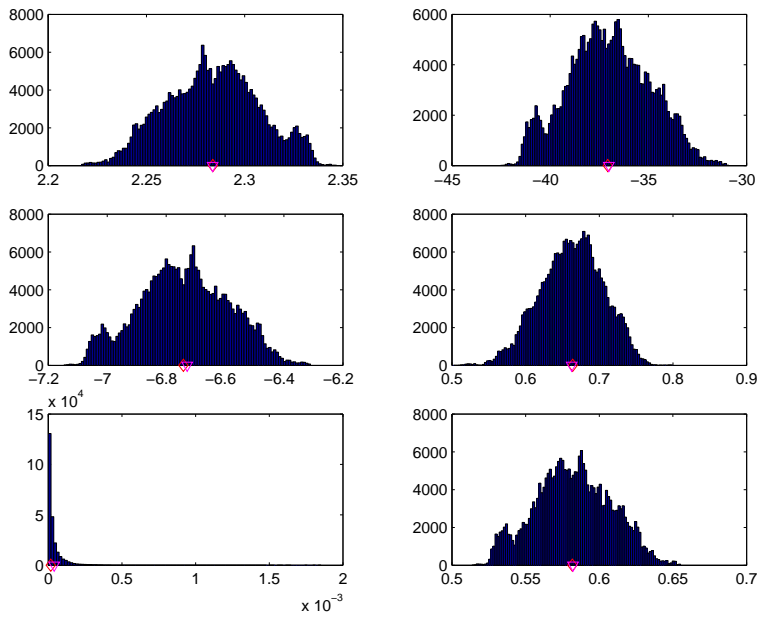
Figure C.53: **From left to right:** b, c, $\ln(a)$, ψ, τ^2 and ϵ. The resulting posterior distributions for each parameter. On each figure the parameter estimates, the mean and the median, are shown.

L
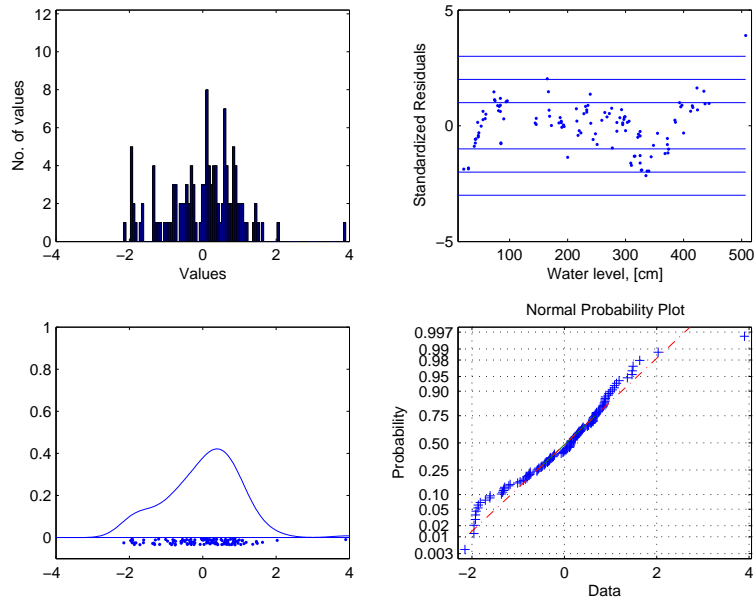
Figure C.54: **Upper left:** A histogram of the standardized residuals. **Upper right:** Standardized residuals from the estimated rating curve as a function of water level. **Lower left:** A smooth representation of the residual density. **Lower right:** A normal probability plot of standardized residuals.
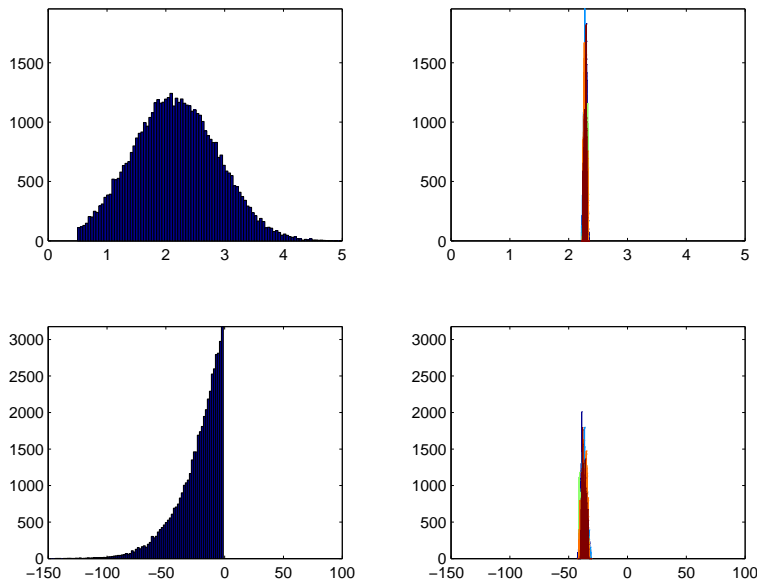
Figure C.55: **Upper left:** The prior distribution for parameter ϵ. **Upper right:** The posterior distribution of parameter ϵ. **Lower left:** The prior distribution for parameter ψ. **Lower right:** The posterior distribution of parameter ψ.
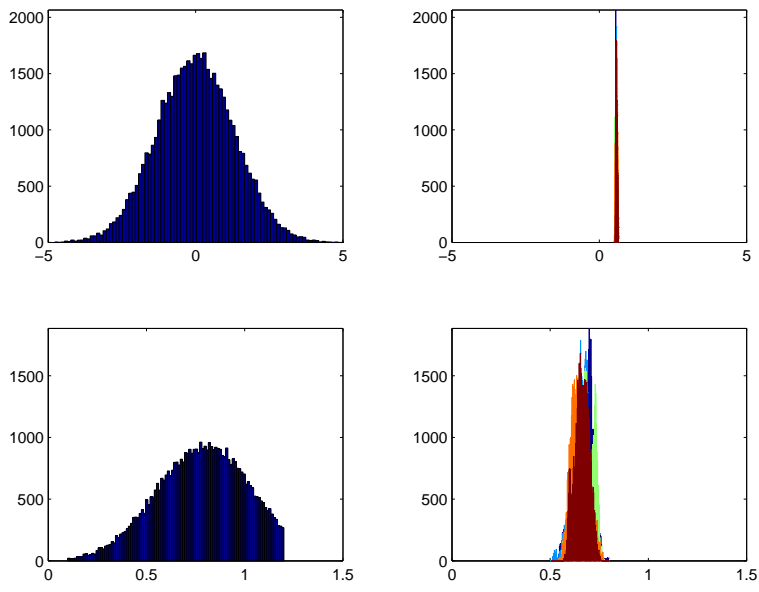
Figure C.56: **Upper left:** The prior distribution for parameter b. **Upper right:** The posterior distribution of parameter b. **Lower left:** The prior distribution for parameter c. **Lower right:** The posterior distribution of parameter c.

C.2   Annual Mean Discharge Estimates

In Figures C.57 through C.63, the estimated credible regions are sometimes very narrow. Hence, they will simply appear as lines instead of intervals.

C.2.1   Case 1, Station DK_1, Skjern å

Table C.8: The estimated annual mean discharge based on the Skjern å data.

| Station no. 1 in Denmark	DK	FI	IS	NO	SE	2.5%	25%	50%	75%	97.5%
Dry year	9.6	9.2	9.9	10.6	9.7	9.18	9.188	9.191	9.194	9.202
Normal year	15.7	15.9	16.4	15.2	16.1	15.79	15.8	15.8	15.8	15.81
Wet year	19.7	19.7	20.6	19	19.93	19.9	19.91	19.92	19.92	19.93
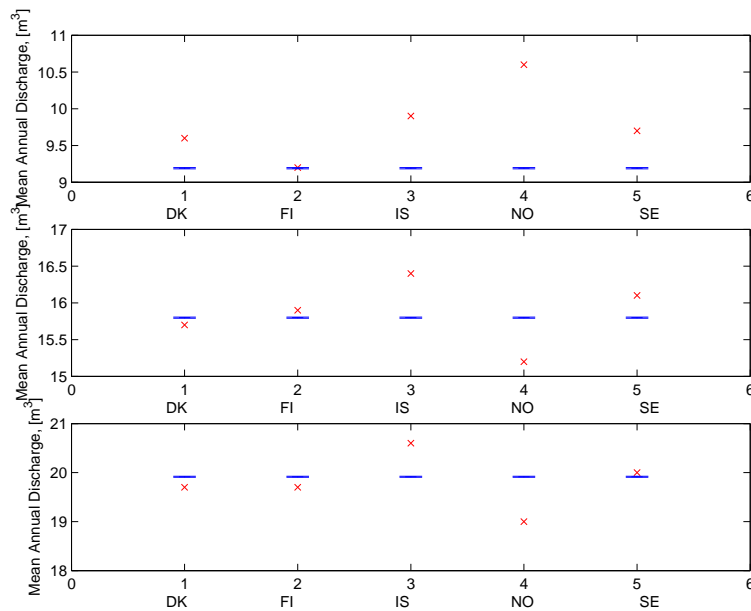
Figure C.57: The CHIN results from each country, compared to the posterior mean and 95% credible regions for the annual mean discharge for three years. **Top:** Dry year. **Middle:** Average year. **Bottom:** Wet year.

C.2.2 Case 2, Station DK_2, Odense å

Table C.9: The estimated annual mean discharge based on the Odense å data.

Station no. 2 in Denmark	DK	FI	IS	NO	SE	2.5%	25%	50%	75%	97.5%
Dry year	1.5	1.5	1.5	1.2	1.5	1.50	1.51	1.51	1.51	1.52
Normal year	3.1	3.3	3.2	3.2	3.2	3.11	3.13	3.13	3.13	3.15
Wet year	4.9	4.7	5.0	4.4	4.9	4.91	4.94	4.96	4.97	5.00
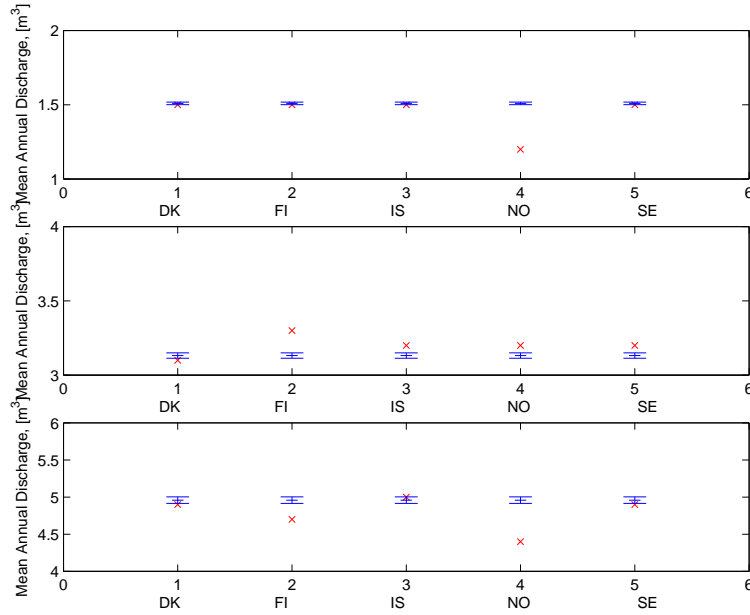
Figure C.58: The CHIN results from each country, compared to the posterior mean and 95% credible regions for the annual mean discharge for three years. **Top:** Dry year. **Middle:** Average year. **Bottom:** Wet year.

C.2.3 Case 3, Station FI_1, Lake Lannevesi

Table C.10: The estimated annual mean discharge based on the Lake Lannevesi data.

| Station no. 1 in Finland	DK	FI	IS	NO	SE	2.5%	25%	50%	75%	97.5%
Dry year	2.2	2.3	2.3	2.2	2.2	2.17	2.20	2.21	2.22	2.25
Normal year	3.3	3.4	3.4	3.3	3.3	3.29	3.34	3.34	3.34	3.39
Wet year	4.0	4.1	4.0	4.0	3.9	3.88	3.93	3.94	3.95	3.99

Figure C.59: The CHIN results from each country, compared to the posterior mean and 95% credible regions for the annual mean discharge for three years. **Top:** Dry year. **Middle:** Average year. **Bottom:** Wet year.

C.2.4 Case 4, Station FI_2, Lake Vahvajarvi

Table C.11: The estimated annual mean discharge based on the Lake Vahvajarvi data.

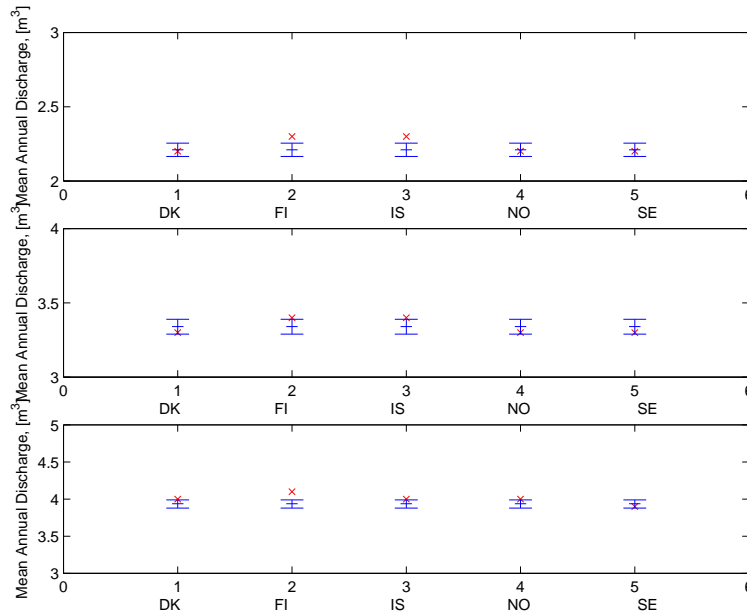| Station no. 2 in Finland	DK	FI	IS	NO	SE	2.5%	25%	50%	75%	97.5%
Dry year	22.9	22.9	22.9	22.9	23.0	22.84	22.91	22.92	22.92	22.99
Normal year	27.5	27.5	27.6	27.6	27.6	27.57	27.66	27.67	27.67	27.75
Wet year	29.0	29.1	29.1	29.1	29.2	29.10	29.18	29.19	29.20	29.28

Figure C.60: The CHIN results from each country, compared to the posterior mean and 95% credible regions for the annual mean discharge for three years. **Top:** Dry year. **Middle:** Average year. **Bottom:** Wet year.

C.2.5 Case 5, Station IS_1, Skjálfandafljót

Table C.12: The estimated annual mean discharge based on the Skjálfandafljót data.

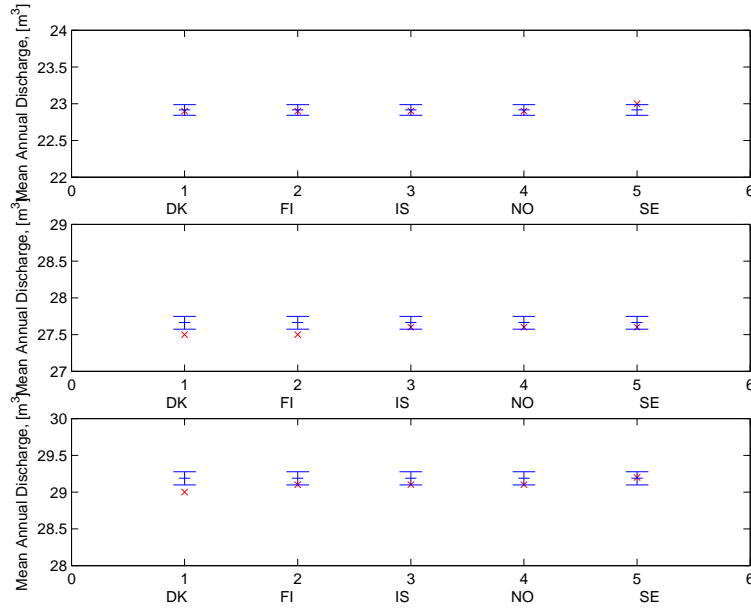| Station no. 1 in Iceland	DK	FI	IS	NO	SE	2.5%	25%	50%	75%	97.5%
Dry year	43.3	43.2	43.0	43.1	43.0	42.54	42.89	42.99	43.09	43.46
Normal year	49.2	48.8	48.8	48.8	48.8	48.16	48.56	48.65	48.74	49.16
Wet year	54.7	54.3	54.3	54.3	54.3	53.70	54.14	54.22	54.31	54.75

Figure C.61: The CHIN results from each country, compared to the posterior mean and 95% credible regions for the annual mean discharge for three years. **Top:** Dry year. **Middle:** Average year. **Bottom:** Wet year.

C.2.6 Case 6, Station IS_2, Fnjóská

Table C.13: The estimated annual mean discharge based on the Fnjóská data.

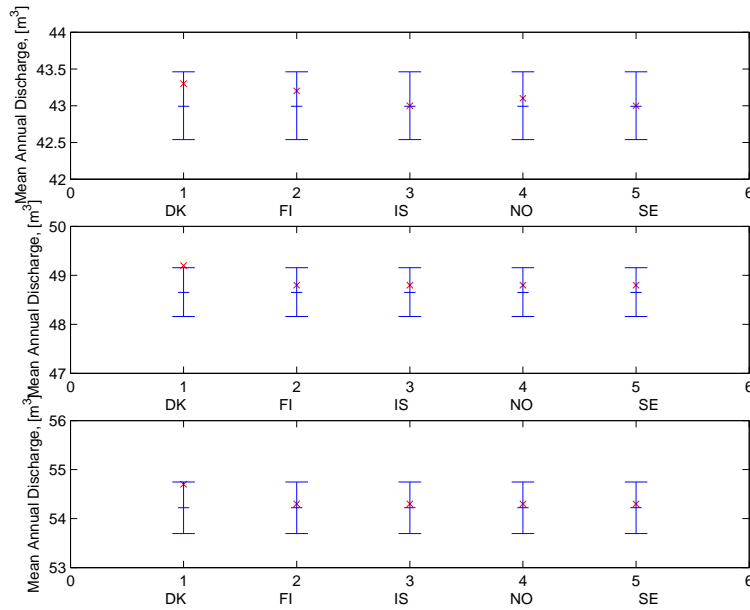| Station no. 2 in Iceland	DK	FI	IS	NO	SE	2.5%	25%	50%	75%	97.5%
Dry year	30.3	30.6	30.8	30.3	30.0	29.86	30.28	30.39	30.50	30.89
Normal year	38.9	41.0	39.4	38.9	38.7	38.45	38.92	39.03	39.15	39.62
Wet year	51.4	57.7	51.4	51.3	51.4	50.96	51.56	51.72	51.89	52.51
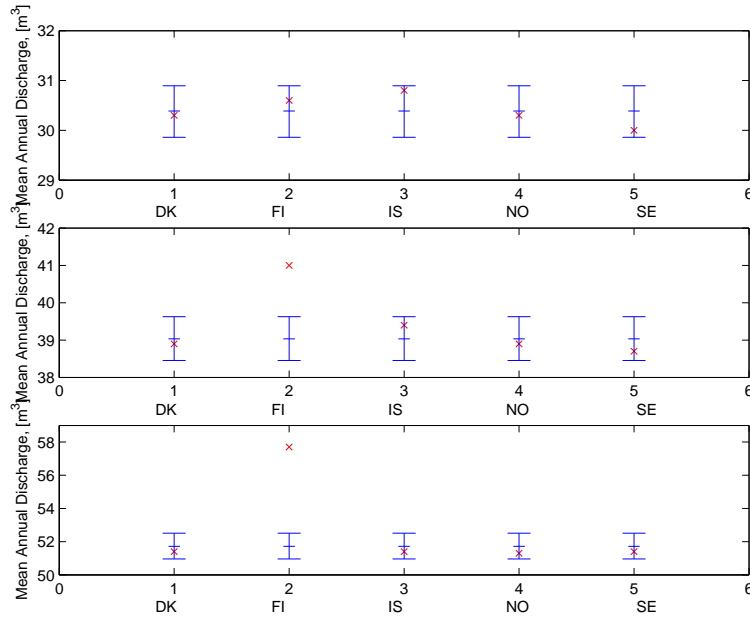
Figure C.62: The CHIN results from each country, compared to the posterior mean and 95% credible regions for the annual mean discharge for three years. **Top:** Dry year. **Middle:** Average year. **Bottom:** Wet year. for three years. **Top:** Dry year. **Middle:** Average year. **Bottom:** Wet year.

C.2.7 Case 7, Station NO_1, Gudbrandsdalslågen

Table C.14: The estimated annual mean values based on the Gudbrandsdalslågen data.

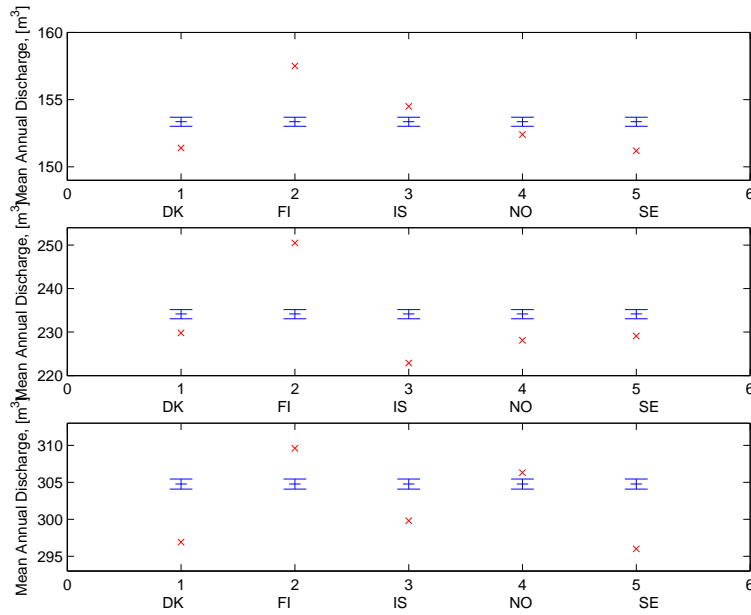| Station no. 1 in Norway	DK	FI	IS	NO	SE	2.5%	25%	50%	75%	97.5%
Dry year	151.4	157.5	154.5	152.4	151.2	153.02	153.26	153.36	153.44	153.69
Normal year	229.8	250.5	222.9	228.1	229.1	233.04	233.77	234.16	234.56	235.17
Wet year	296.9	309.6	299.8	306.3	296.0	304.08	304.53	304.76	304.99	305.43

Figure C.63: The CHIN results from each country, compared to the posterior mean and 95% credible regions for the annual mean discharge for three years. **Top:** Dry year. **Middle:** Average year. **Bottom:** Wet year.

C.3 Maximum and Minimum Discharge Estimates

C.3.1 Case 1, Station DK_1, Skjern å

Table C.15: The estimated maximum and minimum discharge values based on the Skjern å data.

Station no. 1 in Denmark	DK	FI	IS	NO	SE	2.5%	25%	50%	75%	97.5%
Highest calculated discharge	57.6	48.2	58.5	48.0	52.4	54.93	55.01	55.06	55.10	55.19
Lowest calculated discharge	0.0	3.6	0.0	5.5	0.0	4.33	4.34	4.35	4.36	4.37

Figure C.64: The CHIN results from each country, compared to the posterior mean and 95% credible regions for the maximum and minimum discharge. **Upper:** The maximum discharge. **Lower:** The minimum discharge.

C.3.2 Case 2, Station DK_1, Odense å

Table C.16: The estimated maximum and minimum discharge values based on the Odense å data.

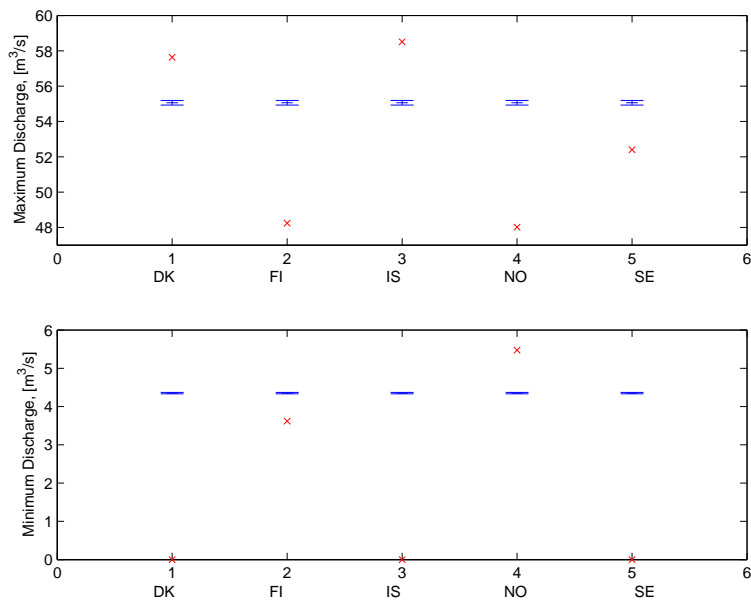| Station no. 2 in Denmark	DK	FI	IS	NO	SE	2.5%	25%	50%	75%	97.5%
Highest calculated discharge	37.5	20.8	30.2	30.1	33.6	37.54	38.16	38.60	39.05	39.81
Lowest calculated discharge	0.2	0.0	0.2	0.0	0.1	0.19	0.19	0.19	0.20	0.20

Figure C.65: The CHIN results from each country, compared to the posterior mean and 95% credible regions for the maximum and minimum discharge. **Upper:** The maximum discharge. **Lower:** The minimum discharge.

C.3.3 Case 3, Station FI_1, Lake Lannevesi

Table C.17: The estimated maximum and minimum discharge values based on the Lake Lann-evesi data.

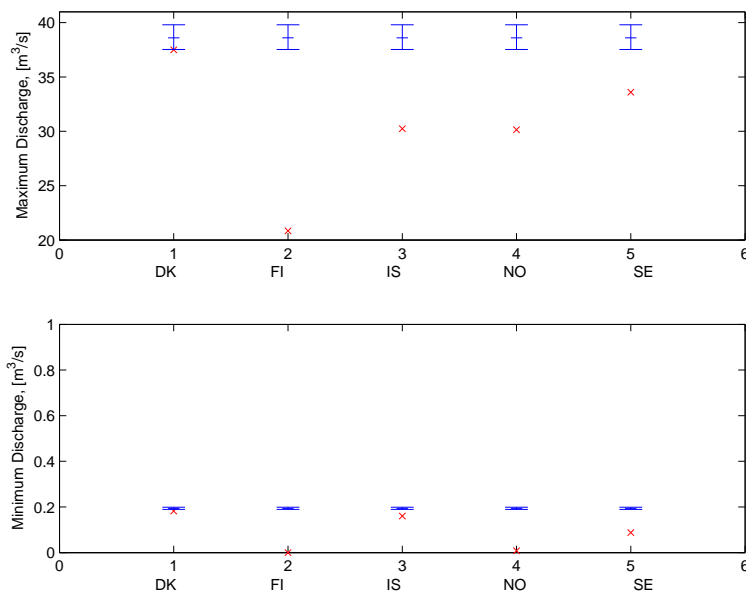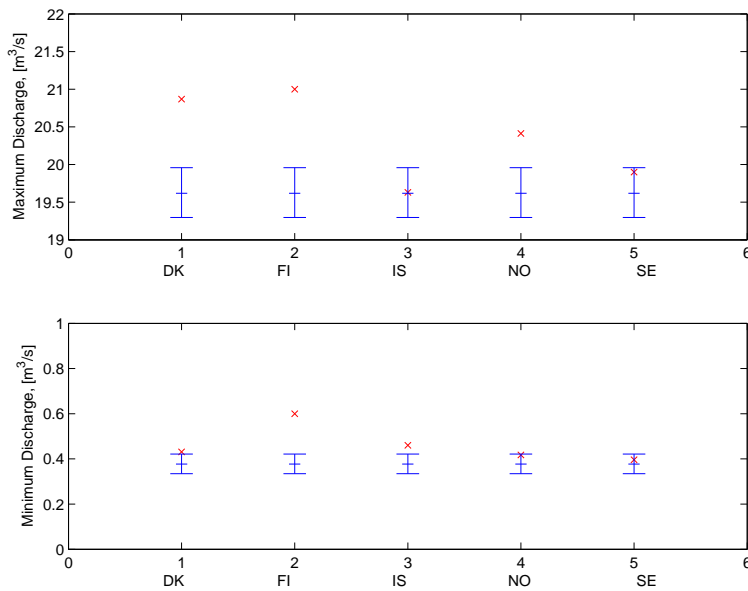| Station no. 1 in Finland	DK	FI	IS	NO	SE	2.5%	25%	50%	75%	97.5%
Highest calculated discharge	20.9	21.0	19.6	20.4	19.9	19.30	19.50	19.62	19.76	19.96
Lowest calculated discharge	0.4	0.6	0.5	0.4	0.4	0.33	0.36	0.38	0.39	0.42

Figure C.66: The CHIN results from each country, compared to the posterior mean and 95% credible regions for the maximum and minimum discharge. **Upper:** The maximum discharge. **Lower:** The minimum discharge.

C.3.4 Case 4, Station FI_2, Lake Vahvajarvi

Table C.18: The estimated maximum and minimum discharge values based on the Lake Vah-
vajarvi data.

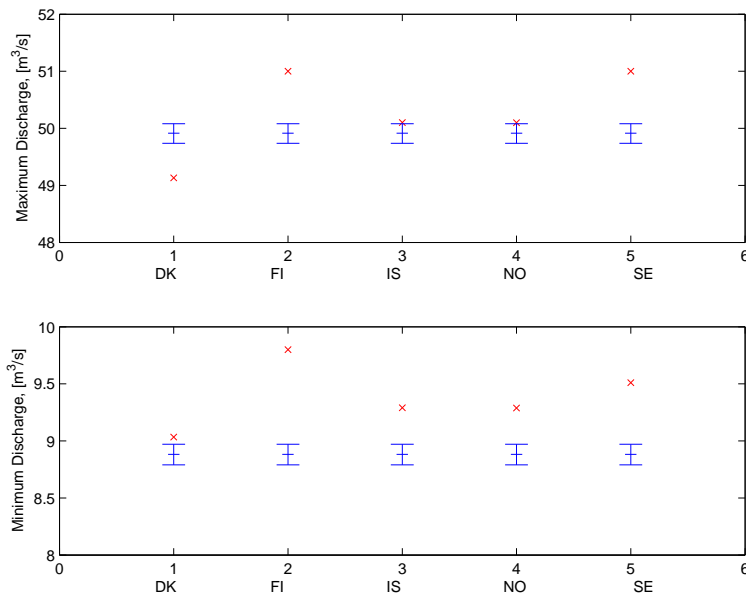| Station no. 2 in Finland	DK	FI	IS	NO	SE	2.5%	25%	50%	75%	97.5%
Highest calculated discharge	49.1	51.0	50.1	50.1	51.0	49.74	49.87	49.91	49.96	50.08
Lowest calculated discharge	9.0	9.8	9.3	9.3	9.5	8.79	8.85	8.88	8.91	8.97

Figure C.67: The CHIN results from each country, compared to the posterior mean and 95%
credible regions for the maximum and minimum discharge. **Upper:** The maximum discharge.
Lower: The minimum discharge.

C.3.5   Case 5, Station IS_1, Skjálfandafljót

Table C.19: The estimated maximum and minimum discharge values based on the Skjálfandafljót data.

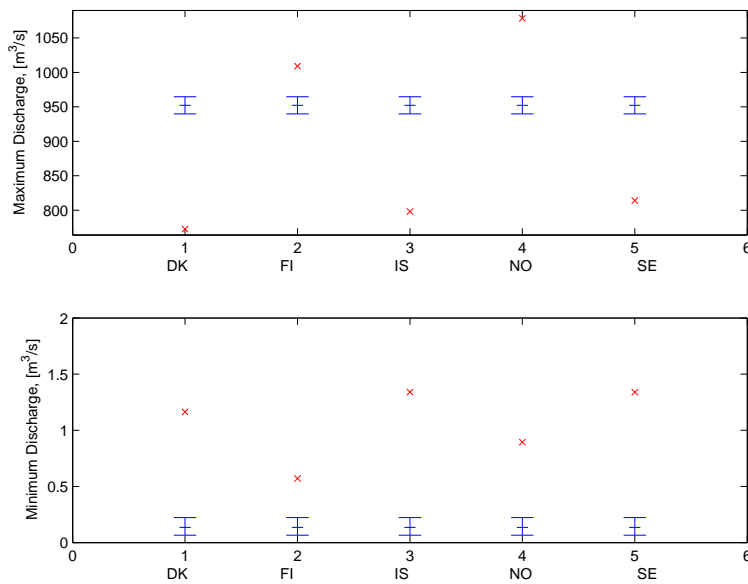| Station no. 1 in Iceland	DK	FI	IS	NO	SE	2.5%	25%	50%	75%	97.5%
Highest calculated discharge	772.5	1009.1	798.2	1078.6	814.0	939.9	947.9	952.3	956.6	964.6
Lowest calculated discharge	1.2	0.6	1.3	0.9	1.3	0.07	0.11	0.14	0.17	0.22

Figure C.68: The CHIN results from each country, compared to the posterior mean and 95% credible regions for the maximum and minimum discharge. **Upper:** The maximum discharge. **Lower:** The minimum discharge.

C.3.6 Case 6, Station IS_2, Fnjóská

Table C.20: The estimated maximum and minimum discharge values based on the Fnjóská data.

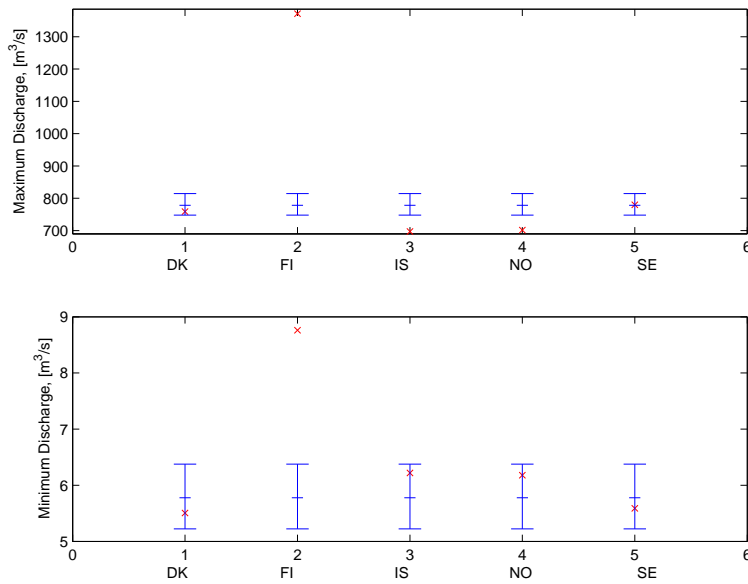| Station no. 2 in Iceland	DK	FI	IS	NO	SE	2.5%	25%	50%	75%	97.5%
Highest calculated discharge	758.9	1371.1	697.0	701.6	780.0	748.0	768.4	778.3	790.1	814.7
Lowest calculated discharge	5.5	8.8	6.2	6.2	5.6	5.22	5.60	5.78	5.98	6.38

Figure C.69: The CHIN results from each country, compared to the posterior mean and 95% credible regions for the maximum and minimum discharge. **Upper:** The maximum discharge. **Lower:** The minimum discharge.

C.3.7 Case 7, Station NO_1, Gudbrandsdalslågen

Table C.21: The estimated maximum and minimum discharge values based on the Gudbrandsdalslågen data.

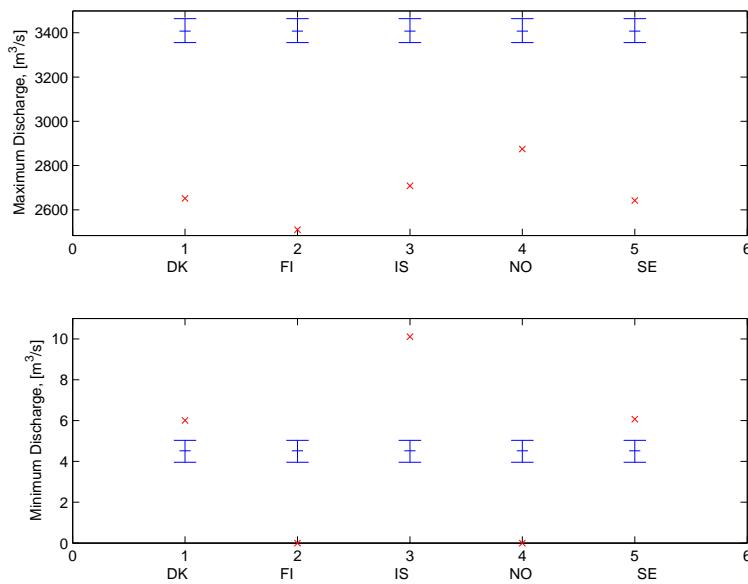| Station no. 1 in Norway	DK	FI	IS	NO	SE	2.5%	25%	50%	75%	97.5%
Highest calculated discharge	2651.5	2509.7	2708.6	2642.0	2642.0	3330.1	3339.4	3341.1	3345.4	3374.4
Lowest calculated discharge	6.0	0.0	10.2	0.0	6.1	3.70	4.11	4.33	4.5	4.95

Figure C.70: The CHIN results from each country, compared to the posterior mean and 95% credible regions for the maximum and minimum discharge. **Upper:** The maximum discharge. **Lower:** The minimum discharge.